Science
AAAS

Supplementary Materials for

Genomic inference of a severe human bottleneck during the Early to Middle Pleistocene transition

Wangjie Hu, Ziqian Hao, Pengyuan Du, Fabio Di Vincenzo, Giorgio Manzi, Jialong Cui, Yun-Xin Fu, Yi-Hsuan Pan, Haipeng Li

Corresponding authors: yxpan@sat.ecnu.edu.cn; lihaipeng@sinh.ac.cn

This PDF file includes:

This is the author's version of the work. It is posted here by permission of the AAAS for personal use, not for redistribution. The definitive version was published in *Science* on September 1, 2023, DOI: 10.1126/science.abq7487.

Click the link to download the published version: https://doi.org/10.1126/science.abq7487

Contents

Materials and Methods

Coalescent time

The coalescent time is the time period between two successive coalescent events. There are three different time measurements. First, time was measured in generations or years. Second, time τ, as one-point scaled time, was scaled by $2N(0)$ generations, where $N(\cdot)$, a function of reverse time, denoted the population size history (i.e., the dynamic of population size). Third, time t was scaled by $2N(t)$ generations (*15, 22, 47*). To distinguish it from the one-point scaled time τ, time t was designated as the standard coalescent time.

Fast infinitesimal time coalescent (FitCoal) process

It is assumed that a sample was obtained by random selection of *n* sequences from a diploid population. FitCoal traced lineages of the sample to the common ancestor. This long period of time was partitioned into millions of infinitesimal time intervals to ensure the accuracy of calculation. FitCoal then calculated the expected branch length for each category of site frequency spectrum (SFS) with an arbitrary population size history $N(\cdot)$. A category of SFS is the proportion of mutations of the same size in the sample. The size of a mutation is the number of sequences with the mutation (*48*). Since SFS categories are also referred to as SFS types, both terms are used interchangeably in this study.

A sample was designated to be in the coalescent state l ($l = 2, \cdots, n$) at time t if it had exactly l ancestral lineages at this time (Fig. 1). The probability of state l at time t was denoted $p_l(t)$. In a coalescent tree, a branch was designated type i if it had i descendants. Based on Kingman's coalescent (*15*),

$$\frac{\mathrm{d}}{\mathrm{d}t}p_l(t) = \begin{cases} \binom{l+1}{2}p_{l+1}(t) - \binom{l}{2}p_l(t) & l = 2, \cdots, n-1 \\ -\binom{l}{2}p_l(t) & l = n \end{cases}.$$

When Δt was extremely small (Fig. 1), there was almost no or only one coalescent event during t and $t + \Delta t$, leading to

$$p_l(t+\Delta t) = \begin{cases} \binom{l+1}{2}\Delta t p_{l+1}(t) + \left(1 - \binom{l}{2}\Delta t\right)p_l(t) & l = 2, \cdots, n-1 \\ \left(1 - \binom{l}{2}\Delta t\right)p_l(t) & l = n \end{cases}.$$

The branch length was in units of generations. The expected branch length of state l during t and $t + \Delta t$ was calculated as $\int_t^{t+\Delta t} 2\,N(t)p_l(t)l\mathrm{d}t$. The probability that a branch of state l was of type i was $\frac{\binom{n-i-1}{l-2}}{\binom{n-1}{l-1}}$ (*15*). The expected branch length of type i of state l during t and $t + \Delta t$ was $\int_t^{t+\Delta t} 2\,N(t)p_l(t)l\frac{\binom{n-i-1}{l-2}}{\binom{n-1}{l-1}}\mathrm{d}t$. Therefore, the expected branch length $BL_i(N(\cdot))$ of type i was

$$\sum_{l=2}^{n-i+1}\int_0^{\infty} 2\,N(t)p_l(t)l\mathrm{d}t\frac{\binom{n-i-1}{l-2}}{\binom{n-1}{l-1}}. \quad (1)$$

A FitCoal time partition was denoted $\{t_0, t_1, \cdots, t_m\}$, where $0 = t_0 < t_1 < \cdots < t_m$. Thus $p_l(t_0) = \begin{cases} 1 & l = n \\ 0 & \text{else} \end{cases}$. For a large positive number m, if t_m was large and $(t_k - t_{k-1})$ was small for $k = 1, \cdots, m$,

$$p_l(t_k) = \begin{cases} \left(1 - \binom{l}{2}(t_k - t_{k-1})\right) p_l(t_{k-1}) & l = n \\ \left(1 - \binom{l}{2}(t_k - t_{k-1})\right) p_l(t_{k-1}) + \binom{l+1}{2}(t_k - t_{k-1}) p_{l+1}(t_{k-1}) & \text{else} \end{cases}$$, where $k = 1, \cdots, m$.

The expected branch length of type i was calculated as

$$BL_i(N(\cdot)) = \sum_{l=2}^{n-i+1} l \frac{\binom{n-i-1}{l-2}}{\binom{n-1}{l-1}} \left(\sum_{k=1}^{m} 2N(t_{k-1}) p_l\,(t_{k-1})(t_k - t_{k-1})\right).$$

To determine the time partition, the coalescent probability was set less than 10^{-4} during t_{k-1} and t_k ($k = 1, \cdots, m$), and the probability of common ancestor (i.e., the probability of state 1) at t_m was larger than $(1 - 10^{-6})$. When the sample size was 10, $m =$ 1,571,200. When the sample size was 200, $m =$ 7,038,398. Thus, each Δt was extremely small for precise calculation of expected branch length.

Several analytical formulae for SFS were derived in two previous studies (*16*, *17*). Both studies relied on the joint probability density function of coalescent times, which resulted in large numerical errors when the sample size was not small (e.g., $n > 50$). To avoid large numerical errors, the Polanski-Kimmel method was developed (*16*). This method was then implemented in fastNeutrino (*19*).

FitCoal has no such numerical-error problems because it does not rely on the joint density among different coalescent times (Fig. 1). Moreover, FitCoal calculated branch lengths were nearly identical to those calculated with the Živković-Wiehe method (*17*) when the sample size was very small (e.g., $n = 10$) (table S13). When the sample size was very large (e.g., $n =$ 1,000), FitCoal precisely calculated the expected branch lengths (table S14). The differences between FitCoal and the Živković-Wiehe method are summarized in table S15.

Accelerated calculation of FitCoal

The expected branch length of each type or category can be calculated for arbitrary time intervals according to the procedure described above. For tabulated time partition $\{t_0, t_1, \cdots, t_{m'}\}$ ($0 = t_0 < t_1 < \cdots < t_{m'}$), the expected branch length of each type is equal to the sum of the expected branch lengths of this type during each tabulated time interval; thus, the latter was rescaled, tabulated, and stored. These pre-stored values were re-used to calculate the expected branch lengths.

The rescaled expected branch length $BL_{i,t}$ of type i during 0 and t was $BL_{i,t} = \sum_{l=2}^{n-i+1} \int_0^t p_s\,(l) l \frac{\binom{n-i-1}{l-2}}{\binom{n-1}{l-1}} \mathrm{d}s$, where $i = 1, \cdots, n-1$. For tabulated time partition $\{t_0, t_1, \cdots, t_{m'}\}$, BL_{i,t_0}, BL_{i,t_1}, $\cdots$, and $BL_{i,t_{m'}}$ were tabulated. As an example, when $n = 10$ and 200, $m' = 231$ and 529, respectively.

$BL_{i,t}$ was used to calculate the expected branch lengths under arbitrary population size histories. When $\tilde{t} \in [t_{k-1}, t_k)$,

$$BL_{i,\tilde{t}} \approx \frac{t_k - \tilde{t}}{t_k - t_{k-1}} BL_{i,t_{k-1}} + \frac{\tilde{t} - t_{k-1}}{t_k - t_{k-1}} BL_{i,t_k}.$$

When $N(t)$ was a piecewise constant, a demographic time partition $\{\tilde{t}_0, \tilde{t}_1, \cdots, \tilde{t}_{\tilde{m}}\}$ was present, such that $N(t) = N_k$ for $t \in [\tilde{t}_k, \tilde{t}_{k+1})$, $k = 0, \cdots, \tilde{m}$. The expected branch length of type i was then calculated as

$$BL_i(N(\cdot)) = \sum_{k=1}^{\tilde{m}} 2N_k \left(BL_{i,\tilde{t}_k} - BL_{i,\tilde{t}_{k-1}}\right).$$

When $N(t)$ was complex, the population size history was approximated by a piecewise constant function.

FitCoal composite likelihood

The mutation rate per base pair per generation was denoted by μ, and $\vec{\xi} = (\xi_i)$ was the observed SFS. ξ_i is the number of mutations of the same size *i* in the sample (n sequences with σ base pair), where $i = 1, \cdots, n-1$. The expected SFS was $\vec{\lambda} = (\lambda_i)$, where $\lambda_i = \mu\sigma BL_i(N(\cdot))$. Based on the commonly used Poisson probability (*19*, *49-51*), the composite likelihood function was determined as

$$L_{\mu,\iota}(\vec{\xi}, N(\cdot)) = \prod_{i=1}^{n-1} \frac{\lambda_i^{\xi_i} e^{-\lambda_i}}{\xi_i!}.$$

The composite likelihood function was extended for data set with missing data. Assuming that $\sigma^{(n)}$ base pairs were sequenced in n sequences and S was the set of all sample sizes, the observed SFS of $n(\in S)$ sequences was $\vec{\xi}^{(n)} = \left(\xi_1^{(n)}, \cdots, \xi_{n-1}^{(n)}\right)$. The expected SFS of n sequences $\vec{\lambda}^{(n)} = \left(\lambda_1^{(n)}, \cdots, \lambda_{n-1}^{(n)}\right)$, where $\lambda_i^{(n)} = \mu\sigma^{(n)} BL_i^{(n)}(N(\cdot))$, $BL_i^{(n)}(N(\cdot))$ was the expected branch length of type i with n sequences under the population size history $N(\cdot)$. The total number of base pairs was $\sigma(S) := \sum_{n\in S} \sigma^{(n)}$, and the composite likelihood function was

$$\begin{aligned} & L_{\mu,(\iota^{(n)})_{n\in S}}((\vec{\xi}^{(n)})_{n\in S}, N(\cdot)) \\ &= \prod_{n\in S} L_{\mu,\iota^{(n)}}(\vec{\xi}^{(n)}, N(\cdot)) \\ &= \prod_{n\in S} \prod_{i=1}^{n-1} \frac{(\lambda_i^{(n)})^{\xi_i^{(n)}} e^{-\lambda_i^{(n)}}}{\xi_i^{(n)}!} \end{aligned}.$$

It has been recommended to combine (*19*) or truncate (*6*) high frequency mutations when inferring demography. The former collapses (combines) the high frequency mutations represented by the tail end of an SFS into one category (*19*). The latter calculates likelihood using a subset of SFS by discarding certain categories of an SFS (*6*). Both approaches are appropriate as different categories of an SFS are independent from each other. Therefore, if an SFS "curve" was found to have a raised tail end, truncated SFS $\vec{\xi}^{T} = (\xi_i)$ was used, where $i = 1, \cdots, k$. Its composite likelihood function was

$$L_{\mu,\iota}(\vec{\xi}^{T}, N(\cdot)) = \prod_{i=1}^{k} \frac{\lambda_i^{\xi_i} e^{-\lambda_i}}{\xi_i!}.$$

When an SFS was partially collapsed, its composite likelihood function was

$$L_{\mu,\iota}(\vec{\xi}^{B}, N(\cdot)) = \frac{\lambda_B^{\xi_B} e^{-\lambda_B}}{\xi_B!} \prod_{i=1}^{k} \frac{\lambda_i^{\xi_i} e^{-\lambda_i}}{\xi_i!},$$

where the partially collapsed SFS $\vec{\xi}^{B} = (\xi_1, \xi_2, \ldots\ldots, \xi_k, \xi_B)$, $\xi_B = \sum_{i=k+1}^{n-1} \xi_i$, and $\lambda_B = \sum_{i=k+1}^{n-1} \lambda_i$.

As sequencing errors could affect rare mutations in a sample, singletons and mutations with a size $(n-1)$ were discarded. The composite likelihood function of an SFS without these mutations was

$$L_{\mu,\iota}(\vec{\xi}, N(\cdot)) = \prod_{i=2}^{n-2} \frac{\lambda_i^{\xi_i} e^{-\lambda_i}}{\xi_i!}.$$

An SFS is referred as folded SFS when ancestral/derived status of mutations is not inferred. As previously described (*19, 52*), when *n* was an odd number, the composite likelihood of the folded SFS was

$$L_{\mu,\iota}(\vec{\xi}, N(\cdot)) = \prod_{i=1}^{n/2} \frac{(\lambda_i+\lambda_{n-i})^{(\xi_i+\xi_{n-i})} e^{-(\lambda_i+\lambda_{n-i})}}{(\xi_i+\xi_{n-i})!}.$$

When *n* was an even number, the composite likelihood was

$$L_{\mu,\iota}(\vec{\xi}, N(\cdot)) = \frac{\lambda_{n/2}{}^{\xi_{n/2}} e^{-\xi_{n/2}}}{\xi_{n/2}!} \prod_{i=1}^{\frac{n}{2}-1} \frac{(\lambda_i+\lambda_{n-i})^{(\xi_i+\xi_{n-i})} e^{-(\lambda_i+\lambda_{n-i})}}{(\xi_i+\xi_{n-i})!}.$$

When the tail of an SFS "curve" was raised upward, truncated (*6*) or collapsed (*19*) SFS was used for FitCoal demographic inference.

FitCoal demographic inference

FitCoal first fitted the observed SFS using a constant size model with one time interval, and the number of time intervals was increased by one at a time to generate more complex models. The Local Unimodal Sampling (LUS) algorithm (*53*) was used to maximize the likelihood and estimate parameters of population size history. A log-likelihood promotion rate (LLPR) was used to determine the best model to explain the observed SFS, and 20% was used as the threshold.

A series of demography with m pieces was denoted by a set of $S(m)$, where $S(m)$ contained all of the following m pieces of population size:

$$N(t|N0 > 0, N_{(m)}, t_{(m)}, c_{(m)})$$
$$= \begin{cases} N_m N0 & t \geq t_m \\ N_k N0 & t_k \leq t < t_{k+1}, c_k \in \mathcal{C}, k = 1, \cdots, m-1, \\ \frac{(t_{k+1}-t_k) N_{k+1} N_k N0}{(t-t_k) N_k + (t_{k+1}-t) N_{k+1}} & t_k \leq t < t_{k+1}, c_k \in \mathcal{E}, k = 1, \cdots, m-1 \end{cases}$$

where $N_{(m)} = (N_1, \cdots, N_m) \in N[m]$, $t_{(m)} = (t_1, \cdots, t_m) \in t[m]$, $c_{(m)} = (c_1, \cdots, c_m) \in c[m]$, $N[m] = \{(N_1, \cdots, N_m) | N_1 = 1, N_i > 0 \text{ for } i > 1\}$, $t[m] = \{(t_1, \cdots, t_m) | 0 = t_1 < \cdots < t_m\}$, $c[m] = \{(c_1, \cdots, c_m) | c_m \in \mathcal{C}, c_i \in \mathcal{C} \cup \mathcal{E} \text{ for } = 1, \cdots, m-1\}$, $\mathcal{C} = \{\text{constant}\}$, and $\mathcal{E} = \{\text{exponential}\}$. $N0$ was the effective population size at present, and N_k was the population size relative to $N0$, where $k = 1, \cdots, m-1$.

The $S(m)$ set was used as the wide-range parameter space to determine the maximum likelihood. To find the best population size history to explain the observed SFS, the following procedures were used:

(1) The number of inference time intervals (or pieces) m was initially set to 1, and the maximum likelihood $\max L_1$ was determined with the constant size model (i.e., the demographic model in $S(1)$).

(2) The number of time intervals (m) was increased by 1. For each change of type $c_{(m)}$, parameters $N_{(m)} = (N_1, \cdots, N_m)$ and $t_{(m)} = (t_1 = 0, t_2, \cdots, t_m)$ were searched to maximize the likelihood by the LUS algorithm to fit the observed SFS. The maximum likelihood $\max L_m$ was calculated with models in S(m) with all possible change types.

(3) Step 2 was repeated until $(1 + \text{threshold}) \cdot \log(\max L_m) < \log(\max L_{m-1})$ was obtained. The best model corresponding $\max L_{m-1}$ was determined to explain the observed SFS.

(4) To avoid local optima, steps 1–3 were repeated K times to find the best model. $K = 10$ was used to analyze simulated samples, and $K = 200$ was used to analyze the observed SFSs of the populations in 1000GP and the HGDP-CEPH panel.

To make FitCoal suitable for most cases and to determine the search range of parameter space by avoiding the so-called "runaway behavior" in optimization (*54*), the minimum length of each epoch was set to 0.001 (measured as the standard coalescent time) and 50 generations. Moreover, $0.01 \leq \frac{N_i}{N_{(i-1)}} \leq 100$ and $0.001 \leq \frac{N_i}{N_1} \leq 1000$ were applied for all cases.

The number of inference time intervals was determined by the threshold of log-likelihood promotion rate (LLPR). To find the best threshold of LLPR for FitCoal analyses, a large number of simulations were performed (table S16). As described above, the estimation was conducted with two models that differed by one inference time interval (i.e., time intervals m and $m+1$, respectively) using different thresholds of LLPR (e.g., 10, 20, and 30%). If the estimated number of inference time intervals was larger than the true number of inference time intervals, overfitting was recorded. When the former was smaller than the latter, underfitting was considered. Results of numerous such analyses showed that 20% was the best threshold of LLPR as 100% of the simulations in all models estimated population sizes correctly without any over-fitting or under-fitting cases (table S16). Therefore, this threshold of LLPR (20%) was used for all subsequent FitCoal analyses.

Data simulation

DNA polymorphism data were simulated using *ms* (*55*), MaCS (*56*), and msprime (*57*) software. Unless otherwise specified, a generation time was assumed to be 24 years (*6, 20*), the mutation rate μ was set for 1.2×10^{-8} per base per generation (*6, 21, 58, 59*), and the recombination rate was $r = 0.8\mu$. For each model, 200 SFSs were simulated to calculate the median and 2.5 and 97.5 percentiles. When verifying the inferred population size histories, eight DNA fragments with the length of 100 Mb each were used for simulation.

Monotonically decreasing SFS in neutrally evolved single populations

The expected SFS of a sample was denoted by $\vec{\lambda} = (\lambda_1, \dots, \lambda_{n-1})$. If the sample was collected from a single varying size population, it was expected that $\lambda_{\lceil n/2 \rceil} > \cdots > \lambda_{n-1}$. The expectation was proved as follows: the expected branch length of type *i* was $L(i) = \sum_{l=2}^{n-i+1} \int_0^\infty N(t) p_l(t) \mathrm{d}t \frac{\binom{n-i-1}{l-2}}{\binom{n-1}{l-1}}$. If $i_1 > i_2$,

$$L(i_1) = \sum_{l=2}^{n-i_1+1} \int_0^\infty N(t) p_l(t) \mathrm{d}t \frac{\binom{n-i_1-1}{l-2}}{\binom{n-1}{l-1}}$$

$$\leq \sum_{l=2}^{n-i_1+1} \int_0^\infty N(t) p_l(t) \mathrm{d}t \frac{\binom{n-i_2-1}{l-2}}{\binom{n-1}{l-1}} \quad .$$

$$< \sum_{l=2}^{n-i_2+1} \int_0^\infty N(t) p_l(t) \mathrm{d}t \frac{\binom{n-i_2-1}{l-2}}{\binom{n-1}{l-1}} = L(i_2)$$

When $L(i_1) < L(i_2)$, and $\lambda_{\lceil n/2 \rceil} > \cdots > \lambda_{n-1}$, monotonically decreasing SFS was observed in neutrally evolved single populations.

SFS truncation and collapse

The genome-wide SFS was expected to be monotonically decreasing in a neutrally evolved single population; however, the observed SFS curve of $\vec{\xi} = (\xi_1, \ldots, \xi_{n-1})$ was raised upward at the tail end (figs. S25 and S26), indicating excessive high frequency mutations probably because of hitchhiking effects of positive selection (*25*) and migration effects among different sub-populations (*28*). Such situations might result in a bias during demographic inference because the neutrally evolved single population failed to model excessive high frequency mutations of SFS. An m-dimension vector $\vec{V} = (v_1, \ldots, v_m)$ would have a raised tail end when $z \in \{1, \cdots, m-1\}$ and $v_z < \cdots < v_m$.

As each type of mutations ξ_i was determined by population size history $N(\cdot)$, the exclusion of ξ_i from FitCoal analysis would not introduce a bias in the estimated demography but would decrease its accuracy because less information was available (fig. S5). However, a bottleneck was inferred by FitCoal accurately even when only 10% of SFS categories were used for the analysis (fig. S5).

A simple procedure was developed to determine the cut-off threshold for exclusion of SFS types with high frequency mutations with a small window sliding through the SFS as follows: The cut-off threshold was determined if ξ_i exceeded its random fluctuation range. Let $\hat{n}(\vec{\xi}) = \max_{k \in \{1,\cdots,n-1\}} \left\{k | \overline{w}_k(\vec{\xi}) - 3SD_k(\vec{\xi}) < w_{k-i(n)+1}, \cdots, w_k < \overline{w}_k(\vec{\xi}) + 3SD_k(\vec{\xi})\right\}$, where $\overline{w}_k(\vec{\xi}) = \frac{1}{i(n)} \sum_{a=k-i(n)+1}^{k} \xi_a$, $SD_k(\vec{\xi}) = \sqrt{\overline{w}_k(\vec{\xi})}$, and

$$i(n) = \begin{cases} 3, & n \leq 50 \\ 4, & 50 < n \leq 100 \\ 5, & 100 < n \leq 300 \\ 10, & 300 < n \leq 500 \\ 20, & 500 < n \leq 1000 \\ 30, & 1000 < n \leq 2000 \\ 40, & 2000 < n \leq 3000 \\ 50, & n > 3000 \end{cases}$$

. The truncated SFS $\vec{\xi}^T = (\xi_i)$, where $i = 1, \cdots, k$. The proportion of truncated SFS types was calculated by $(n-1-k)/(n-1)$.

This procedure was also used to determine the high frequency boundary of SFS to be combined. The SFS combining procedure has been proposed to collapse these components (i.e., high frequency mutations) into one category to improve the efficiency of demography inference (*19*).

1000 Genomes Project data

Sequences of autosomal SNPs in 1000GP phase 3 (*23*) were downloaded from the 1000GP ftp server (table S2), and 26 populations were analyzed, including seven African populations (ACB, ASW, ESN, GWD, LWK, MSL, and YRI), five European populations (CEU, FIN, GBR, IBS, and TSI), five East Asian populations (CDX, CHB, CHS, JPT, and KHV), five South Asian populations (BEB, GIH, ITU, PJL, and STU), and four American populations (CLM, MXL, PEL, and PUR) (tables S3 and S5). The 1000 GP strict mask was used to exclude artifacts in SNP calling. Non-coding regions, except pseudogenes, defined by GENCODE release 35 (*60*), were examined to partially avoid potential effects of purifying selection. The number of sites that passed the filtering was 826,649,529 in the human genome. Bi-allelic polymorphic sites with

high-confidence ancestral allele inference, according to 1000GP annotations, were used. To avoid the effect of positive selection, high frequency mutations were excluded, and the truncated SFS was used to infer population size history (fig. S25 and table S17). The average proportion of excluded high frequency SNPs of all populations in 1000GP was 4.40%.

To verify the results, remote non-coding regions were re-analyzed. These regions were at least 10kb away from coding regions (fig. S23). In these cases, the 1000 GP strict mask was not used.

HGDP-CEPH data

HGDP-CEPH data are whole genome sequencing data obtained from the Human Genome Diversity Project (HGDP) of the Centre d'Étude du Polymorphisme Humain (CEPH) (*24*) (table S2). Populations with more than 15 individuals each were examined. In total, 24 populations in the HGDP-CEPH panel were analyzed, including three African populations (Biaka, Mandeka, and Yoruba), five European populations (Adygei, Basque, French, Russian, and Sardinian), four Middle East populations (Bedouin, Druze, Mozabite, and Palestinian), three East Asian populations (Han, Japanese, and Yakut), eight Central and South Asian populations (Balochi, Brahui, Burusho, Hazara, Kalash, Makrani, Pathan, and Sindhi), and one American population (Maya) (tables S4 and S6). Only bi-allelic SNPs in GENCODE non-coding regions (*60*) except pseudogenes that passed HGDP-CEPH filtering were used. HGDP-CEPH accessible mask was also used to filter SNPs (*24*). The number of sites that passed the filtering was 791,999,125 in the human genome. Missing data were allowed to avoid artifacts due to imputation. The proportion of sites with two or more missing individuals was less than 3% for all populations (table S18). Each population had two SFSs, with one calculated from sites with no missing data, and the other from sites with one missing individual (figs. S26 and S27, and table S19). Truncated SFSs were used to avoid the effect of positive selection. The average proportion of excluded high frequency SNPs of all 24 populations was 7.18%.

To confirm the ancient severe bottleneck, two South African populations (San and BantuSouthAfrica) were analyzed. These two populations were excluded in formal analyses (table S4) because of small sample sizes (6 and 8 individuals, respectively). To verify the results, all other 24 populations were re-analyzed, and remote non-coding regions were also examined (fig. S23). For these cases, HGDP-CEPH accessible mask was not applied.

FitCoal inference for the recent and ancient human population size histories

In this study, 200 repeats ($K = 200$) were performed to maximize the likelihood and analyze observed human SFSs. To estimate the recent and ancient human population size histories, it was assumed that a generation time was 24 years (*6, 20*) and that the mutation rate was 1.2×10^{-8} per site per generation (*6, 21, 58, 59*). The recent population size histories indicate the dynamic of population size since the emergence of modern humans (*1-3*).

Stairway Plot, PSMC, SMC++, and Relate population size inference

The default parameters of Stairway Plot (*6*), PSMC (*7*), SMC++ (*8*), and Relate (*27*) were applied when analyzing the genetic data of African YRI population in 1000GP and African Yoruba population in the HGDP-CEPH panel, and using simulated data to infer population size

histories. Because Relate requires phased data, SHAPEIT (*61*) and IMPUTE2 (*62*) were used to phase and impute missing genotypes of Yoruba population. To avoid potential influence of phasing and imputation errors, this phased and imputed data was only used in Relate estimation, and the original Yoruba data was used in Stairway Plot, PSMC, and SMC++ analyses.

YRI genetic map (*63*) was used when estimating Relate population size histories for the two African populations. Simulated data were analyzed under a uniform recombination rate.

Models and corresponding simulation commands in Fig. 2

All scripts are provided in the supplementary files. Unless otherwise specified, the default mutation rate μ was 1.2×10^{-8} per base per generation, and the recombination rate was $r = 0.8\mu$. The generation time was 24 years. All models were simulated with 200 replications using the software msprime (*57*).

1. Constant size model

The effective population size was assumed to be 10,000, and 30 sequences of 10 Mb each were simulated.

2. Instantaneous increase model

This model was used to mimic the demography of an African population (*64*) with the following assumptions: ancient population size, 7,778; current population size, 25,636; and instantaneous population increase occurred 6,809 generations ago. 30 sequences of 10 Mb each were simulated.

3. Bottleneck model

This model was based on the "standard simulation" model in PSMC publication (*7*). 170 sequences of 30Mb each were simulated.

4. Exponential growth model I

Current population size of 50,000 and a growth rate $r = 0.004$ were assumed. 30 sequences of 10 Mb each were simulated.

5. Exponential growth model II

This model was used to mimic the demography of a European population (*12*) with the following parameters: ancient population size 1,000, current population size 29,525, and exponential population growth occurred 848 generations ago. 30 sequences of 10 Mb each were simulated.

6. Exponential growth model III

In this model, the ancient population size was assumed to be 8,000 with instantaneous population decrease to 7,900 followed by an exponential growth to 900,000. 170 sequences of 10 Mb each were simulated.

Models and corresponding simulation commands in Fig. 4 and fig. S28

Unless otherwise specified, the default mutation rate μ was 1.2×10^{-8} per base per generation, and the recombination rate was $r = 0.8\mu$. The generation time was 24 years. All models were simulated with 200 replications using the software msprime (*57*). For each replication, 800 Mb data was generated by simulating 8 DNA fragments of 100 Mb in length.

1. Bottleneck I model

This model was used to mimic the demography of African populations. The ancient population size was assumed to be 93,000. It was also assumed that the population experienced

an instantaneous decrease to 1,300 around 38,000 generations ago and instantaneous growth to 27,000 around 33,000 generations ago, followed by an exponential growth to 82,000 around 1000 generations ago. The sample size was 188 sequences.

2. Bottleneck II model

This model was used to mimic the FitCoal inferred demography of non-African populations. The ancient population size was assumed to be 20,000. It was also assumed that the population experienced an exponential decrease to 7,500 around 15,000 generations ago and an exponential growth to 120,000 around 1,000 generations ago. The sample size was 194 sequences.

3. Bottleneck III model

This model was used to mimic the demography of non-African populations. The ancient population size was assumed to be 93,000. It was also assumed that the population experienced an instantaneous decrease to 1,300 around 38,000 generations ago and an instantaneous growth to 27,000 around 33,000 generations ago, followed by an exponential decline to 7,500 around 19,284 generations ago and then an instantaneous increased to 120,000 around 1,000 generations ago. The sample size was 194 sequences.

4. Bottleneck IV model

This model was used to mimic a slow size reduction starting 1.5 million years ago in African populations. The ancient population size was assumed to be 93,000. It was also assumed that the population experienced an exponential decrease to 1,300 around 62,500 generations ago and an instantaneous growth to 27,000 around 33,000 generations ago, followed by an exponential growth to 82,000 around 1000 generations ago. The sample size was 188 sequences.

5. Bottleneck V model

This model was used to mimic an ancient moderate bottleneck in African populations. The ancient population size was assumed to be 93,000. It was also assumed that the population experienced an instantaneous decrease to 3,000 around 38,000 generations ago and an instantaneous growth to 27,000 around 33,000 generations ago, followed by an exponential growth to 82,000 around 1000 generations ago. The sample size was 188 sequences.

6. Bottleneck VI model

This model was used to mimic an ancient mild bottleneck of African populations. The ancient population size was assumed to be 93,000. It was also assumed that the population experienced an instantaneous decrease to 13,000 around 38,000 generations ago and an instantaneous growth to 27,000 around 33,000 generations ago, followed by an exponential growth to 82,000 around 1000 generations ago. The sample size was 188 sequences.

<u>Models and corresponding simulation commands in figs. S3, S29, and S30</u>

Unless otherwise specified, the default mutation rate μ was 1.2×10^{-8} per base per generation, and the recombination rate was $r = 0.8\mu$. The generation time was 24 years. All models were simulated with 200 replications using *ms* (*55*) or MaCS (*56*). The time was scaled by $4N_0$ generations, and the population size was scaled by N_0 as required by the simulation software.

1. Constant size model (figs. S3A, S29A, and S30A)

The effective population size was assumed to be 10,000, and 30 sequences of 10 Mb each were simulated. The corresponding *ms* command is

ms 30 200 -t 4800 -r 3800 10000000

2. Instantaneous increase model (figs. S3B, S29B, and S30B)

This model was used to mimic the demography of an African population (*64*). It was also assumed that the ancient population size was 7,778, the current population size was 25,636 and that the population began an instantaneous increase around 6,809 generations ago. 30 sequences of 10 Mb each were simulated. The corresponding ms command for the simulation is

ms 30 200 -t 12310 -r 9750 10000000 -eN 0.066 0.3

3. Bottleneck model (figs. S3C, S29C, and S30C)

This model was based on the "standard simulation" model described previously (*7*). 170 sequences of 30Mb each were simulated. The corresponding MaCS command for this simulation is

macs 170 30000000 -i 200 -h 1e3 -t 0.002732 -r 0.002179 -h 1e3 -eN 0.01 0.05 -eN 0.0375 0.5 -eN 1.25 1

4. Exponential growth model I (figs. S3D, S29D, and S30D)

The current population size was assumed to be 50,000, and the growth rate was $r = 0.004$. 30 sequences of 10 Mb each were simulated. The corresponding *ms* command for the simulation is

ms 30 200 -t 24000 -r 19000 10000000 -G 800

5. Exponential growth model II (figs. S3E, S29E, and S30E)

This model was used to mimic the demography of a European populations (*12*). It was also assumed that the ancient population size was 1,000, that the current population size was 29,525, and that the population began exponential growth around 848 generations ago. 30 sequences of 10 Mb each were simulated. The corresponding *ms* command for the simulation is

ms 30 200 -t 14172 -r 10629 10000000 -G 472.4 -eN 0.00718 0.0339

6. Exponential growth model III (figs. S3F, S29F, and S30F)

The ancient population size was assumed to be 8,000. It was also assumed that the population experienced an instantaneous decrease to 7,900, followed by an exponential growth to 900,000. 30 sequences of 10 Mb each were simulated. The corresponding *ms* command for the simulation is

ms 170 200 -t 432000 -r 340000 10000000 -G 46368 -eN 0.0001027 0.008889

<u>Models and corresponding simulation commands in figs. S4 and S31</u>

Unless otherwise specified, the default mutation rate μ was 1.2×10^{-8} per base per generation, and the recombination rate was $r = 0.8\mu$. The generation time was 24 years. All models were simulated with 200 replications using *ms* (*55*) or MaCS (*56*). The time was scaled by $4N_0$ generations, and the population size was scaled by N_0 as required by the simulation software.

1. PSMC "sim-YH" model (figs. S4A and S31A)

This model is the same as that described previously (*7*). 170 sequences of 30 Mb each were simulated. The corresponding MaCS command for the simulation is

macs 170 30000000 -i 200 -h 1e3 -t 0.002171 -r 0.001731 -eN 0.0055 0.0832 -eN 0.0089 0.0489 -eN 0.0130 0.0607 -eN 0.0177 0.1072 -eN 0.0233 0.2093 -eN 0.0299 0.3630 -eN 0.0375 0.5041 -eN 0.0465 0.5870 -eN 0.0571 0.6343 -eN 0.0695 0.6138 -eN 0.0840 0.5292 -eN 0.1010 0.4409 -eN 0.1210 0.3749 -eN 0.1444 0.3313 -eN 0.1718 0.3066 -eN 0.2040 0.2952 -eN 0.2418 0.2915 -eN 0.2860 0.2950 -eN 0.3379 0.3103 -eN 0.3988 0.3458 -eN 0.4701 0.4109 -eN 0.5538 0.5048 -eN 0.6520 0.6520 -eN 0.7671 0.6440 -eN 0.9020 0.6178 -eN 1.0603 0.5345 -eN 1.4635 1.7931

2. PSMC “sim-1” model (figs. S4B and S31B)

This model is also the same as that described previously (*7*). 170 sequences of 30 Mb each were simulated. The corresponding MaCS command for the simulation is

macs 170 30000000 -i 200 -h 1e3 -t 0.001 -r 0.0008 -eN 0.01 0.1 -eN 0.06 1 -eN 0.2 0.5 -eN 1 1 -eN 2 2

3. PSMC “sim-2” model (figs. S4C and S31C)

This model is the same as that described previously (*7*). 170 sequences of 30 Mb each were simulated. The corresponding MaCS command for the simulation is

macs 170 30000000 -i 200 -h 1e3 -t 0.0001 -r 0.00008 -eN 0.1 5 -eN 0.6 20 -eN 2 5 -eN 10 10 -eN 20 5

4. PSMC “sim-3” model (figs. S4D and S31D)

This model is the same as that described previously (*7*). 170 sequences of 30 Mb each were simulated. The corresponding MaCS command for the simulation is

macs 170 30000000 -i 200 -h 1e3 -t 0.002 -r 0.0016 -eN 0.01 0.05 -eN 0.0150 0.5 -eN 0.05 0.25 -eN 0.5 0.5

5. Complicated model III (figs. S4E and S31E)

The ancient population size was assumed to be 4,167. It was also assumed that the population experienced an instantaneous increase to 20,833 around 33,333 generations ago and an instantaneous decrease to 2,083 around 2,500 generations ago, followed by an instantaneous increase to 41,667 around 833 generations ago. 170 sequences of 30 Mb each were simulated. The corresponding MaCS command for the simulation is

macs 170 30000000 -i 200 -h 1e3 -t 0.002 -r 0.0016 -eN 0.005 0.05 -eN 0.0150 0.5 -eN 0.2 0.1

6. Complicated model II (figs. S4F and S31F)

The ancient population size was assumed to be 1,250. It was also assumed that the population experienced an instantaneous increase to 33,333 around 33,333 generations ago, an instantaneous decrease to 12,500 around 16,667 generations ago, an instantaneous increase to 20,833 around 8,333 generations ago, an instantaneous decrease to 8,333 around 4,167 generations ago, an instantaneous decrease to 2,083 around 1,667 generations ago, and an instantaneous increase to 41,667 around 833 generations ago. 170 sequences of 30 Mb each were simulated. The corresponding MaCS command for the simulation is

macs 170 30000000 -i 200 -h 1e3 -t 0.002 -r 0.0016 -eN 0.005 0.05 -eN 0.01 0.2 -eN 0.0250 0.5 -eN 0.05 0.3 -eN 0.1 0.8 -eN 0.2 0.03

7. Exponential growth model IV (figs. S4G and S31G)

The ancient population size was assumed to be 20,000. It was also assumed that the population experienced an instantaneous decrease to 1,000 around 4,000 generations ago, and an exponential growth to 20,000 around 2,000 generations ago. 170 sequences of 30 Mb each were simulated. The corresponding MaCS command for the simulation is

macs 170 30000000 -i 200 -h 1e3 -t 0.001 -r 0.0008 -G 120 -eG 0.025 0 -eN 0.05 1

8. Exponential growth model V (figs. S4H and S31H)

The ancient population size was assumed to be 15,000. It was also assumed that the population experienced an instantaneous decrease to 6,000 around 4,000 generations ago, and an exponential growth to 30,000 around 2,000 generations ago. 170 sequences of 30 Mb each were simulated. The corresponding MaCS command for the simulation is

macs 170 30000000 -i 200 -h 1e3 -t 0.00144 -r 0.00115 -G 96.37 -eG 0.0167 0 -eN 0.033 0.5

9. Exponential growth model VI (figs. S4I and S31I)

The ancient population size was assumed to be 15,000. It was also assumed that the population experienced an exponential decrease to 6,000 around 5,000 generations ago, and an exponential growth to 30,000 around 2,000 generations ago. 170 sequences of 30 Mb each were simulated. The corresponding ms command for the simulation is

ms 170 200 -t 43200 -r 34560 30000000 -G 96.56627474604602 -eG 0.01666666666667 -36.65162927 -eN 0.0416666666667 0.5

Models for studying influence factors of FitCoal in fig. S2

Unless otherwise specified, the default mutation rate μ was 1.2×10^{-8} per base per generation, and the recombination rate was $r = 0.8\mu$. All models were simulated with 200 replications using *ms* (*55*) or MaCS (*56*). The time was scaled by $4N_0$ generations and the population size was scaled by N_0 as required by the simulation software.

Variations of the Exponential growth model V were simulated by increasing or decreasing the number of sequences, length of sequences, and recombination rate as follows:

1. Number of sequence *n* = 170, sequence length *L* = 1 Mb, recombination rate $\rho = 0.8\mu$ (fig. S2A). The corresponding *ms* command for the simulation is

   ms 170 1 -t 1440 -r 1152 1000000 -G 96.56627474604602 -eN 0.016666666666666666 0.2 -eN 0.03333333333333333 0.5
2. Number of sequence *n* = 170, sequence length *L* = 10 Mb, recombination rate $\rho = 0.8\mu$ (fig. S2B). The corresponding *ms* command for the simulation is

   ms 170 10 -t 1440 -r 1152 1000000 -G 96.56627474604602 -eN 0.016666666666666666 0.2 -eN 0.03333333333333333 0.5
3. Number of sequence *n* = 170, sequence length *L* = 100 Mb, recombination rate $\rho = 0.8\mu$ (figs. S2C, S2F, and S2H). The corresponding *ms* command for the simulation is

   ms 170 100 -t 1440 -r 1152 1000000 -G 96.56627474604602 -eN 0.016666666666666666 0.2 -eN 0.03333333333333333 0.5
4. Number of sequence *n* = 10, sequence length *L* = 100 Mb, recombination rate $\rho = 0.8\mu$ (fig. S2D). The corresponding *ms* command for the simulation is

   ms 10 100 -t 1440 -r 1152 1000000 -G 96.56627474604602 -eN 0.016666666666666666 0.2 -eN 0.03333333333333333 0.5
5. Number of sequence *n* = 100, sequence length *L* = 100 Mb, recombination rate $\rho = 0.8\mu$ (fig. S2E). The corresponding *ms* command for the simulation is

   ms 100 100 -t 1440 -r 1152 1000000 -G 96.56627474604602 -eN 0.016666666666666666 0.2 -eN 0.03333333333333333 0.5
6. Number of sequence *n* = 170, sequence length *L* = 100 Mb, recombination rate $\rho = 0.1\mu$ (fig. S2G). The corresponding *ms* command for the simulation is

   ms 170 100 -t 1440 -r 144 1000000 -G 96.56627474604602 -eN 0.016666666666666666 0.2 -eN 0.03333333333333333 0.5
7. Number of sequence *n* = 170, sequence length *L* = 100 Mb, recombination rate $\rho = 10\mu$ (fig. S2I). The corresponding *ms* command for the simulation is

   ms 170 100 -t 1440 -r 14400 1000000 -G 96.56627474604602 -eN 0.016666666666666666 0.2 -eN 0.03333333333333333 0.5

Models for investigating the ancient severe bottleneck in figs. S9 and S10

The default mutation rate μ was 1.2×10^{-8} per base per generation, and the recombination rate was $r = 0.8\mu$. All models were simulated with 200 replications using *ms* (*55*) or MaCS (*56*). For each replication, 800 Mb data was generated by simulating 80,000 sequences of 10 kb in length.

For 1000GP populations (fig. S9), recent population expansion parameters of YRI and CHB were used for African and non-African population, respectively. Average values of parameters inferred from African and non-African populations were used. The models used were the same as those models in Figs. 4A, 4B, and 4C.

For HGDP-CEPH populations (fig. S10), recent population expansion parameters of Yoruba and Han were used for African and non-African population, respectively. Average values of parameters inferred from African, except Biaka, and non-African populations were used. As the Biaka, a hunter-gatherer population, was found to have a recent population decline and a relatively large population size after the ancient severe bottleneck was relieved, this population was not considered in building the recent demographic model.

1. Bottleneck model for HGDP-CEPH populations (fig. S10A)

This model was used to mimic the demography of African populations. The ancient population size was assumed to be 120,000. It was assumed that the population experienced an instantaneous decrease to 1,400 around 41,000 generations ago, an instantaneous growth to 28,000 around 35,000 generations ago, and another instantaneous growth to 50,000 around 500 generations ago. 44 sequences of 800 Mb each were simulated. The corresponding *ms* command for the simulation is

ms 44 80000 -t 24 -r 19.19 10000 -eN 0.0025 0.56 -eN 0.17500000000000002 0.028 -eN 0.205 2.4

2. Bottleneck model for HGDP-CEPH (fig. S10B)

This model was used to mimic the inferred population size history of non-African populations. The ancient population size was assumed to be 21,000. It was assumed that the population experienced an exponential decrease to 6,000 around 20,000 generations ago, and an exponential growth to 300,000 around 1,000 generations ago. 56 sequences of 800 Mb each were simulated. The corresponding *ms* command for the simulation is

ms 56 80000 -t 144 -r 115.19 10000 -G 4694.427606513776 -eN 8.333333333333333E-4 0.02 -eG 8.333333333333333E-4 -79.1218716944443 -eN 0.016666666666666666 0.07

3. Bottleneck model for HGDP-CEPH (fig. S10C)

This model was used to mimic the real demography of non-African populations. The ancient population size was assumed to be 120,000. It was also assumed that the population experienced an instantaneous decrease to 1,400 around 41,000 generations ago, and an instantaneous growth to 25,000 around 35,000 generations ago, followed by an exponential decline to 6,000 around 24,363 generations ago and an instantaneous increased to 300,000 around 1,000 generations ago. 56 sequences of 800 Mb each were simulated. The corresponding *ms* command for the simulation is

ms 56 80000 -t 144 -r 115.19 10000 -G 4694.427606513776 -eN 8.333333333333333E-4 0.02 -eG 8.333333333333333E-4 -79.12228948065652 -eN 0.0203025 0.09333333333333334 -eN 0.029166666666666667 0.004666666666666667 -eN 0.034166666666666665 0.4

Models and corresponding simulation commands in fig. S32

Unless otherwise specified, the default mutation rate μ was 1.2×10^{-8} per base per generation, and the recombination rate was $r = 0.8\mu$. The generation time was 24 years. All models were simulated with 200 replications using *ms* (*55*) or MaCS (*56*). The time was scaled by $4N_0$ generations, and the population size was scaled by N_0 as required by the simulation software.

1. Split model I (fig. S32A)

This model was used to mimic the split demography of African hunter-gatherer and agriculturist populations. The ancient population size was assumed to be 20,833. It was also assumed that the ancient population split into two subpopulations around 6,667 generations ago, that the first population experienced an instantaneous increase to 41,667 around 500 generations ago, and that the second population experienced an instantaneous decline to 8,333 around 1,250 generations ago. 170 sequences of 30 Mb each were simulated. The corresponding MaCS command for the simulation is

macs 340 30000000 -i 1 -h 1e3 -t 0.002 -r 0.0016 -I 2 170 170 4 -n 2 0.2 -en 0.003 1 0.5 -en 0.0075 2 0.5 -ej 0.04 2 1

2. Split model II (fig. S32B)

This model was used to mimic the split demography of African and European populations and was based on the following assumptions: the ancient population size was 20,833 and split into two subpopulations around 5,000 generations ago, the size of the first population declined to 83,303 followed by an instantaneous increase to 20,833 around 833 generations ago, and the second population had an instantaneous increase to 41,667 around 500 generations ago. 170 sequences of 30 Mb each were simulated. The corresponding MaCS command for the simulation is

macs 340 30000000 -i 1 -h 1e3 -t 0.004 -r 0.0032 -I 2 170 170 4 -n 2 0.5 -en 0.0015 2 0.25 -en 0.0025 1 0.1 -ej 0.015 1 2

3. Split model III (fig. S32C)

The ancient population size was assumed to be 4,167. It was also assumed that the ancient population experienced an instantaneous growth to 20,833 around 8,333 generations ago and split into two subpopulations around 2,500 generations ago. The size of the first population decreased to 2,083 around 1,666 generations ago and increased to 20,833 around 833 generations ago. The size of the second population remained constant. 170 sequences of 100 Mb each were simulated. The corresponding MaCS command for the simulation is

macs 340 1000000 -i 100 -h 1e3 -t 0.001 -r 0.0008 -I 2 170 170 4 -eN 0 1 -en 0.01 1 0.1 -en 0.02 1 1 -ej 0.03 2 1 -eN 0.10 0.2 -eN 1 1

Models and corresponding simulation commands in fig. S33

Coalescent trees ($n = 10$) were simulated with 1,000,000 replications using the software *ms* (*55*) to calculate the average branch length for each SFS type (category). The time was scaled by $4N_0$ generations, and the population size was scaled by N_0 as required by the simulation software.

1. Constant size model (fig. S33A)

The corresponding ms command is

ms 10 1000000 -L -T

2. Exponential growth model (fig. S33B)

The scaled ancient population size was assumed to be 0.5. The population began an exponential growth to the current scaled size of 1.0 when the time was 0.17328679513998632. The corresponding *ms* command is

ms 10 1000000 -G 4.0 -eN 0.17328679513998632 0.5 -L -T

3. Bottleneck model (fig. S33C)

The scaled population size was 1.0 when the time was between 0 and 0.1, and a scaled population size was 0.5 when the time was between 0.1 and 0.25. The corresponding *ms* command is

ms 10 1000000 -eN 0.1 0.5 -eN 0.25 1.0 -L -T

4. Complex model (fig. S33D)

The scaled ancient population size was assumed to be 0.5. The population experienced a bottleneck with the scaled population size decreased to 0.2 when the time was between 0.11465735902799726 to 0.08465735902799726 and then exponentially increased to the scaled current size of 1.0. The corresponding *ms* command for the simulation is

ms 10 1000000 -G 20.0 -eN 0.03465735902799726 0.5 -eN 0.08465735902799726 0.2 -eN 0.11465735902799726 0.5 -L –T

Models and corresponding simulation commands in table S13

To ensure the accuracy of FitCoal, the expected branch length of FitCoal ($n = 10$) was compared with that determined with Živković-Wiehe's method (*17*). The time was scaled by $4N_0$ generations, and the population size was scaled by N_0 as required by Živković-Wiehe's method.

1. Constant size model

The corresponding input parameters of Živković-Wiehe's method are

unfoldedfreq[10, 0.0, 0.0, 1.0, 1.0]

2. Instantaneous growth model

It was assumed that the current population size was 1.0. The scaled population size was decreased instantaneously to 0.5 at the time of 0.5. The corresponding input parameters of Živković-Wiehe's method are

unfoldedfreq[10, 0.5, 0.0, 0.5, 0.5]

3. Bottleneck model

The scaled population size was assumed to be 1.0 when the time was between 0 and 0.1. The scaled population size was 0.5 when the time was between 0.1 and 0.25. The scaled ancestral population size was 1.0. The corresponding input parameters of Živković-Wiehe's method are

unfoldedfreq[10, 0.2, 0.6, 0.5, 1]

Simulation commands for determination of confidence intervals in figs. S34 – S44

The default mutation rate μ was 1.2×10^{-8} per base per generation, and the recombination rate was $r = 0.8\mu$. All models were simulated with 200 replications using *ms* (*55*) or MaCS (*56*). For each replication, 800 Mb data were generated by simulating 80,000 sequences of 10 kb each.

The inferred demographic parameters of various populations in the 1000GP dataset were provided in the command lines (figs. S34 – S38):

ACB:

ms 192 80000 -t 37.725120000000004 -r 30.180096000000002 10000 -G 307.97400639367373 -eN 0.0033742698361377437 0.35374201592996923 -eN 0.10237507717670723 0.012990813548107999 -eN 0.1132253281877044 0.9123469984986132

ASW:

ms 122 80000 -t 26.50224 -r 21.201792 10000 -G 56.10026737541272 -eN 0.01390929179691329 0.4582616412801333 -eN 0.1538498233982067 0.013891655950591346 -eN 0.16560167778269375 1.3718870555847353

BEB:

ms 172 80000 -t 62.65536 -r 50.124288 10000 -G 1215.8971532452542 -eN 0.0023403111314833293 0.058100695614868386 -eG 0.0023403111314833293 -30.907477873075123 -eN 0.03371108514231231 0.15320381209205405

CDX:

ms 186 80000 -t 25.248 -r 20.1984 10000 -G 495.40037108442965 -eN 0.004604646549934852 0.10216730038022814 -eG 0.004604646549934852 -17.489419084798488 -eN 0.0835118490009135 0.4061216730038023

CEU:

ms 198 80000 -t 76.50768000000001 -r 61.206144 10000 -G 3486.9981711123683 -eN 8.189396733027973E-4 0.057518931432765964 -eN 0.01896877424771246 0.1280749854132291

CHB:

ms 206 80000 -t 148.45488 -r 118.763904 10000 -G 7477.99792685936 -eN 5.168378866508531E-4 0.020964753735276336 -eN 0.006336402867008054 0.06404208470614102

CHS:

ms 210 80000 -t 87.9024 -r 70.32192 10000 -G 4112.853998070424 -eN 8.149360963103421E-4 0.03502429967782449 -eN 0.011161187141954527 0.1114290394801507

CLM:

ms 188 80000 -t 26.05104 -r 20.840832 10000 -eN 0.006899708256449607 0.17470933981906286 -eN 0.04654813479653858 0.35472518563558303

ESN:

ms 198 80000 -t 32.99376 -r 26.395008 10000 -G 1399.7970544542743 -eN 6.732730258474137E-4 0.38967368375110933 -eN 0.11907424073256923 0.025241136505812008 -eN 0.14645778743979765 1.6907342479305179

FIN:

ms 198 80000 -t 21.88368 -r 17.506944 10000 -G 1545.9307685858762 -eN 0.0010069648928517855 0.21083108508258208 -eN 0.079627651288076 0.4667149218047421

GBR:

ms 182 80000 -t 68.96448 -r 55.171584 10000 -G 4780.2465803320365 -eN 4.8660205464359964E-4 0.09767810907876055 -eG 4.8660205464359964E-4 299.83121839376906 -eN 0.0026469357311387233 0.051108048665051926 -eG 0.0026469357311387233 -38.53061553796807 -eN 0.02777287031733699 0.1345666638826248

GIH:

ms 206 80000 -t 22.5384 -r 18.03072 10000 -G 319.3657263289911 -eN 0.005331789062104143 0.18217442231924183 -eG 0.005331789062104143 -7.108545561599834 -eN 0.1312801904940001 0.4459801938025769

GWD:

ms 226 80000 -t 71.53488 -r 57.227904 10000 -G 2480.4594823364796 -eN 6.955466408858352E-4 0.17812401446678877 -eN 0.055221144353749266 0.008796827505686736 -eN 0.06446476441787029 0.7480725486643718

IBS:

ms 214 80000 -t 101.40288 -r 81.122304 10000 -G 3879.3899843730937 -eN 7.379412692860351E-4 0.05711080395349718 -eN 0.001639355380662806 0.03441322376642557 -eG 0.001639355380662806 -55.51532072601329 -eN 0.019312961005874058 0.09179857613511569

ITU:

ms 204 80000 -t 45.81072 -r 36.648576 10000 -G 942.7096023053382 -eN 0.002494089782323459 0.09525456050461552 -eN 0.026664885830212617 0.2086358826056434

JPT:

ms 208 80000 -t 55.95024 -r 44.760192 10000 -G 3128.7376262633884 -eN 8.114087494514677E-4 0.07897017063733774 -eN 0.002182047525463559 0.04600945411494213 -eG 0.002182047525463559 -42.38616087573135 -eN 0.03372169017138904 0.17515849797963332

KHV:

ms 198 80000 -t 57.9072 -r 46.32576 10000 -G 1588.3658354039515 -eN 0.0019264561851523535 0.04689157824933687 -eG 0.0019264561851523535 -36.60290382061524 -eN 0.03792001517437307 0.17509118037135277

LWK:

ms 198 80000 -t 21.33888 -r 17.071104000000002 10000 -G 34.458048510849686 -eN 0.014319371341156495 0.6105362605722512 -eN 0.18803659662764166 0.02145942055065683 -eN 0.20879409785416014 2.0908763721432426

MSL:

ms 170 80000 -t 21.25872 -r 17.006976 10000 -G 127.20491855898698 -eN 0.003279354257615819 0.6589220799747115 -eN 0.18195660752091394 0.04585788796315112 -eN 0.2357981142165514 2.9051457472510105

MXL:

ms 128 80000 -t 72.2232 -r 57.77856 10000 -G 1185.9983336956855 -eN 0.0025552519587115612 0.04829030006978367 -eG 0.0025552519587115612 -35.997766981810344 -eN 0.030770096213141897 0.13333997939720202

PEL:

ms 170 80000 -t 104.52432 -r 83.619456 10000 -G 2449.33558491349 -eN 0.0014410414433505075 0.029316813541575778 -eN 0.01066574560965878 0.0949030809289168 3

PJL:

ms 192 80000 -t 40.10544 -r 32.084352 10000 -G 658.1508823918153 -eN 0.003516549012580939 2 0.09882350125070315 -eG 0.003516549012580939 2 -14.935034208218648 -eN 0.06458715193043525 0.2460234821011813

PUR:

ms 208 80000 -t 23.60832 -r 18.886656 10000 -eN 0.0038497802945414656 0.6750365972674041 -eN 0.014388104698224359 0.1546437865972674 -eG 0.014388104698224359 -15.582101828279491 -eN 0.07286054886643582 0.3846169486011711

STU:

ms 204 80000 -t 34.572 -r 27.657600000000002 10000 -G 510.43071934664556 -eN 0.004267252624293807 0.11325234293648039 -eN 0.02525451461678291 0.2616869142658799

TSI:

ms 214 80000 -t 75.82608 -r 60.660864000000004 10000 -G 2569.467980386571 -eN 0.0011371059177742527 0.05383899576504548 -eG 0.0011371059177742527 -19.704497360903815 -eN 0.04986270865479367 0.14062707712175018

YRI:

ms 216 80000 -t 64.91088 -r 51.928704 10000 -G 4776.570655987927 -eN 3.3888995289779744E-4 0.19814983250881826 -eN 0.0625962626099122 0.007882807936050167 -eN 0.06835272805758985 0.4330589879539455

The inferred demographic parameters of various populations in the HGDP-CEPH panel were provided in the command lines (figs. S39 to S44):

Adygei:

ms 32 80000 -t 19.19712 -r 15.357696 10000 -eN 0.005250411630207267 0.19837975696354454 -eG 0.005250411630207267 -8.596593090355556 -eN 0.11548669953457971 0.5117517627644147

Balochi:

ms 48 80000 -t 50.949600000000004 -r 40.75968 10000 -G 623.264941916954 -eN 0.004223024540924805 0.0719299072024118 -eG 0.004223024540924805 -32.99343443398211 -eN 0.032825823542035906 0.18482264826416694

Basque:

ms 46 80000 -t 26.153760000000002 -r 20.923008 10000 -G 751.4700408942055 -eN 0.0025016313707249523 0.15260520858186355 -eG 0.0025016313707249523 -8.224106050612061 -eN 0.1199670757097625 0.40097637968689775

Bedouin:

ms 92 80000 -t 36.622080000000004 -r 29.297664 10000 -G 244.38587570241546 -eN 0.008841200644961786 0.11524850581944007 -eG 0.008841200644961786 -16.31003863953942 -eN 0.05738997874929217 0.2544039005976722

Biaka:

ms 44 80000 -t 4.5912 -r 3.6729600000000002 10000 -eN 0.009592435429723692 3.6935703084161005 -eN 0.9319760745921495 0.09492943021432305 -eG 0.9319760745921495 -11.520947944349727 -eN 1.3098356260554107 7.379299529534762

Brahui:

ms 50 80000 -t 36.26112 -r 29.008896 10000 -G 372.4275509762127 -eN 0.006063547988128193 0.10453510536905644 -eG 0.006063547988128193 -20.411278092113488 -eN 0.05182198032003567 0.26600391824632

Burusho:

ms 48 80000 -t 11.5464 -r 9.23712 10000 -eN 0.015366836965198416 0.29627935980045733 -eG 0.015366836965198416 -8.16350928074288 -eN 0.1408168183093884 0.8250259821242986

Druze:

ms 84 80000 -t 16.18944 -r 12.951552 10000 -G 109.07256817628162 -eN 0.01288215226934864 0.24534511385199242 -eG 0.01288215226934864 -7.35809820577746 -eN 0.13234063031350007 0.5909037001897534

French:

ms 56 80000 -t 79.18416 -r 63.347328000000005 10000 -G 2198.9359820452387 -eN 0.001348902384433904 0.051501209332775646 -eG 0.001348902384433904 -24.36290322377743 -eN 0.03939915284814332 0.13014117975110173

Han:

ms 86 80000 -t 159.24816 -r 127.398528 10000 -G 5363.756025025552 -eN 7.370989032405503E-4 0.0191851510246649 -eN 0.005252449909354633 0.05743488653181299

Hazara:

ms 38 80000 -t 12.69792 -r 10.158336 10000 -eN 0.014217614003750299 0.25629394420503515 -eG 0.014217614003750299 -9.884907873225844 -eN 0.12245692270731047 0.7471459892643834

Japanese:

ms 54 80000 -t 33.88464 -r 27.107712 10000 -G 636.5261153273832 -eN 0.004000435354218995 0.07836471038204922 -eG 0.004000435354218995 -26.629980477176918 -eN 0.0528258276856906 0.2876064198999901

Kalash:

ms 44 80000 -t 3.04608 -r 2.436864 10000 -G -2.415743522809092 -eN 0.47028502523586235 3.1145603529782537

Makrani:

ms 50 80000 -t 24.11088 -r 19.288704 10000 -eN 0.00980388240380426 0.14526885787661006 -eG 0.00980388240380426 -17.111271203295853 -eN 0.06723955104118398 0.388146761959746

Mandenka:

ms 44 80000 -t 13.10688 -r 10.485504 10000 -eN 0.3296277261231593 0.048304401962938545 -eG 0.3296277261231593 -17.85185708722175 -eN 0.5825077171252933 4.411191679484362

Maya:

ms 42 80000 -t 16.673280000000002 -r 13.338624000000001 10000 -eN 0.008589230112361738 0.09687356057116536 -eG 0.008589230112361738 -25.14802627151756 -eN 0.08111110798113147 0.600155458314141

Mozabite:

ms 54 80000 -t 17.42304 -r 13.938432 10000 -G 34.034495761040134 -eN 0.03302787085100088 0.32494903300457323 -eG 0.03302787085100088 -4.504618045303915 -eN 0.1472698871889101 0.543638767976197

Palestinian:

ms 92 80000 -t 22.33968 -r 17.871744 10000 -eN 0.008844463035145432 0.1913151844610129 -eG 0.008844463035145432 -7.866119095624621 -eN 0.11128708520369861 0.4282675490427795

Pathan:

ms 48 80000 -t 42.96432 -r 34.371456 10000 -G 497.59849646988573 -eN 0.005312881946315924 0.07109899563172419 -eG 0.005312881946315924 -47.5703288285576 -eN 0.02861662601453915 0.21543085052899708

Russian:

ms 50 80000 -t 22.14048 -r 17.712384 10000 -G 258.609263568537 -eN 0.006473721471777433 0.1874647704114816 -eN 0.047392730886604 0.4300394571391406

Sardinian:

ms 56 80000 -t 19.90512 -r 15.924096 10000 -G 209.67966756103402 -eN 0.008361464215634221 0.17321372591574427 -eG 0.008361464215634221 -11.622404927783043 -eN 0.09674763618341507 0.48385541006535

Sindhi:

ms 48 80000 -t 28.07088 -r 22.456704000000002 10000 -eN 0.006697787857121225 0.12812708401019132 -eG 0.006697787857121225 -17.75301871013936 -eN 0.06131324436460199 0.33785331988167094

Yakut:

ms 50 80000 -t 10.99008 -r 8.792064 10000 -G 107.01050381191519 -eN 0.010397096462590117 0.32870370370370366 -eN 0.09403222060369128 0.8740391334730957

Yoruba:

ms 44 80000 -t 30.6816 -r 24.54528 10000 -G 298.1592873494309 -eN 0.0028204398926000218 0.4313047559449311 -eN 0.1396195363438095 0.026126408010012515 -eN 0.16980043486634022 2.1113579474342927

Supplementary Text

Validation of expected branch lengths calculated by FitCoal

Under the constant size model, when the sample size was small (e.g., $n = 5$, where *n* is the number of sequences) or extremely large (e.g., $n = 1{,}000$), FitCoal calculated the expected branch lengths correctly (fig. S33 and table S14). Such high accuracy is essential for the precise determination of population size history (i.e., the dynamic of population size).

FitCoal calculated branch lengths were nearly identical to those calculated with the method of Živković and Wiehe's (*17*) under three demographic models (table S13). For more complex models, the average branch lengths were obtained from extensive coalescent simulations. The simulated results were consistent with those calculated by FitCoal with different demographic models (table S20).

FitCoal- and simulation-based likelihood graph

With an instantaneous growth model, the effectiveness of FitCoal in the calculation of likelihood values was compared with that of the commonly used simulation method of Li and Stephan (*9*). In this model, the population size was increased from N_1 (10,000) to N_0 (20,000) at the standard coalescent time of 0.2, and an SFS was obtained by multiplying the expected branch lengths by θl ($= 4\mathrm{N}_0\mu$), where $\mu l = 1.0$. The number of sequences was 100. Results of this

comparison are presented with a graph composed of numerous dots with each dot representing a likelihood value (fig. S1). To draw the likelihood graphs, grid searches were performed in a parameter space, ranging from N_1 (9,800 – 10,200) to N_0 (19,600 – 20,400), conditional on the standard coalescent time of 0.2. To calculate simulation-based likelihood values, 100,000 coalescent-based simulations were performed. The graphed image of FitCoal likelihood was smooth, but that of simulation-based likelihood was rugged (fig. S1), suggesting that FitCoal is much more effective than the method of Li and Stephan (*9*) in likelihood determination. FitCoal likelihood values were also larger than those of simulations because FitCoal expected branch lengths fit the data better than the average branch lengths obtained from the simulations.

FitCoal demographic inference on simulated data

To validate the accuracy of FitCoal inference and to ensure fair comparisons with other state-of-art methods, six different demographic models were tested by simulating 200 independent data sets for each model as described previously (*6*). FitCoal precisely inferred the population size histories in all six models (Fig. 2).

FitCoal gains benefit from a priori knowledge of population size history. In some circumstances, a slow and continuous change in the size of a population was more biologically relevant than a quick and sudden change. FitCoal also performed well with an exponential or instantaneous change within each inference time interval (figs. S29 and S30). Results showed that the accuracy of FitCoal inference is increased in the presence of correct priori knowledge. Even if the condition was mis-specified, the inferred population size histories were similar to those of the true models.

FitCoal was model flexible, and the number of inference time intervals was dependent on the complexity of a population. For more complex populations, FitCoal might have missed slight changes in population size in short time periods but successfully detected major changes in all complex populations examined (figs. S4 and S31). When the two-population split models were used (fig. S32), FitCoal also performed well although a slightly larger recent population size was inferred, probably due to the effects of population migration.

Effects of positive selection on FitCoal inference under a constant size model.

To simulate the effects of positive selection, a two-locus model (*65, 66*) was used with a constant size model. The effective population size was set as 27,000, the number of neutral fragments used for simulations was 10,000, and 10 or 20% of them were partially linked to selected alleles. The distance between the neutral and the selected loci was 20kb, and the recombination rate was 1cM per Mb. The sample size was 202 (the average sample size of populations in 1000GP). The selection coefficient (*s*) was 0.01 or 0.05, and the mutation rate was 1.2×10^{-8} per base per generation. To compare among different cases, the average number of single nucleotide polymorphisms (SNPs, 5,882,885) in populations in 1000GP was designated as the expected number of SNPs for the simulations.

All simulated samples were found to have excessive high frequency mutations (*25*). As the genetic diversity of selected loci was low, their contribution to the genome-wide diversity was relatively low, and only a slight excess of rare mutations (*67*) was observed. The ratio between the number of singletons and doubletons was in the range of 2.008 to 2.110 in the simulated samples, only slightly larger than the expected value (2.0) under neutrality.

FitCoal was then used to infer demography. For simplicity, the last 21 SFS categories of high frequency mutations were excluded for analysis (table S17). As a result, a relatively correct population size history with a slight population expansion was estimated to occur within one million years (fig. S6A). When full size (complete) SFSs were used, the population size was found to remain constant for 2,000 kyr (fig. S6B). The constant size model was inferred because all optimization processes were prematurely stopped at the stage of one phase when the SFSs with high frequency mutations were analyzed. The population size estimated from simulations was slightly smaller than the true parameter (~25,200 *vs* 27,000).

Population size histories of African populations

To infer population size histories of African populations, seven African populations in the 1000GP (*23*) were analyzed by the FitCoal (table S3). Only autosomal non-coding regions were used to partially avoid the effect of purifying selection. To avoid hitchhiking effect due to positive selection (*25*), high-frequency mutations were excluded from the analysis. Results showed that all seven African populations went through a severe bottleneck around 915 (range: 854–1,003) kyr BP and that this bottleneck was relieved about 793 (range: 772–815) kyr BP (Fig. 3, A and B, fig. S7). The average effective population size (i.e., the number of breeding individuals) (*26*) of African populations during the bottleneck period was 1,270 (range: 770–2,030). After the bottleneck was relieved, the population size was increased to an average of 27,080 (range: 25,300–29,180), a 20-fold increase, around 793 kyr BP. The population size remained relatively constant and did not begin to expand significantly until 10–80 kyr BP.

To avoid the potential effects of low sequencing depth, sequences with high sequencing coverage (~35x) of autosomal non-coding regions of populations in the HGDP-CEPH panel were analyzed (*24*). Results showed that the severe bottleneck occurred in all three African populations in the HGDP-CEPH panel between 1,257 (range: 1,042–1,527) and 859 (range: 856–864) kyr BP (Fig. 3, C and D, fig. S8) and that the average population size during the bottleneck period was 1,300 (range: 910–1,670). This population size is very similar to that (1,270) estimated from the data of 1000GP.

After the ancient severe bottleneck was relieved, the population sizes of the two African agriculturalist populations in the HGDP-CEPH panel were increased to 27,300 and 27,570, respectively (Fig. 3D, fig. S8, and table S4), consistent with the estimated size of 27,280 from 1000GP. The Biaka, an African hunter-gatherer population, had a larger population size of 35,330, suggesting a deep divergence between this and other agriculturalist populations (*68-70*). The Biaka population was found to have a recent population decline (Fig. 3D and fig. S8), as previously observed (*24*). These results suggested that the hunter-gatherer populations were widely spread and decreased when the agriculturalist populations were expanded in Africa.

The discovery of the ancient severe bottleneck is robust with sample size, since it could be detected in two South African populations with small sample sizes (San: 6 individuals; BantuSouthAfrica: 8 individuals) in the HGDP-CEPH panel (fig. S46). When the 10 African populations in the two data sets were re-analyzed using remote non-coding regions (at least 10kb away from coding regions), the severe bottleneck was again detected (fig. S23). To avoid the impact of low or high frequency mutations resulting from positive selection, negative selection, or sequencing error (*67*), FitCoal analyses were re-performed with these mutations excluded, and the severe bottleneck was again detected (fig. S47). Furthermore, when complete SFSs were used (i.e., SFSs without the precautionary data truncation), population size histories were inferred

conditional on the same number of inference time intervals, which is very similar to that estimated using truncated SFSs (figs. S48 and S49).

Recent population size histories of non-African populations

The out-of-Africa dispersal was detected in all 40 non-African populations (tables S5 and S6). The Middle East populations had the weakest founder effect during the dispersal, while the Maya, an American population, had the strongest effect. European and South Asian populations were found to have a weaker founder effect during the out-of-Africa dispersal than East Asian populations. Generally, a positive correlation was observed between the founder effect severity of the out-of-Africa dispersal and their geographic distance to Africa, consistent with the observed correlation between heterozygosity and geographic distance (*5*, *71*). A weak founder effect during the out-of-Africa dispersal was observed in American populations (non-Maya), probably because of recent admixture (*23*). All non-African populations were found to increase in size recently, except an isolated Kalash population, as previously observed (*24, 72*). Therefore, the FitCoal inferred recent population size histories, including population size expansion or reduction and the out-of-Africa dispersal, are consistent with those of previous studies (*5-8, 23, 24*).

SFS truncation and collapse for analysis of human populations

A monotonically decreasing genome-wide SFS was expected in neutrally evolved single populations. However, all human populations examined were found to have excessive high frequency mutations (figs. S25, S26, and S27) probably because of hitchhiking effects of positive selection (*25*) and migration effects among different sub-populations (*28*). Thus, the model of neutrally evolved single population failed to explain the excessive high frequency mutations in human populations.

When the full-size SFSs were considered, analysis of these populations with the neutral single population model also failed because optimization processes prematurely stopped (fig. S22B), thus introducing an underfitting in demographic inference. This problem was avoided by excluding excessive high frequency mutations (fig. S22A). Therefore, a truncated SFS was used for analysis of each human population. The proportions of truncated sizes are listed in tables S17 and S19.

For neutrally evolved single populations, FitCoal-inferred population size histories with truncated SFSs were very similar to that estimated with complete SFS (Fig. 2 *vs* fig. S3; fig. S4 *vs* S31). For populations with excessive high frequency mutations, FitCoal-inferred population size histories with truncated SFSs were also very similar to that estimated with complete SFS if the analysis was performed conditional on the same number of time intervals (figs. S28, S48, and S49). As the number of time intervals was usually unknown for real populations, the confidence interval of inferred histories was affected by population structure in some cases when full-size SFSs were used for analysis (fig. S20, simulated East African population).

Collapsed SFSs in which a portion of high frequency mutations were combined into one category were also used for FitCoal analysis of human populations. Both truncating and collapsing approaches were found to infer population size histories correctly (figs. S50 and S51). Therefore, use of truncated (*6*) or collapsed (*19*) SFSs is recommended for inference of

population size histories to minimize the adverse effect of sequencing errors, hitchhiking effects of positive selection, and migration effects among different sub-populations on FitCoal analysis.

Verification of inferred human population size histories

To evaluate the accuracy of inferred population size histories (Fig. 3), 200 DNA polymorphism data sets were simulated for each population examined. Results showed that the SFSs obtained from simulations were nearly identical to those obtained from real populations (figs. S52 and S53) with very narrow confidence intervals of inferred demography (figs. S34 – S44), indicating that FitCoal has accurately inferred the population size histories of human populations.

To investigate why the ancient severe bottleneck was not detected in non-African populations, various factors were examined. The effect of SFS truncation on FitCoal analysis was first analyzed. When SFS truncation was performed, the proportion of truncated SFS was found to be different for different populations (tables S17 and S19). To determine whether this difference was the cause for the discrepancy in the inference of population size histories, FitCoal analysis was re-performed with the same proportion of SFS truncated for all populations in the same database (10% for 1000GP and 15% for HGDP-CEPH populations). Results showed that the population size histories inferred with a fixed proportion of SFS truncated for all populations were very similar to those inferred with different proportions of SFS truncated for different populations (fig. S45). This result suggests that the amount of exclusion of SFS categories with high frequency mutations is not critical for FitCoal analysis and is consistent with the finding that as little as 10% of an SFS is sufficient for accurate determination of population size history (fig. S5).

Similar to SFS truncation, different proportions of SNPs were found to be discarded in FitCoal analyses (table S17). The average proportion of truncated SNPs in African and non-African populations of 1000GP was 3.23% and 4.83%, respectively. For the 19 non-African populations listed in table S17, the following proportions were excluded: 3.33%, 3.19%, 3.31%, 3.20%, 3.23%, 3.08%, 3.29%, 3.16%, 3.29%, 3.12%, 3.32%, 3.21%, 3.24%, 2.98%, 3.25%, 3.09%, 3.32%, 3.17%, and 3.36%. The average of these 19 different proportions is 3.22%, nearly identical to that of African populations (3.23%). All 19 non-African populations were re-analyzed with this proportion of SNPs excluded. Results obtained were found to be similar to that derived from exclusion of more proportions of SNPs for non-African populations (fig. S54).

Since positive selection may affect the abundance of rare mutations (*67*), both singletons and high frequency mutations were excluded from FitCoal analysis, and the ancient severe bottleneck was again detected in African populations (fig. S47). The inferred demographic histories of non-African populations were also similar to those of previously inferred (fig. S55). These results suggest that rare mutations have little effect on ancient population size histories because single lineages (i.e., leaves) are relatively unlikely to be traced back to ancient stages.

To further examine the effects of SFS truncation, FitCoal analysis was re-performed with complete SFSs that contained all high frequency mutations, and the analysis was conducted using fixed number of time intervals to minimize the effects of high frequency mutations. With this approach, the ancient severe bottleneck was detected in African populations but not in non-African populations (figs. S48 and S49), suggesting that the detection of the ancient severe bottleneck was not resulted from partial SFS truncation.

Another approach in which SFS categories with high frequency mutations were combined into one category by a process called "collapse" was employed (*19*). With this strategy, the ancient severe bottleneck was detected in six of the seven African populations in 1000GP (fig. S50), and the inferred recent demographic histories of the 19 non-African populations in 1000GP were similar to those inferred with truncated SFS (fig. S51). These results indicated that combining SFS categories with high frequency mutations into one category is also an effective method for FitCoal analysis.

Results of extensive simulations with different demographic models indicated that 20% is a proper LLPR threshold to determine the optimal number of time intervals for each model (table S16). It was then examined whether the inferred human population size histories are robust to this threshold. Generally, FitCoal-inferred population size histories were found to be similar to the inferred population size histories with one more time intervals (figs. S56 and S57). Moreover, the LLPR of two adjacent time intervals (i.e., the time interval of m and $m + 1$) was examined for each population (tables S21 and S22). When the 20% LLPR threshold was applied, the best time interval was 3 for the CEU population because the LLPR of time intervals between 2 and 3 (2471.16%) was much larger than that between 3 and 4 (17.07%) for this population.

Effects of human migration/introgression on FitCoal analysis

As African populations have a complex population structure (*28, 38, 68-70, 73, 74*), data were simulated for a western rainforest hunter-gatherer (wRHG) and a western farmer (wARG) population according to a previously proposed structure model (fig. S18) (*73*). Although a large recent population size was found for both populations, probably due to frequent migrations, the ancient population size (14,427) was accurately inferred for both populations (14,493 and 14,428). Thus, the detection of the ancient severe bottleneck was not due to the complex African population structure.

To investigate the effects of archaic introgression from ghost populations (*75, 76*), different models were examined by assuming that the introgression occurred in different time periods with different migration rates (fig. S19). Results showed that archaic introgression had no effects on the detection of the ancient severe bottleneck.

As the San population is a highly diverged southern African population, a four-population model with parameters defined in the previous study (*2*) was used. The model included the San, East African, non-African, and Neanderthal populations (fig. S20). Migrations between different populations were considered as single pulsed introgressions. Analyses of simulated sequences of the San and East African populations revealed that FitCoal inferred the ancient severe bottleneck correctly.

To further examine the effects of archaic introgression, more cases of pulsed introgressions were investigated (fig. S21). Two four-population models were established, including African, non-African, Neanderthal, and ghost populations (*2*). Results showed that archaic pulsed introgressions in different time points did not result in an ancient severe bottleneck.

Mathematical explanation for stronger signals of ancient severe bottleneck in African populations

To investigate the reasons why the ancient severe bottleneck was directly found in African populations but not in non-African populations, mathematical modelling and analysis was

performed. Results showed that the inferred number of intervals before time t depends on the dimension of the SFS before time t. Details of the modelling and analysis follow:

Denote the probability of state l at time t from n samples by $p_l^n(t)$, where $l = 2, \cdots, n$. And denote the expected branch length of size i from n samples by $BL_i^n(N(\cdot))$, where $i = 1, \cdots, n-1$. There exists an invertible matrix $\mathcal{X} = \left(x_g^h\right)_{g,h=2,\cdots,n}$ which only depends on n, such that $p_l^n(t) = \sum_{g=2}^{n} x_g^l \, p_g^g(t)$ (*18*, *22*). If positive numbers $m < n$, there exists a matrix $\mathcal{Y} = \left(y_g^h\right)_{g=2,\cdots,m,h=2,\cdots,n}$, which only depends on m and n, such that $p_l^m(t) = \sum_{h=2}^{n} y_l^h \, p_h^n(t)$. Combined with eq(1), there exists a matrix $\mathcal{Z} = \left(z_g^h\right)_{g=1,\cdots,m-1,h=1,\cdots,n-1}$, which only depends on m and n, such that $BL_i^m(N(\cdot)) = \sum_{j=1}^{n-1} z_i^j \, BL_j^n(N(\cdot))$.

Define the population size before time t by $N^t(s) = N(t+s)$. Denote the expected branch length of state l before time t by $B_l(t) = \left(b_{1,l}(t), \cdots, b_{l-1,l}(t)\right)$, where $b_{i,l}(t)$ represents the expected branch length of state l before time t of type i at time t. Then, $b_{j,l}(t) = p_l^n(t) BL_j^l(N^t(\cdot))$. $BL_{i,k}^t$ ($i = 1, \cdots, n-1$) denotes the branch length of type i whose number of lineages are no more than k before time t. Therefore,

$$BL_{i,k}^t = \sum_{l=2}^{k} \sum_{j=1}^{l-1} \frac{p(j \to i) p(l-j \to n-i)}{p(l \to n)} b_{j,l}(t),$$

where $p(a \to b) = \begin{cases} \binom{b-1}{a-1} & b \geq a \geq 1 \\ 0 & \text{else} \end{cases}$.

Then,

$$\begin{aligned} & BL_{i,k}^t \\ = \; & \sum_{l=2}^{k} \sum_{j=1}^{l-1} \frac{p(j \to i) p(l-j \to n-i)}{p(l \to n)} b_{j,l}(t) \\ = \; & \sum_{l=2}^{k} \sum_{j=1}^{l-1} \frac{p(j \to i) p(l-j \to n-i)}{p(l \to n)} p_l^n(t) BL_j^l(N^t(\cdot)) \\ = \; & \sum_{h=1}^{k-1} \left(\sum_{l=2}^{k} \sum_{j=1}^{l-1} \frac{p(j \to i) p(l-j \to n-i)}{p(l \to n)} p_l^n(t) z_j^h \right) BL_h^k(N^t(\cdot)) \end{aligned}$$

Thus, the space that is generated by $BL_{1,k}^t$, $\cdots$, $BL_{n-1,k}^t$ can be generated by $BL_1^k(N^t(\cdot))$, $\cdots$, $BL_{k-1}^k(N^t(\cdot))$. This leads to the dimension of $\left(BL_{i,k}^t\right)_{i=1,\cdots,n-1}$ which is no more than $(k-1)$.

If the number of ancestral lineages is no more than k before a given standard coalescent time t, the number of inference time intervals is less than $(k-1)$ before time t in the inferred population size history without overfitting. For non-African populations, when $t = 1.0$, the number of ancestral lineages was found to be ≤ 3 in more than 90% of the cases (table S23), indicating the effectiveness of a constant size model with one inference time interval or with two inference time intervals for populations with an expansion or a contraction beyond this time point. The end time of the ancient severe bottleneck was determined to be 813 (range: 772–864) kyr BP, and the corresponding standard coalescent time was larger than 1.0 for all non-African populations (fig. S11). As the bottleneck spanned three time intervals, it was not straightforward to infer the ancient severe bottleneck in non-African populations.

<u>Minimum number of African individuals to detect the ancient severe bottleneck</u>

The detection of the ancient severe bottleneck was based on the number of lineages remained, and the number of lineages at time t was positively correlated with the sample size. To estimate this minimum number of individuals for detection of the ancient severe bottleneck,

different YRI sub-samples (Yoruba in Ibadan, Nigeria) were considered. The numbers of sampled individuals were 2, 3, 4, 6, 8, 10, 15, and 20. For one sample size, ten randomly chosen data sets were analyzed (fig. S12). The ancient severe bottleneck was precisely identified when the number of sampled individuals was ≥ 3, which is consistent with the inferred ancient severe bottleneck in San (6 individuals) and BantuSouthAfrica (8 individuals). Therefore, only three African individuals were required to detect the ancient severe bottleneck using FitCoal.

This empirical number was validated by a theoretical coalescent analysis. The standard coalescent time was $t = 0.5$ for the African populations (fig. S7A) and $t = 1.0$ for the non-African populations (figs. S7B to E) when tracing back to the time of ancient severe bottleneck. The expected number of lineages ($\bar{\omega}$) tracing back to the time of ancient severe bottleneck was found to be proportional to sample sizes (fig. S58). For the non-African population, $\bar{\omega} = 2.35$ and 1.71 when the number of sampled individuals was 100 and 2, respectively. Similarly, $\bar{\omega}$ was reduced from 4.27 to 2.32 for the African population when the number of sampled individuals was reduced from 100 to 2. When 2 African and 100 non-African individuals were sampled, $\bar{\omega}$ of the former was slightly smaller than that of the latter (2.32 *vs* 2.35), indicating that the ancient severe bottleneck was not detectable by sampling two African individuals (fig. S12). With three African individuals sampled, more lineages remained, thus providing more information for detection of the ancient severe bottleneck. Therefore, the theoretical minimum number of sampled African individuals is three for detection of the ancient severe bottleneck using FitCoal.

Likelihood of the ancient severe bottleneck calculated by Živković-Wiehe's method

As the ancient severe bottleneck was detected using three African individuals ($n = 6$ sequences), other methods, such as Živković-Wiehe's method (*17*), should also be able to calculate the expected branch lengths precisely. To test this possibility, an YRI subsample ($n = 6$ sequences) was chosen for inference of population size histories with one, two, and three inference time intervals. Results showed that likelihoods obtained by FitCoal and Živković-Wiehe's method were nearly identical (fig. S59), indicating that this bottleneck can also be detected using Živković-Wiehe's method.

Detection of the ancient severe bottleneck from weak signals in non-African populations

As the signal for the existence of the ancient severe bottleneck in non-African populations was weaker than that in African populations, the possibility that the ancient severe bottleneck could be detected by increasing the sample size of non-African populations was explored with a large combined non-African sample in 1000GP ($n = 1{,}843$ individuals or $3{,}686$ sequences). Results showed that the ancient severe bottleneck was not detected (fig. S60). As $\bar{\omega}$ value remained nearly unchanged (2.35 *vs* 2.37) when the number of sampled individuals was increased from 100 to 1,843, this result suggests that increasing the non-African sample size had little effect on the detection of the ancient severe bottleneck.

An R-extended FitCoal was then implemented to detect the ancient severe bottleneck in non-African populations. To eliminate noise effects in the inference of recent population size history, the FitCoal-inferred population size history (i.e., the recent history since the emergence of modern humans) was fixed. For a non-African population, a series of demography with m pieces was inferred using FitCoal and denoted by a set $S(m)$, where $S(m)$ contained all of the following m pieces of population size: $N(t|N0 > 0, N_{(m)}, t_{(m)}, c_{(m)})$, $N_{(m)} = (N_1, \cdots, N_m)$,

$t_{(m)} = (t_1, \cdots, t_m)$ and $c_{(m)} = (c_1, \cdots, c_m)$. One parameter N_m was then set free to change, and two extra pieces were appended at the end of the inferred demography. Instantaneous population changes were considered for the two newly introduced pieces. In total, six parameters (N_m, N_{m+1}, N_{m+2}, t_{m+1}, t_{m+2}) were examined to infer the ancient population size history of non-African populations. These parameters were then jointly examined by maximizing the likelihood with no restrictions in searching parameter spaces.

With this approach, the ancient severe bottleneck was detected in all 19 non-African populations in 1000GP (fig. S13). The estimated bottleneck parameters (table S10) were very similar to the ones inferred in African populations. The ancestral size was determined to be 103,390 (103,390 *vs* 98,130). The ancient severe bottleneck was found to begin around 921 (921 *vs* 930) kyr BP and was relieved about 785 (785 *vs* 813) kyr BP. The average effective population size of ancestral African populations during the bottleneck period was 1,450 (1,450 *vs* 1,280).

Effects of positive selection on FitCoal inference with a bottleneck model mimicking African human populations

To study the effects of positive selection on human populations, the model mimicking the demography of African populations was used (Fig. 4A). The most recent population change was set as instantaneous change to simplify the simulation. It was assumed that the population experienced an instantaneous decrease from 93,000 to 1,300 around 38,000 generations ago, followed by an instantaneous growth to 27,000 around 33,000 generations ago and another increase to 82,000 around 1,000 generations ago. Other parameters in the positive selection model were the same as the one above.

All simulated samples had an excess of high frequency mutations (*25*), and the ratio between the numbers of singletons and doubletons ranged between 2.795 and 2.887 in the simulated samples, only slightly larger than the expected value (2.768) under the neutral demographic scenario.

FitCoal was then used to analyze the data obtained from simulations with the last 21 SFS categories, which had high frequency mutations, truncated (table S17). The ancient severe bottleneck was detected in all simulated cases ($100\% = 40/40$) (fig. S22A). When full size (complete) SFSs were analyzed, the ancient severe bottleneck was found only in 45% ($= 18/40$) of the cases (fig. S22B). To investigate whether FitCoal inference was prematurely terminated due to the excess of high frequency mutations, FitCoal inference was re-performed with four inference time intervals. With this approach, the ancient severe bottleneck was detected in all cases (100%=40/40) (fig. S22C). Therefore, truncation of SFS categories with high frequency mutations (partially) avoided the impact of positive selection on the inference of population size history.

Positive selection was found to have less impact on the inference of recent population expansion because such expansion was precisely inferred in all cases (100%=120/120) (figs. S22A and C).

Loss of current genetic diversity due to the ancient severe bottleneck

To investigate the loss of current human genetic diversity due to the ancient severe bottleneck, the expected human genetic diversity at present was analyzed with or without the

ancient severe bottleneck. The genetic diversity was calculated from the expected tree lengths under the demographic models. To avoid the effect of the bottleneck, the population size during the bottleneck was replaced by the one after the bottleneck was relieved. The expected tree length of the inferred population size history with the bottleneck (ω_1) was compared with that without the bottleneck (ω_0).

The loss of current genetic diversity due to the ancient severe bottleneck was calculated as $(\omega_0 - \omega_1)/\omega_0$. When the actual sample size was used for each population, the genetic diversity was measured as Watterson's θ. The average loss in genetic diversity of these eight populations was 46.22%, ranging from 32.17 to 60.56%.

When $n = 2$, the genetic diversity was measured as π, the pairwise nucleotide diversity. The average loss of current genetic diversity in these eight populations was 65.85%, ranging from 52.71 to 73.60%. This value was larger than that derived from Watterson's θ, probably because the bottleneck was ancient, and the recovery rate of Watterson's θ was faster than that of π (*77*). These results demonstrated the profound effect of the ancient severe bottleneck on human evolution.

Gap in African hominin fossil record during the Early to Middle Pleistocene transition

The hominin fossil record is extremely rare or even absent in Africa and Eurasia between around 950 and 650 kyr BP (fig. S24) (*36*). This time duration largely overlaps with the Early to Middle Pleistocene transition (ca. 1,250 and 700 kyr BP) (*33, 36, 78-80*). During this transition, there was a progressive increase in the amplitude of climate oscillations, with a shift from short-timed interglacial sequences (~41 thousand years) to longer cycles (~100 thousand years) causing a strong increase in the global ice volume. Particularly, an extreme and long-term (ca. 80 thousand years) glaciation occurred during Marine Isotope Stage (MIS) 24 and MIS 22, known as the "0.9 Ma event" (*33*). This dry period was associated with major environmental changes and a large faunal turnover in Africa and Eurasia (*35, 81*).

The archaic morphologies associated with *H. ergaster* (or African *Homo erectus*) seem to disappear from the African fossil record between about 950 and 650 kyr BP. Specimens of uncertain taxonomic attribution, such as OH 12 (in Tanzania), Olorgesailie (in Kenya), Daka (in Ethiopia), and Buia (in Eritrea), were all associated with Mode 2 (Early Stone Age) lithic assemblages (*82*) in the fossil record around 1 million years ago. This discontinuity in the production of Mode 2 artefacts has been noted in different layers of the Melka Kunture formation in Ethiopia, dated from 1.0 to 0.85 million years ago (*83*). According to the study of Shea (*84*), only a small number of the dated archaeological sites (6 on a total of 27) of the later Early Stone Age in East Africa overlapped in time span with the ancient severe bottleneck.

Fossil evidence becomes relatively abundant again after 650 kyr BP, with fossils – such as Bodo (Ethiopia), Elandsfontein (South Africa), and Kabwe (Zambia). These specimens exhibited some derived cranial features with respect to that of the Early Pleistocene including the following: a less receding squama of the frontal bone; a supra-orbital torus not straight but showing a step between supraciliary arch (medially) and trigone (laterally), an enlarged braincase with a volume of about 1,200 ml (the average for *H. erectus* sensu lato is about 1,000 ml) (*37, 85-87*). These specimens were also associated with Mode 2 stone tools, but starting from around 300 Kyr BP Mode 3 Middle Stone Age technology emerges as evidenced by the possible association with the Kabwe cranium dated to that chronological horizon (*88*).

Nevertheless, some evidence of human presence in Africa exists between around 950 and 650 kyr BP. A few archaeological findings and a limited number of fragmentary fossils suggest a possible evolutionary transition in the time period spanning between 900 and 800 kyr BP (*36, 37*). Two cranial fragments from Gombore II in the Melka Kunture area of Ethiopia (about 850 kyr BP) and three isolated mandibles and a parietal bone from the Algerian site of Tighenif or Ternifine (perhaps more than 700 kyr BP) were found. These fossil specimens were long attributed to the variability of *H. erectus*, but more recent analyses denied this attribution and indicated affinities with later *H. heidelbergensis* representatives (*36, 37*). Furthermore, the morphology of the Tighenif mandibles did not show affinities with that of archaic contemporary specimens found in Europe, such as the mandibles from the Gran Dolina sites attributed to *H. antecessor* (*89*).

In the same chronological interval, the fossil record from East Asia includes specimens mostly referred to *H. erectus* (*39*). It does not appear that East Asian *H. erectus* might be related to the ancient severe bottleneck because it has not been found to contribute to the ancestry of modern humans (*38*).

Similar effectiveness of different simulation programs and methods

In this study, two different methods were used to simulate 800 Mb sequences at the population level. The *ms* software (*55*) was first used to generate 80,000 sequence fragments of 10 kb each, taking into the consideration of small fragments split by sequencing mask in 1000GP and HGDP-CEPH data sets. Because these fragments were too short to mimic the entire human genomic sequences, the msprime software (*57*) was also used to generate 800 Mb sequences by simulating 8 sequences of 100 Mb each. Results showed that these two simulation programs and methods were similarly effective in FitCoal demographic inference (Figs. 4A to C, figs. S9A to C, and tables S7 and S8).

Data and software availability

All data are presented in the main text and Supplemental Materials. Raw data has been deposited at Mendeley (https://doi.org/10.17632/xmf5r8nzrn.3) (*45*). FitCoal is a free plug-in of the eGPS software (*90*) and can be downloaded and run as an independent package. FitCoal is written in Java and is very fast. As FitCoal does not require much memory to run, it can be executed on a desktop computer. FitCoal (including its source code and documentation) is available via Zenodo (https://doi.org/10.5281/zenodo.7857456) (*46*), our institute website at http://www.sinh.ac.cn/evolgen/, and eGPS website http://www.egps-software.net/.

FitCoal is free for academic users to conduct non-commercial research. For commercial usage, please contact Shanghai Institute of Nutrition and Health to negotiate a license. Contact email address is guzhili@sinh.ac.cn. Please indicate “FitCoal commercial license” on the email subject. FitCoal cannot be extended, modified, re-distributed, and/or used to train a ChatGPT or any other artificial intelligences without written permission from the corresponding authors.

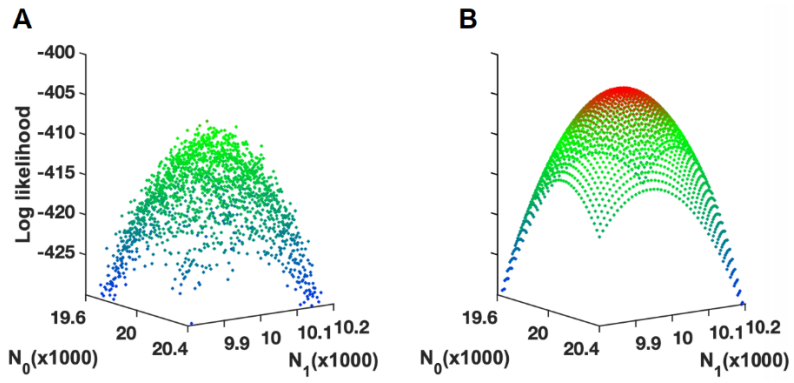

Fig. S1. Comparison of likelihood values of FitCoal with those of simulations.

(**A**) Likelihood values derived from simulations performed with the method of Li and Stephan. To calculate a likelihood value, 100,000 coalescent-based simulations were performed.
(**B**) Likelihood values derived from FitCoal.
The number of sequences analyzed was 100. N_0 is the current effective population size, and N_1 the ancestral effective population size. Red dots indicate large likelihood values; green and blue dots indicate small likelihood values.

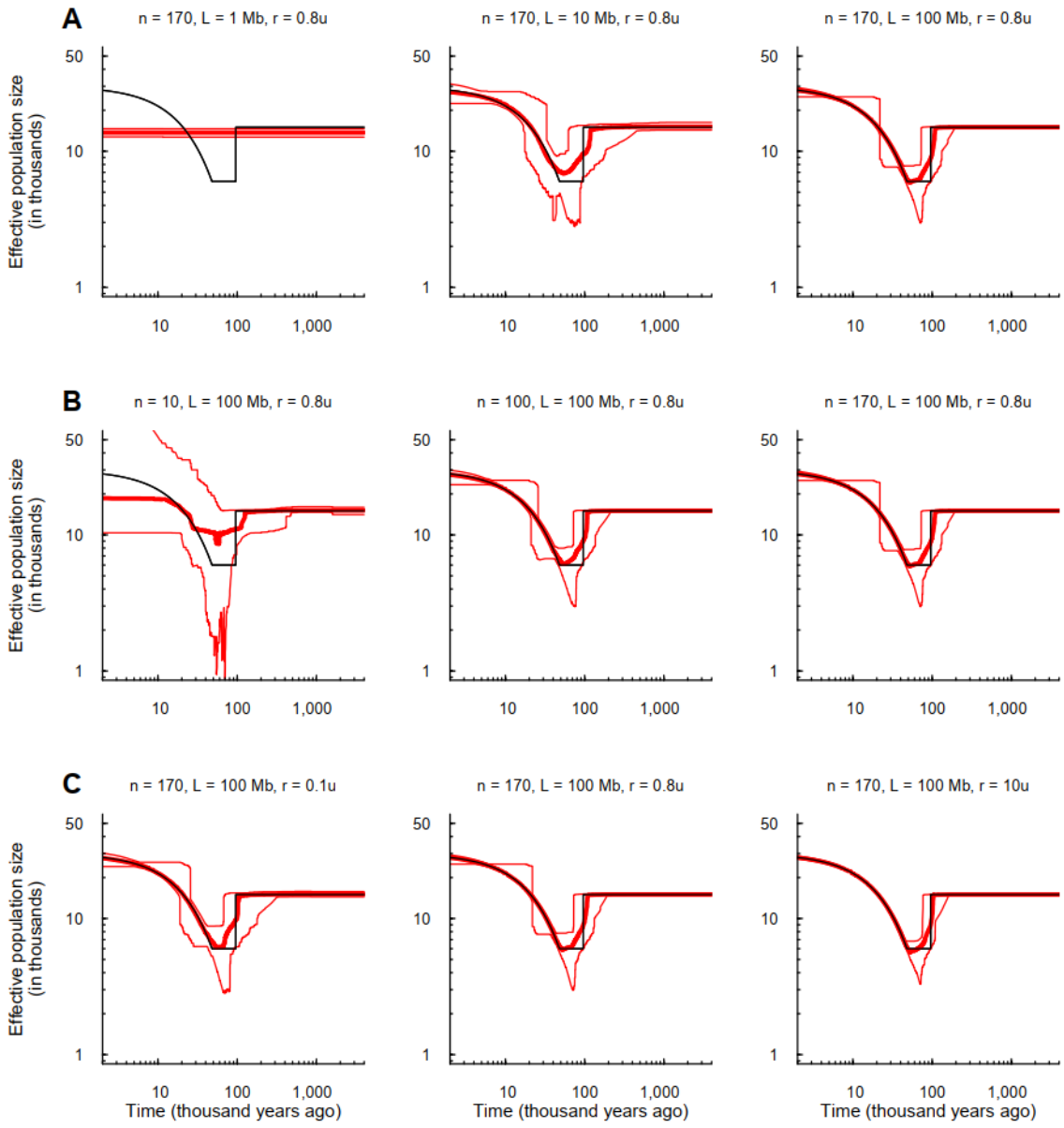

Fig. S2. Effects of sequence length (A), sample size (B), and recombination rate (C) on FitCoal inference.

Black lines indicate true models. Thick red lines present the medians of FitCoal estimated values; thin red lines are 2.5 and 97.5 percentiles of the values. *n* is the number of simulated sequences, *L* is the length of each sequence, and *r* is the recombination rate relative to the mutation rate (μ). Other parameters are the same as those in Fig. 2.

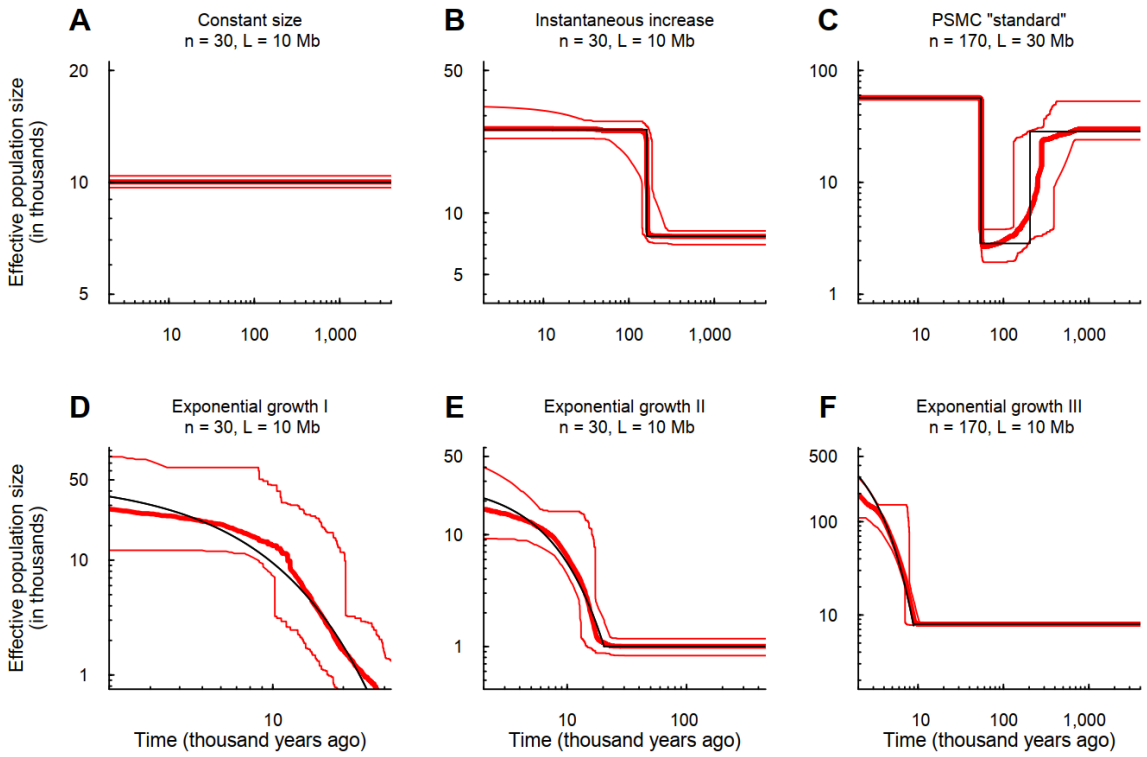

Fig. S3. Verification of FitCoal accuracy with truncated SFS.

(**A**) Constant size model. (**B**) Instantaneous increase model. (**C**) PSMC "standard" model. (**D**) Exponential growth I model. (**E**) Exponential growth II model. (**F**) Exponential growth III model. These six models are the same as those in Fig. 2. Black lines indicate true models. Thick red lines represent the medians of FitCoal estimated values; thin red lines are 2.5 and 97.5 percentiles of the values. *n* is the number of simulated sequences, and *L* is the length of each sequence. 10% of the SFS types with high frequency mutations were discarded (truncated).

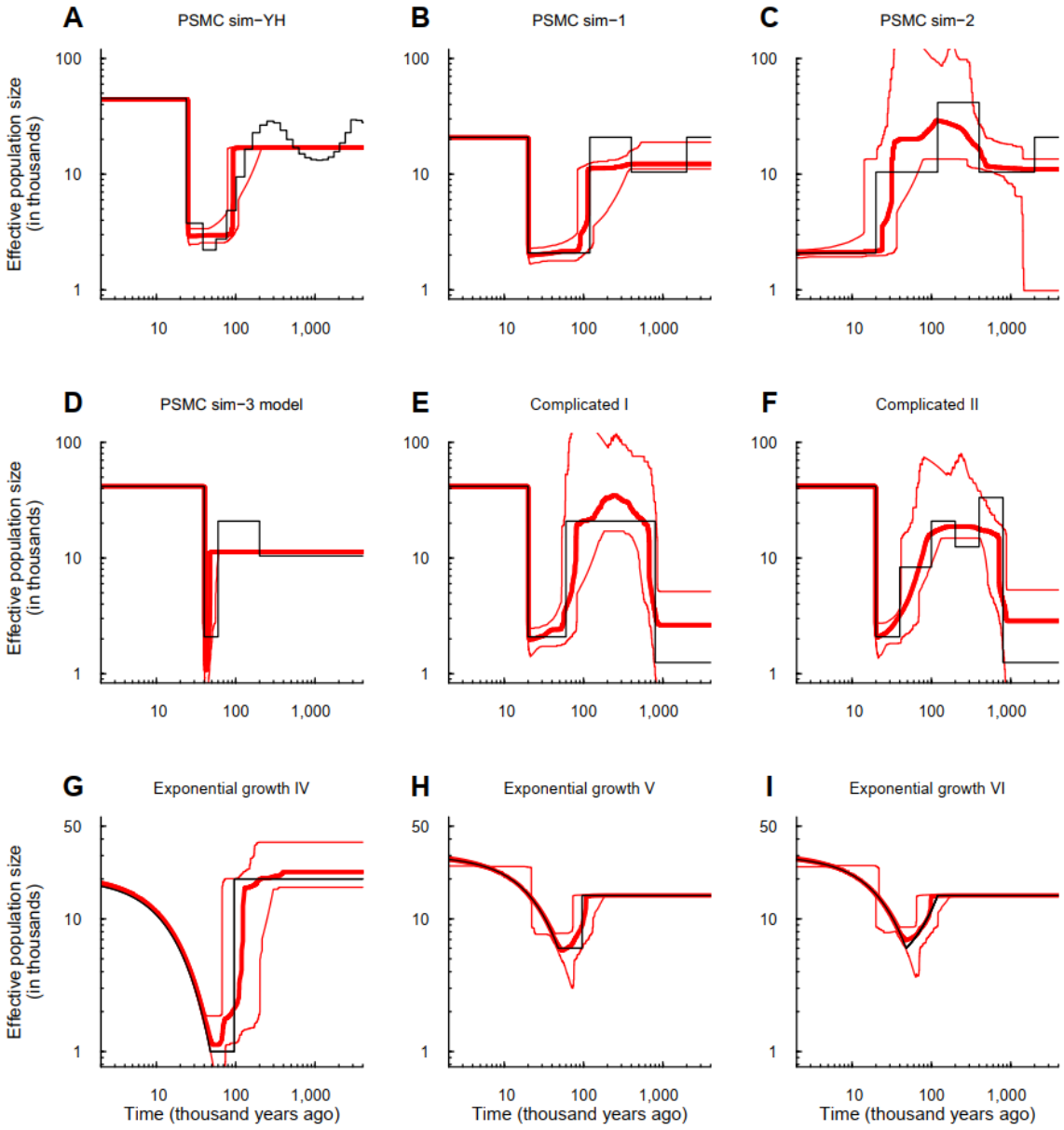

Fig. S4. Verification of FitCoal accuracy using simulated samples with truncated SFS under more complexed models.

(**A**) PSMC sim-YH model. (**B**) PSMC sim-1 model. (**C**) PSMC sim-2 model. (**D**) PSMC sim-3 model. (**E**) Complicated I model. (**F**) Complicated II model. (**G**) Exponential growth IV model. (**H**) Exponential growth V model. (**I**) Exponential growth VI model. Black lines indicate true models. Thick red lines are the medians of FitCoal estimated values; thin red lines are 2.5 and 97.5 percentiles of the values. The number of simulated sequences is 170, and the length of each sequence is 100Mb. 10% of the SFS types (category) with high frequency mutations were discarded (truncated).

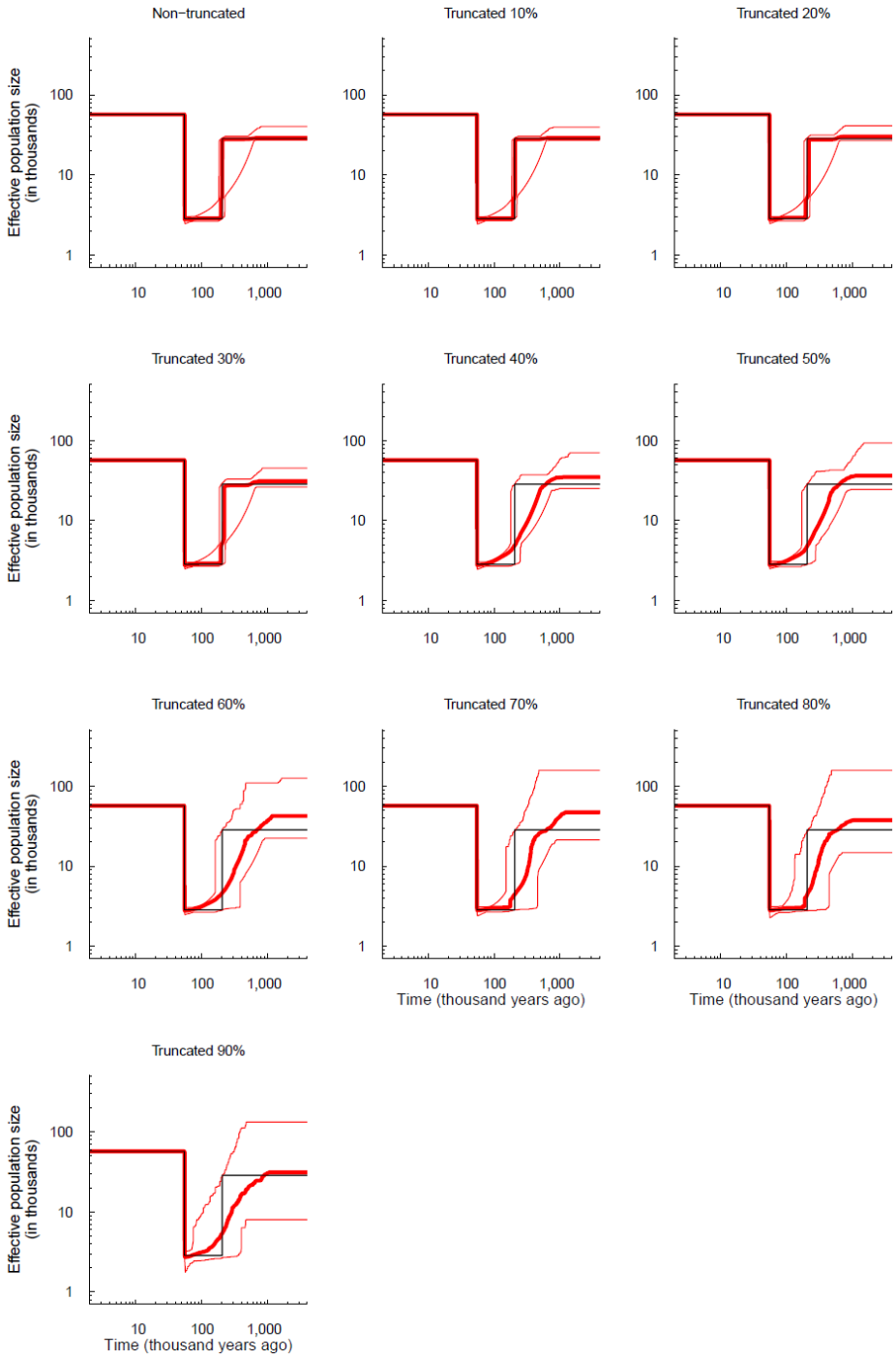

Fig. S5. FitCoal-inferred population size histories under a bottleneck model with different proportions of SFS categories truncated.

This demographic model is the same as the "Bottleneck model" in Fig. 2. The sample size was 188, and eight DNA fragments of 100 Mb each were used for simulation. Black lines indicate true models. Thick red lines represent the medians of FitCoal estimated values; thin red lines are 2.5 and 97.5 percentiles of the values.

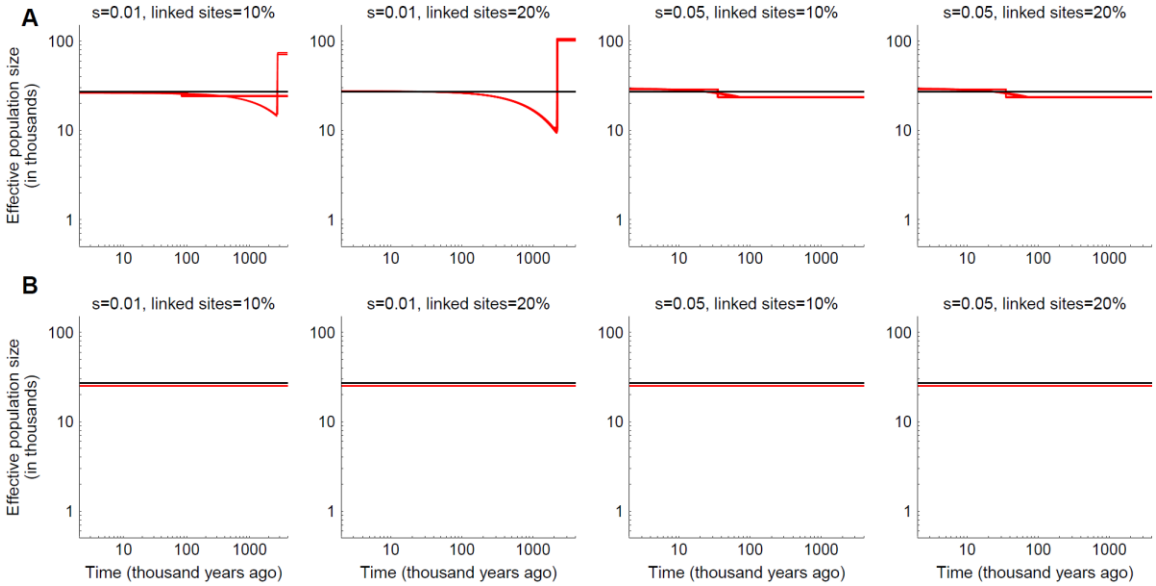

Fig. S6. Effects of positive selection on FitCoal analysis with a constant size model.

(**A**) Inferred population size histories with the last 21 SFS categories of high frequency mutations excluded for analysis.

(**B**) Inferred population size histories using full size (complete) SFSs. Different selection strength (s = 0.01 or 0.05) and percentage (10 or 20%) of loci (linked sites) were used. $n = 202$. Each scenario was examined with 10 replications. The true model (i.e., the constant size model) is indicated with a solid black line. The 10 inferred population size histories were presented with solid red lines.

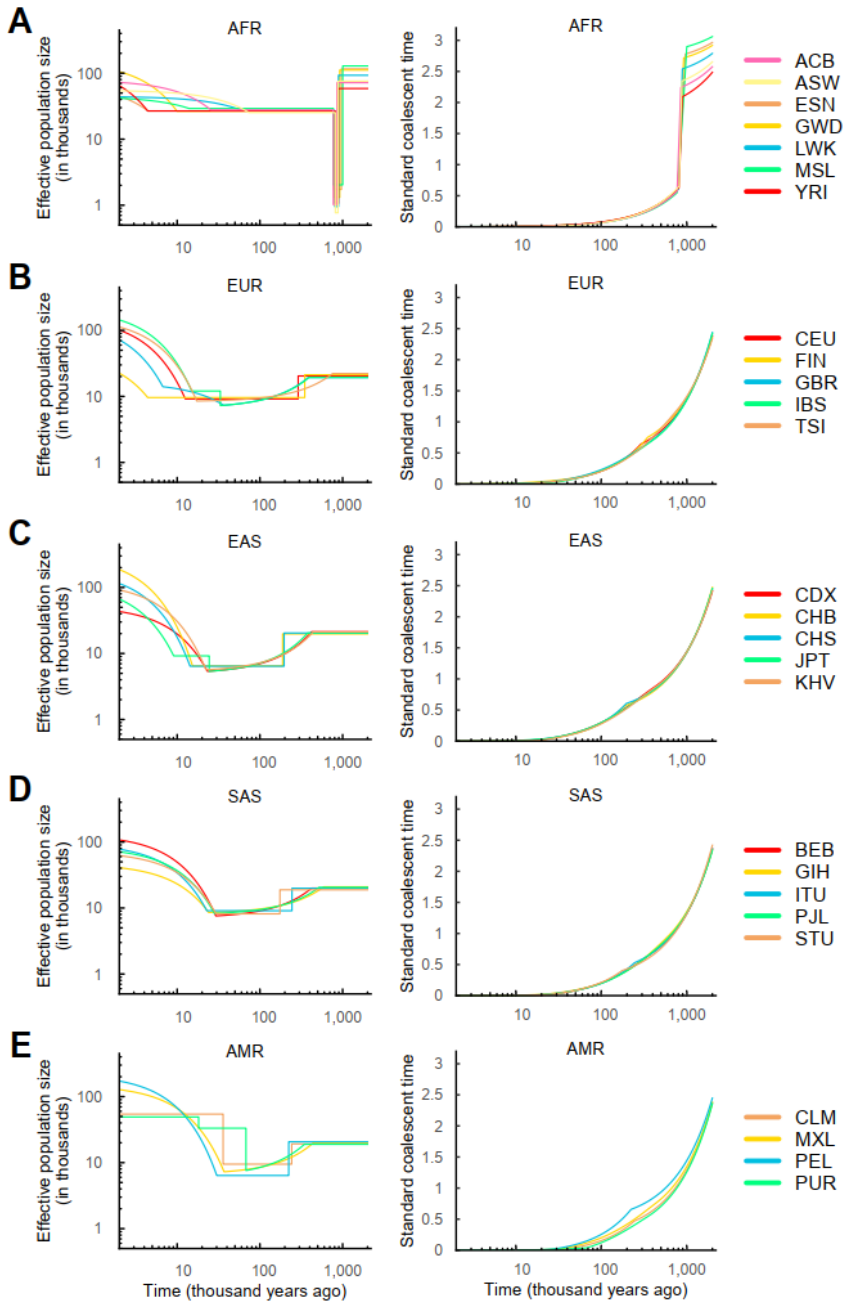

Fig. S7. FitCoal-inferred population size histories and standard coalescent time of various populations in 1000GP.

(**A**) African populations. (**B**) European populations. (**C**) East Asian populations. (**D**) South Asian populations. (**E**) American populations. Left panels show inferred population size histories, and right panels exhibit calendar time *vs* standard coalescent time. The results are the same as those in Fig. 3.

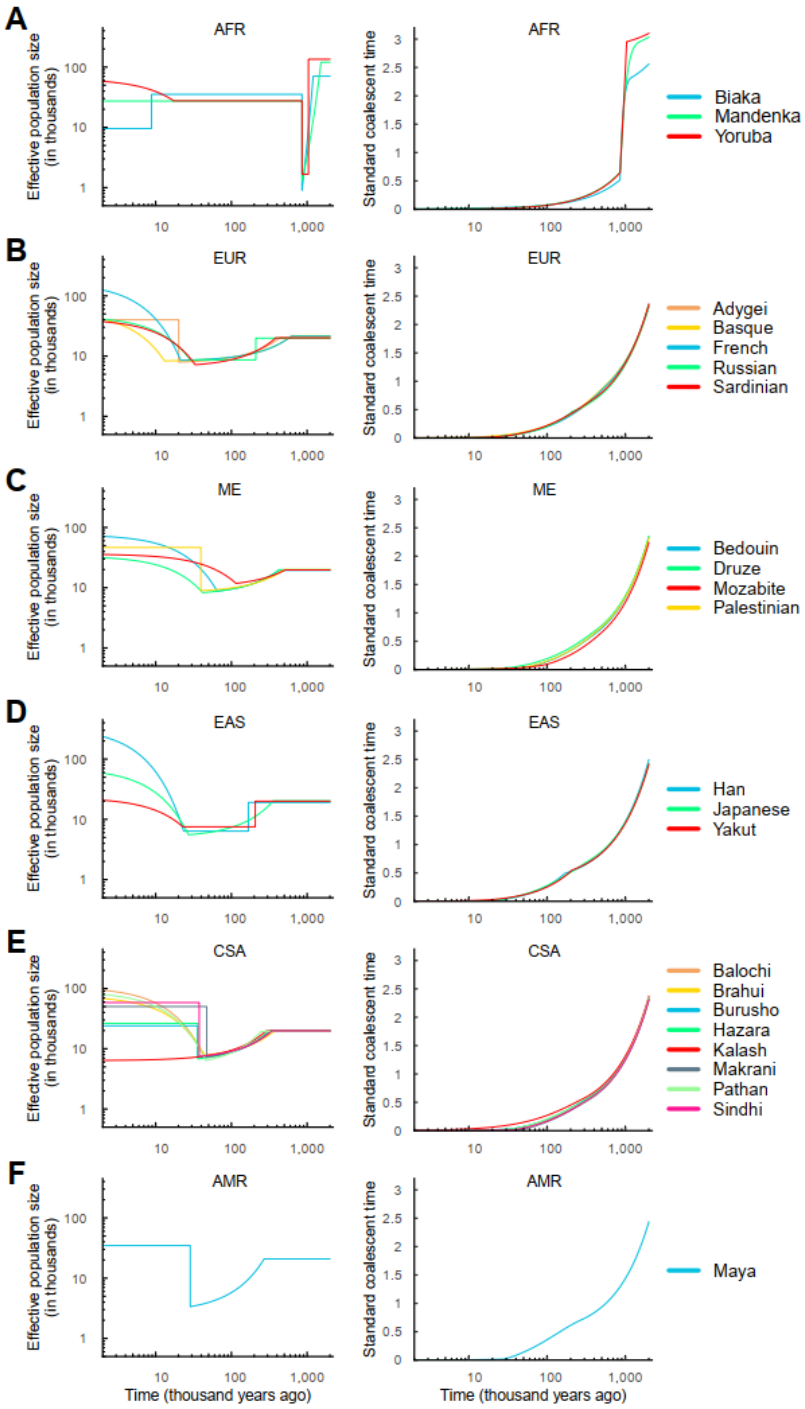

Fig. S8. FitCoal-inferred population size histories and standard coalescent time of various populations in the HGDP-CEPH panel.

(**A**) African populations. (**B**) European populations. (**C**) Middle East populations. (**D**) East Asian populations. (**E**) Central & South Asian populations. (**F**) American population. Left panels show inferred population size histories, and right panels exhibit calendar time *vs* standard coalescent time. The results are the same as those in Fig. 3.

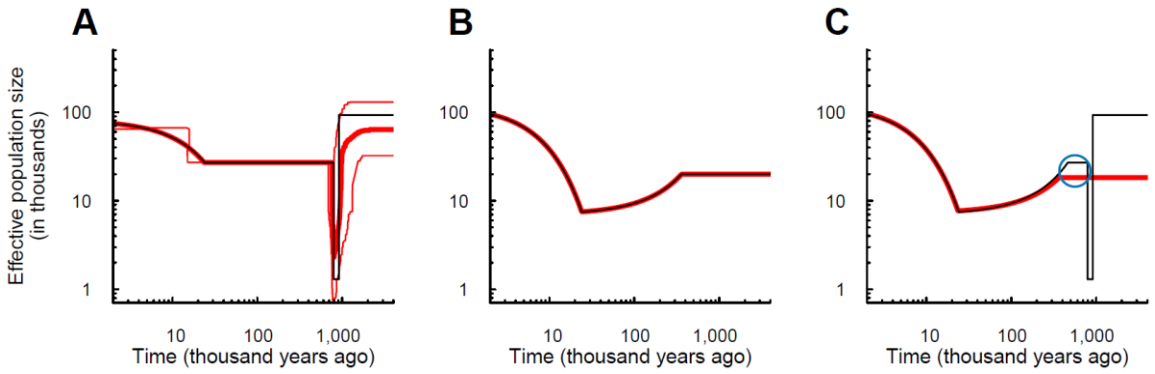

Fig. S9. Verification of the ancient severe bottleneck with short, simulated DNA fragments.
Demographic models are the same as those in Figs. 4A to C. The number of simulated sequences was set according to the cases in 1000GP. All models were simulated with 200 replications. For each replication, 800 Mb sequences were generated by simulating 80,000 fragments of 10 kb each. Black lines indicate true models. Thick red lines represent the medians of FitCoal estimated values; thin red lines denote 2.5 and 97.5 percentiles of the values. 10% of SFS types (categories) with high frequency mutations were discarded.
(**A**) Inferred population size histories with the African Bottleneck model (Bottleneck I model). The number of simulated sequences is 188.
(**B**) Inferred population size histories of Non-African demographic model without the ancient severe bottleneck (Bottleneck II model). The number of simulated sequences is 194.
(**C**) Inferred population size histories of Non-African demographic model with the ancient severe bottleneck (Bottleneck III model). The number of simulated sequences is 194. The blue circle indicates the population gap.

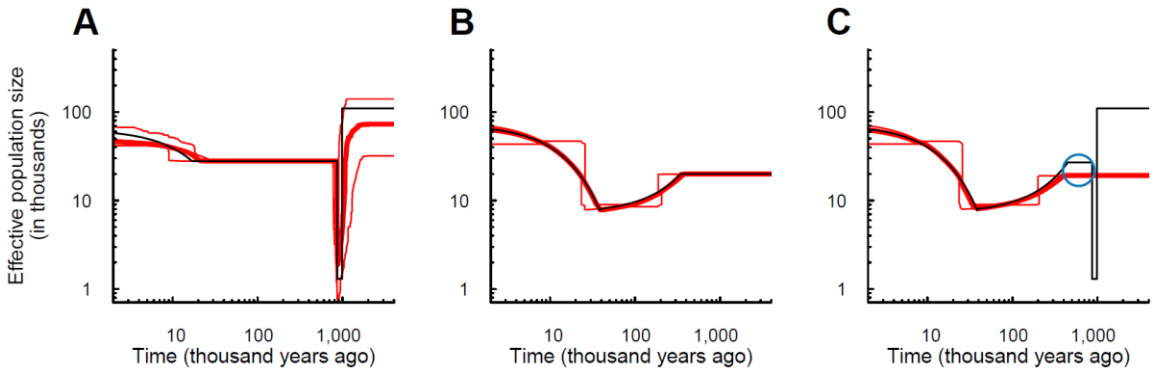

Fig. S10. Verification of the ancient severe bottleneck using parameters from the HGDP-CEPH panel.

Demographic models are very similar to those in Figs. 4A to C. The number of simulated sequences was set according to the cases in the HGDP-CEPH panel. All models were simulated with 200 replications. For each replication, 800 Mb sequences were generated by simulating 80,000 fragments of 10 kb each. Black lines indicate true models. Thick red lines represent the medians of FitCoal estimated values; thin red lines denote 2.5 and 97.5 percentiles of the values. 10% of SFS types (categories) with high frequency mutations were discarded.
(**A**) Inferred population size histories with the African Bottleneck model (Bottleneck I model). The number of simulated sequences is 44.
(**B**) Inferred population size histories of Non-African demographic model without the ancient severe bottleneck (Bottleneck II model). The number of simulated sequences is 56.
(**C**) Inferred population size histories of Non-African demographic model with the ancient severe bottleneck (Bottleneck III model). The number of simulated sequences is 56. The blue circle indicates the population gap.

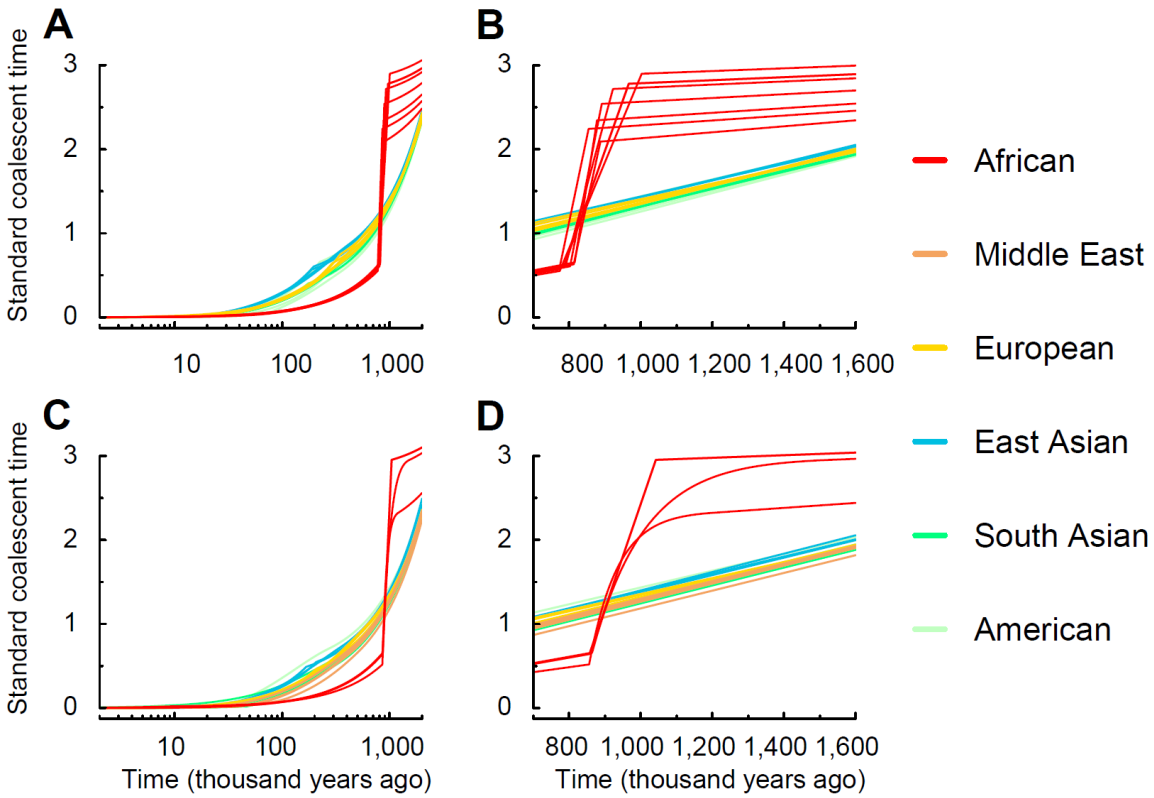

Fig. S11. Estimated standard coalescent time of human populations in 1000GP and the HGDP-CEPH panel.

(A) Calendar time *vs* standard coalescent time of populations in 1000GP. When the standard coalescent time increases, the number of lineages is reduced.
(B) Calendar time *vs* standard coalescent time of populations in 1000GP during the ancient severe bottleneck.
(C) Calendar time *vs* standard coalescent time of populations in the HGDP-CEPH panel.
(D) Calendar time *vs* standard coalescent time of populations in the HGDP-CEPH panel during the ancient severe bottleneck.

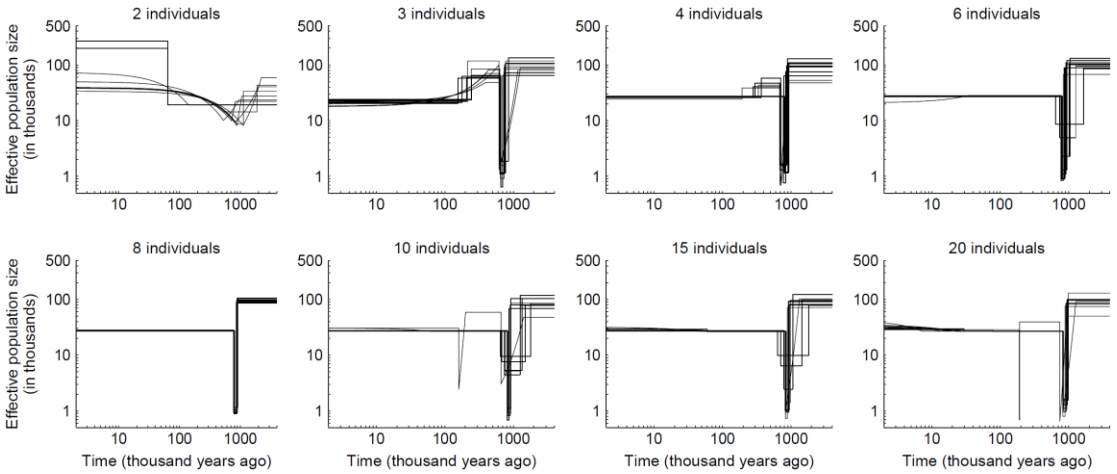

Fig. S12. FitCoal-inferred population size histories of YRI subsamples.

For each subpanel, ten random data sets were used. The number of truncated SFS types was 0, 0, 1, 2, 2, 4, 6, and 7, respectively. When the sample size was $\leq$ 3 individuals, the full SFS was used for analyses because excessive high frequency mutations were not found.

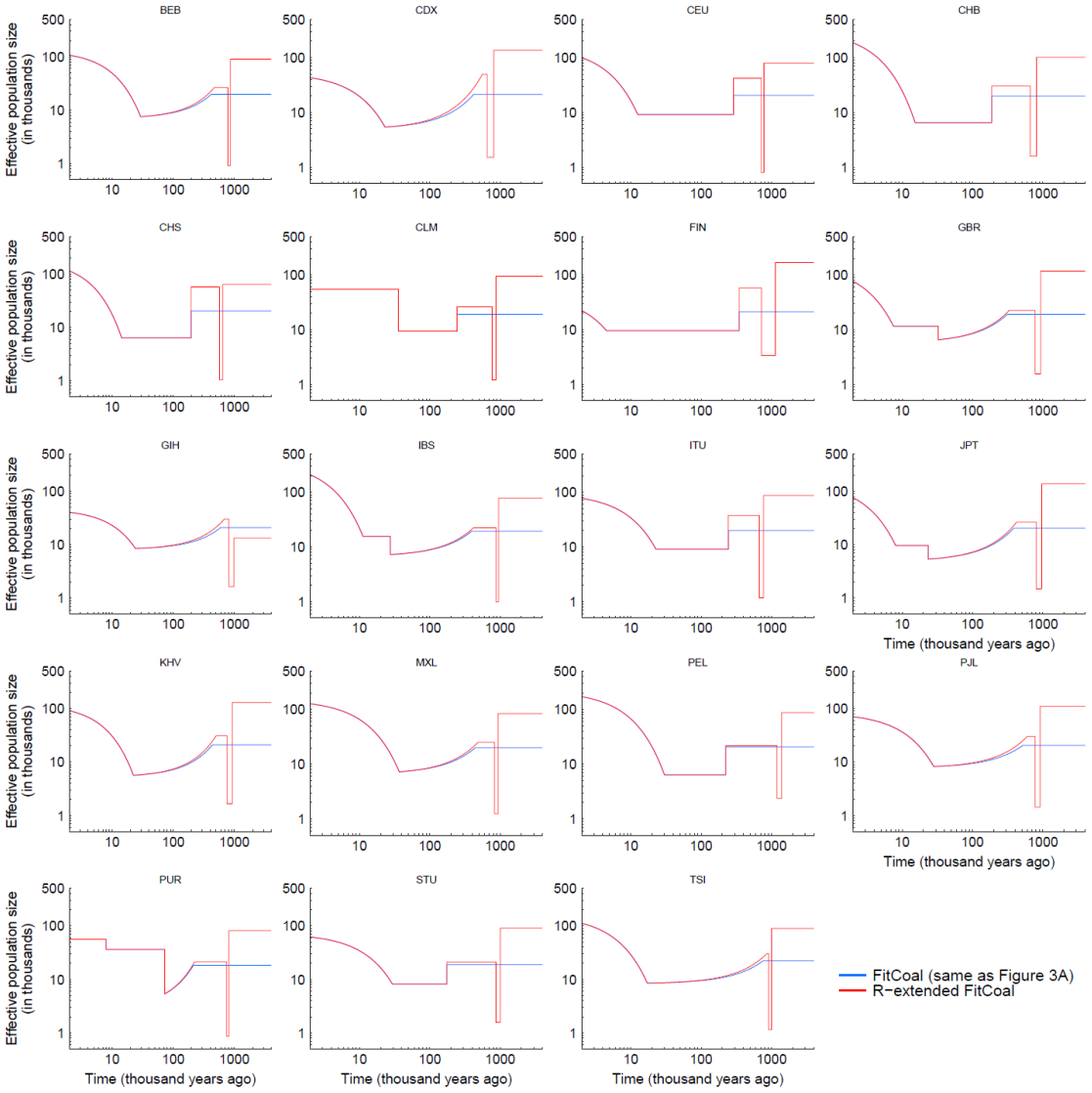

Fig. S13. The ancient severe bottleneck detected in 19 non-African populations in 1000GP using R-extended FitCoal.

Blue lines: FitCoal re-estimated population size histories using the same parameters as those used in Fig. 3A; Red lines: R-extended FitCoal-inferred population size histories.

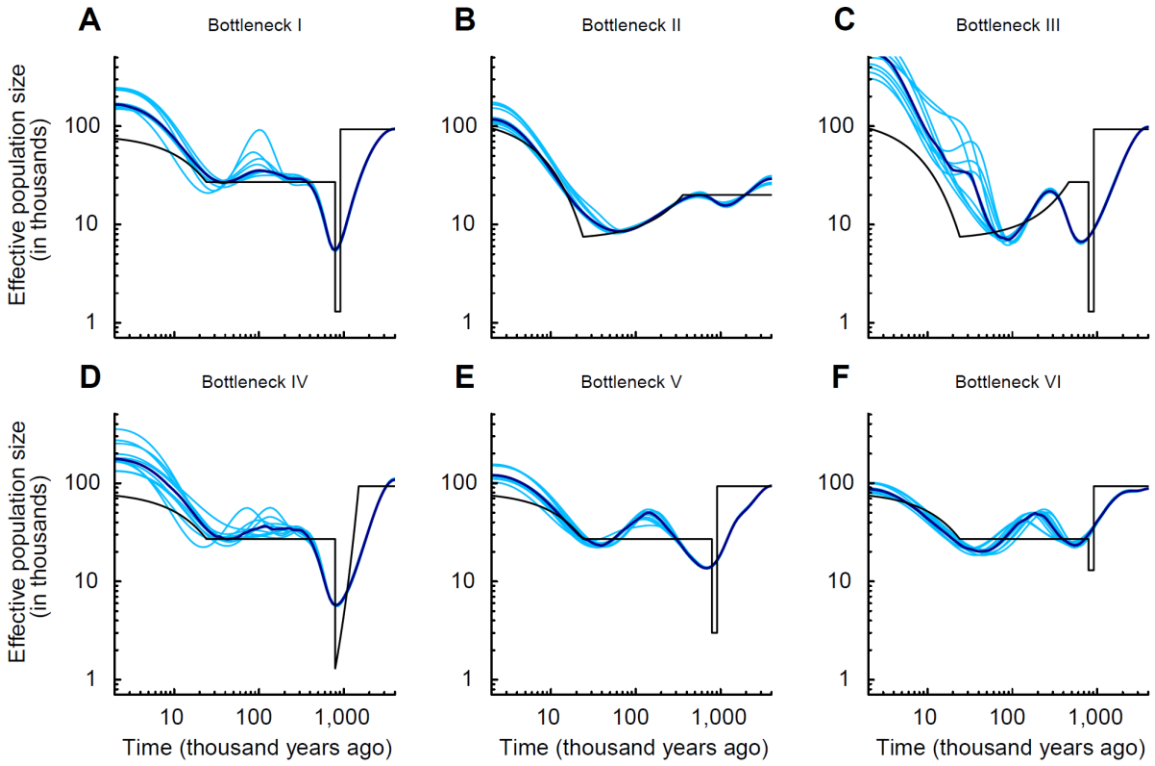

Fig. S14. SMC++ inferred population size histories with six different models in Fig. 4.
(**A**) Bottleneck I model, mimicking the true population size history of African agriculturalist populations. (**B**) Bottleneck II model, mimicking the inferred population size history of non-African populations. (**C**) Bottleneck III model, mimicking the true population size history of non-African populations. (**D**) Bottleneck IV model, mimicking a population with an exponential reduction 1.5 million years ago. (**E**) Bottleneck V model, mimicking a population with a moderate bottleneck. (**F**) Bottleneck VI model, mimicking a population with a weak bottleneck. Black lines indicate the true models as those presented in Fig 4. Blue lines indicate the 10 independently inferred population size histories by SMC++. Thick dark blue lines indicate medians of the 10 runs.

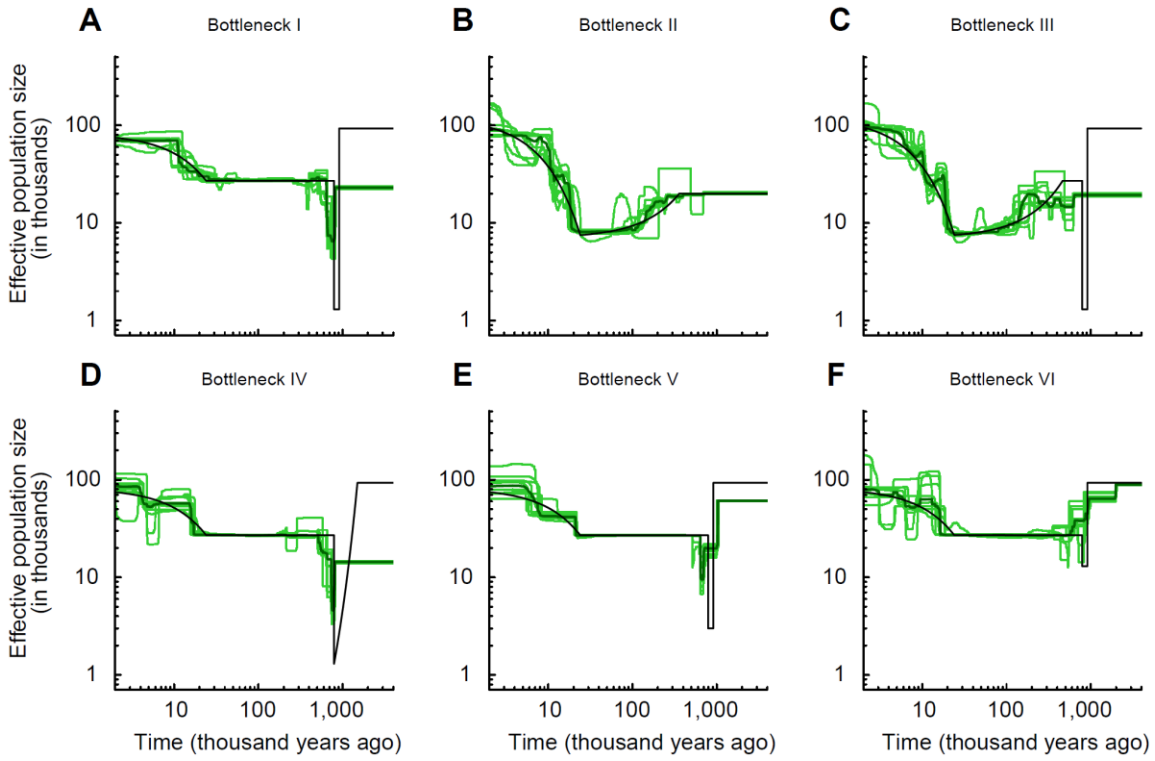

Fig. S15. Stairway Plot inferred population size histories with six different models in Fig. 4. (**A**) Bottleneck I model, mimicking the true population size history of African agriculturalist populations. (**B**) Bottleneck II model, mimicking the inferred population size history of non-African populations. (**C**) Bottleneck III model, mimicking the true population size history of non-African populations. (**D**) Bottleneck IV model, mimicking a population with an exponential reduction 1.5 million years ago. (**E**) Bottleneck V model, mimicking a population with a moderate bottleneck. (**F**) Bottleneck VI model, mimicking a population with a weak bottleneck. Black lines indicate the true models as those presented in Fig 4. Green lines indicate the 10 independently inferred population size histories by Stairway Plot. Thick dark green lines indicate medians of the 10 runs.

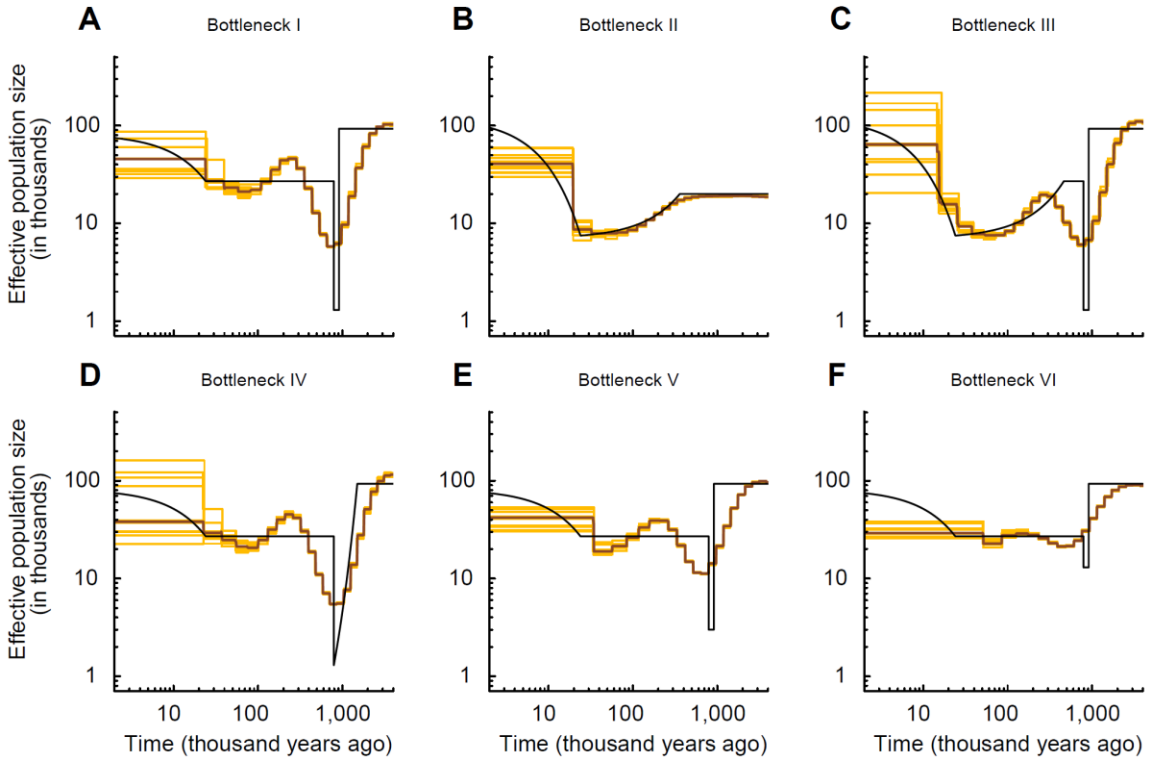

Fig. S16. PSMC inferred population size histories with six different models in Fig. 4.

(**A**) Bottleneck I model, mimicking the true population size history of African agriculturalist populations. (**B**) Bottleneck II model, mimicking the inferred population size history of non-African populations. (**C**) Bottleneck III model, mimicking the true population size history of non-African populations. (**D**) Bottleneck IV model, mimicking a population with an exponential reduction in size 1.5 million years ago. (**E**) Bottleneck V model, mimicking a population with a moderate bottleneck. (**F**) Bottleneck VI model, mimicking a population with a weak bottleneck. Black lines indicate the true models as those presented in Fig 4. Yellow lines indicate the 10 independently inferred population size histories by PSMC. Thick dark yellow lines indicate medians of the 10 runs.

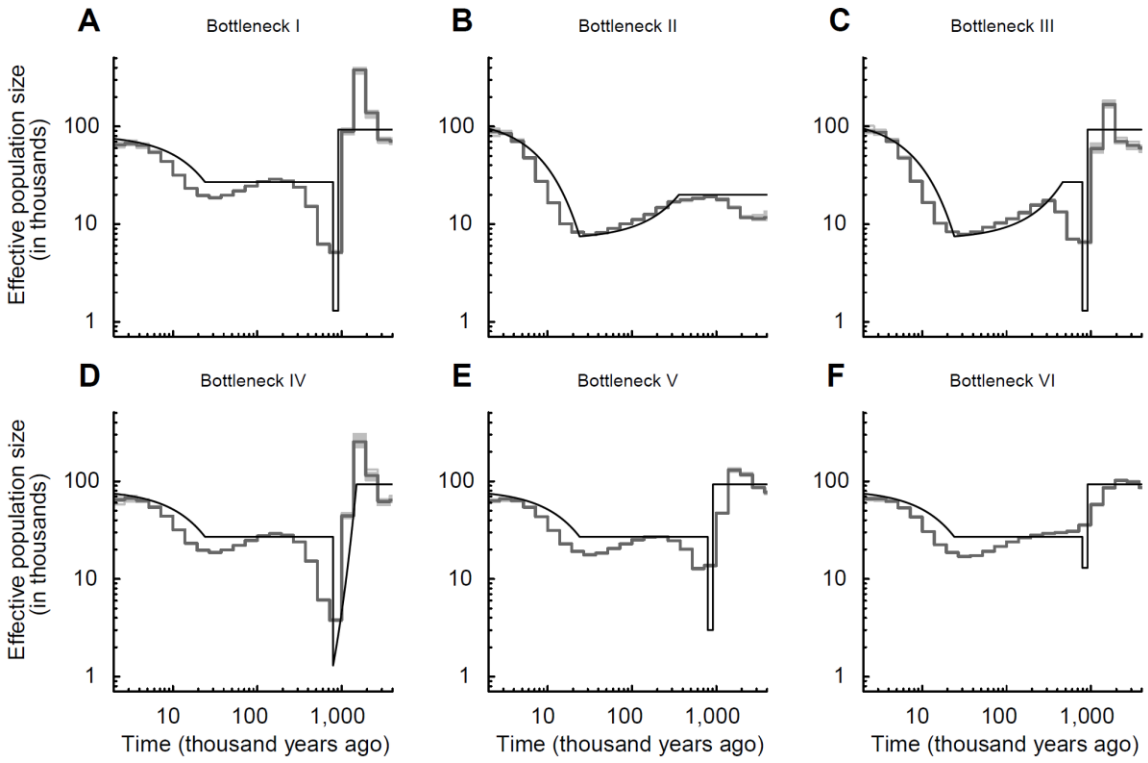

Fig. S17. Relate inferred population size histories with six different models in Fig. 4.
(**A**) Bottleneck I model, mimicking the true population size history of African agriculturalist populations. (**B**) Bottleneck II model, mimicking the inferred population size history of non-African populations. (**C**) Bottleneck III model, mimicking the true population size history of non-African populations. (**D**) Bottleneck IV model, mimicking a population with an exponential reduction 1.5 million years ago. (**E**) Bottleneck V model, mimicking a population with a moderate bottleneck. (**F**) Bottleneck VI model, mimicking a population with a weak bottleneck. Black lines indicate the true models as those presented in Fig 4. Grey lines indicate the 10 independently inferred population size histories by Relate. Thick dark grey lines indicate medians of the 10 runs.

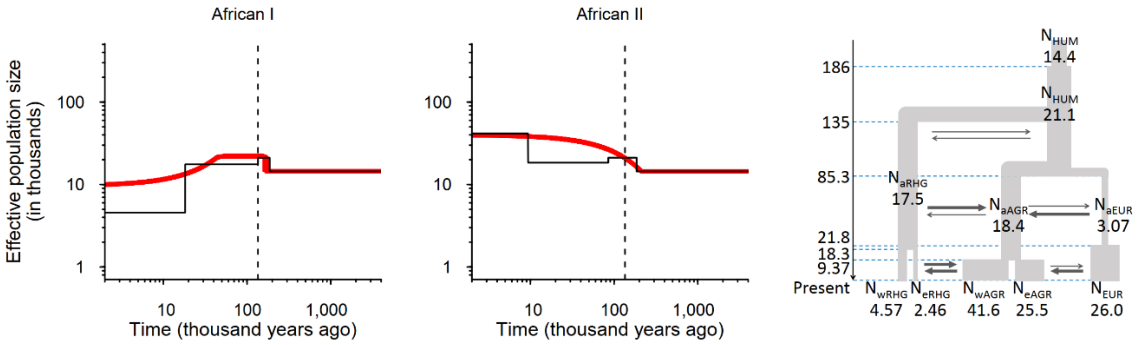

Fig. S18. Verification of FitCoal inference accuracy with a complex human population structure model.

FitCoal was used to estimate the demography of imaginary wRHG (African I) and wAGR (African II) populations. Split time and population sizes are shown in the right panel, in which the unit of time is 1,000 years, and the unit of population size is 1,000. In the left and middle panels, solid black lines indicate the true models. Thick red lines represent the medians of FitCoal estimated values; thin red lines are 2.5 and 97.5 percentiles of the estimated values. Dashed black lines indicate the split time of the two populations. The number of simulated sequences is 170. 200 replications were simulated under the model. For each replication, 800 Mb sequences were generated by simulating 80,000 fragments of 10 kb each. Truncated SFSs of simulated samples were used to infer the population size history.

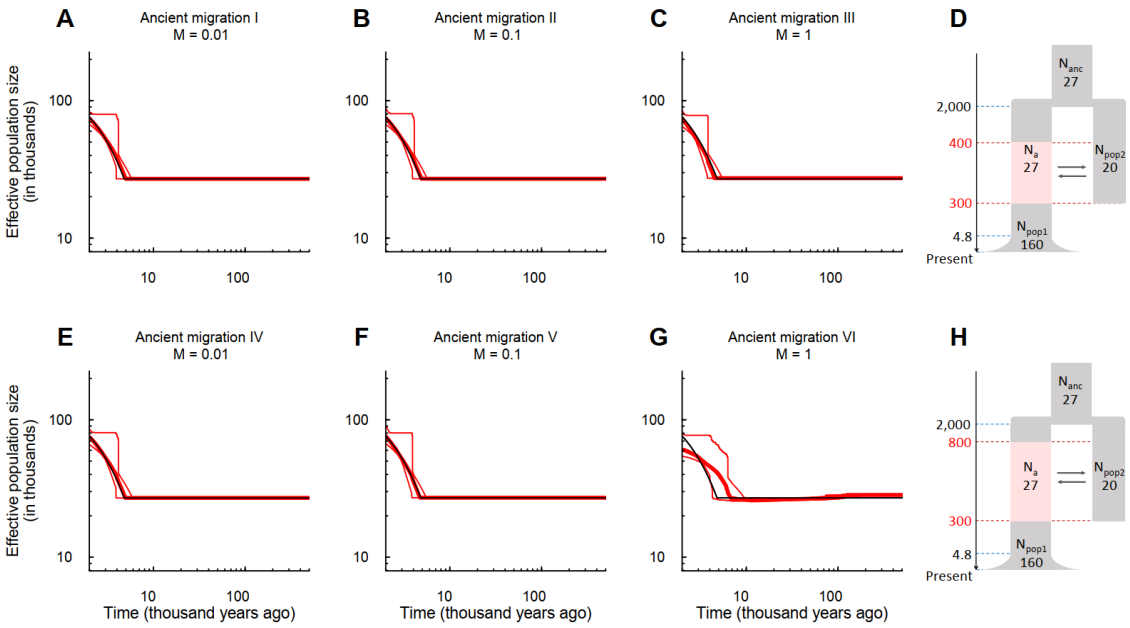

Fig. S19. Verification of FitCoal inference accuracy with an unknown hominin population.
Migration between a population (pop1) and an unknown population was analyzed with two models. In the first model, migration began at 400 kyr BP, and ended at 300 kyr BP (A-D). In the second model, migration began at 800 kyr BP, and ended at 300 kyr BP (E-H). The unit of time is 1,000 years, and the unit of population size is 1,000. *M* is the migration rate ($4Nm$). The pink box in panels D and H indicates the period of migration. The number of simulated sequences is 170, and 200 replications were simulated with each demographic model. For each replication, 800 Mb sequences were generated by simulating 80,000 fragments of 10 kb each. Truncated SFSs were used in FitCoal analysis. Solid black lines indicate the true models. Thick red lines represent the medians of FitCoal estimated values; thin red lines are 2.5 and 97.5 percentiles of the values.

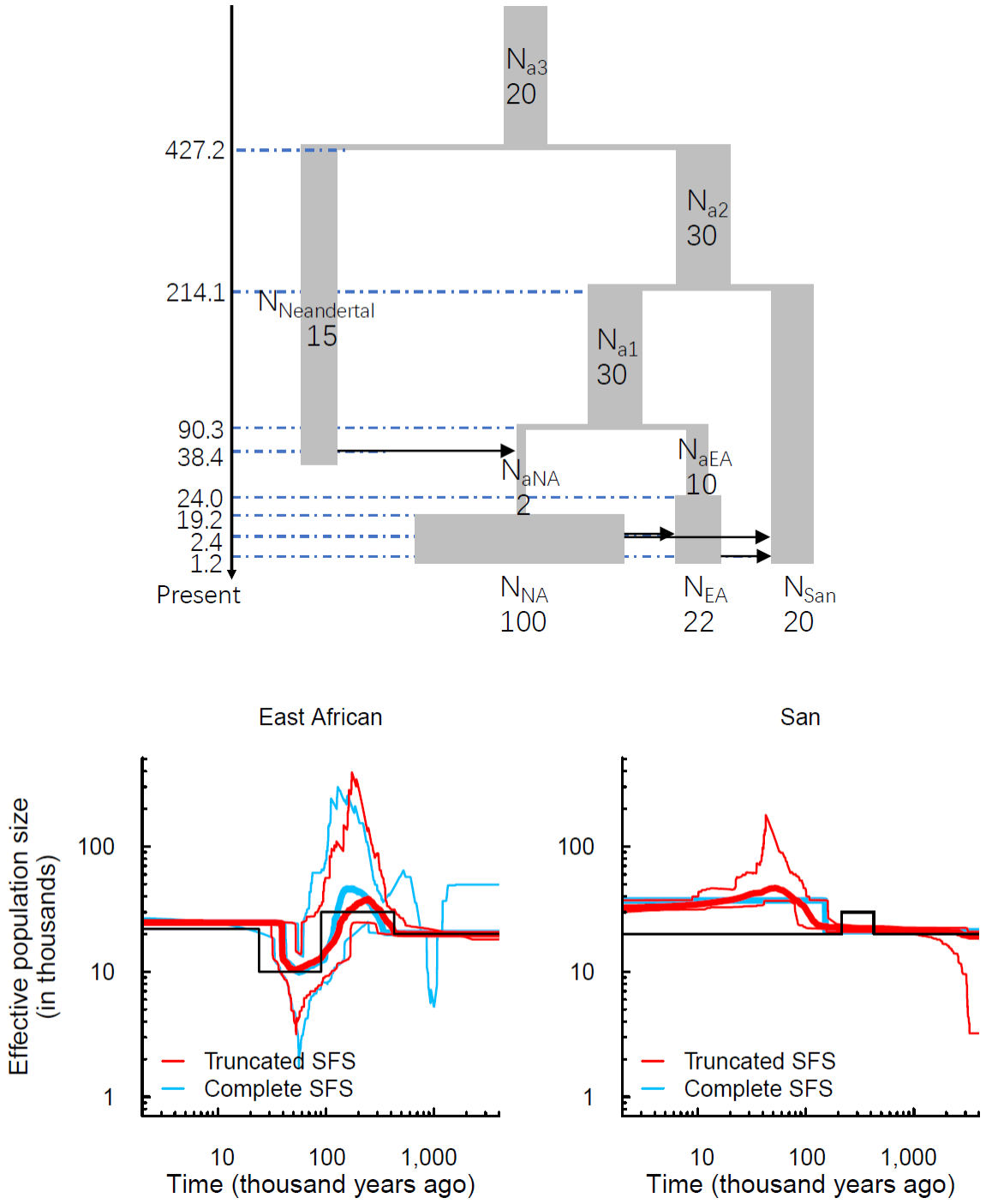

Fig. S20. Verification of inference accuracy with an African structured population model. Values in the upper panel are those of time (unit: 1,000 years) and population sizes (unit: 1,000). The generation time is 24 years. NA: non-African; EA: East African. The modelling was based on the following assumptions: The San population received $0.1N_{EA}$ gene flow from the East African population 50 generations ago and $0.04N_{NA}$ gene flow from the non-African population 100 generations ago. N_{EA} is the effective population size of the East African population, and N_{NA} is the effective population size of the non-African population at the time of pulsed introgression.

The East African population received $0.04N_{NA}$ gene flow from the non-African population 100 generations ago, and the non-African population received $0.02N_{Neander}$ gene flow from the Neanderthal population. $N_{Neanderthal}$ is the effective population sizes of the Neanderthal population at the time of pulsed introgression. The sample size was 188 for each population. 200 simulated replicates were analyzed to obtain the confidence interval of estimated history. For each replicate, 800 Mb sequences were generated by simulating 8 fragments of 100 Mb each. Results are shown in the two lower panels. Both full (blue lines) and truncated (10%) (red lines) SFS types were used for FitCoal analyses. Black lines indicate the true models. Thick lines indicate the medians of FitCoal estimated values; thin lines are 2.5 and 97.5 percentiles of the values.

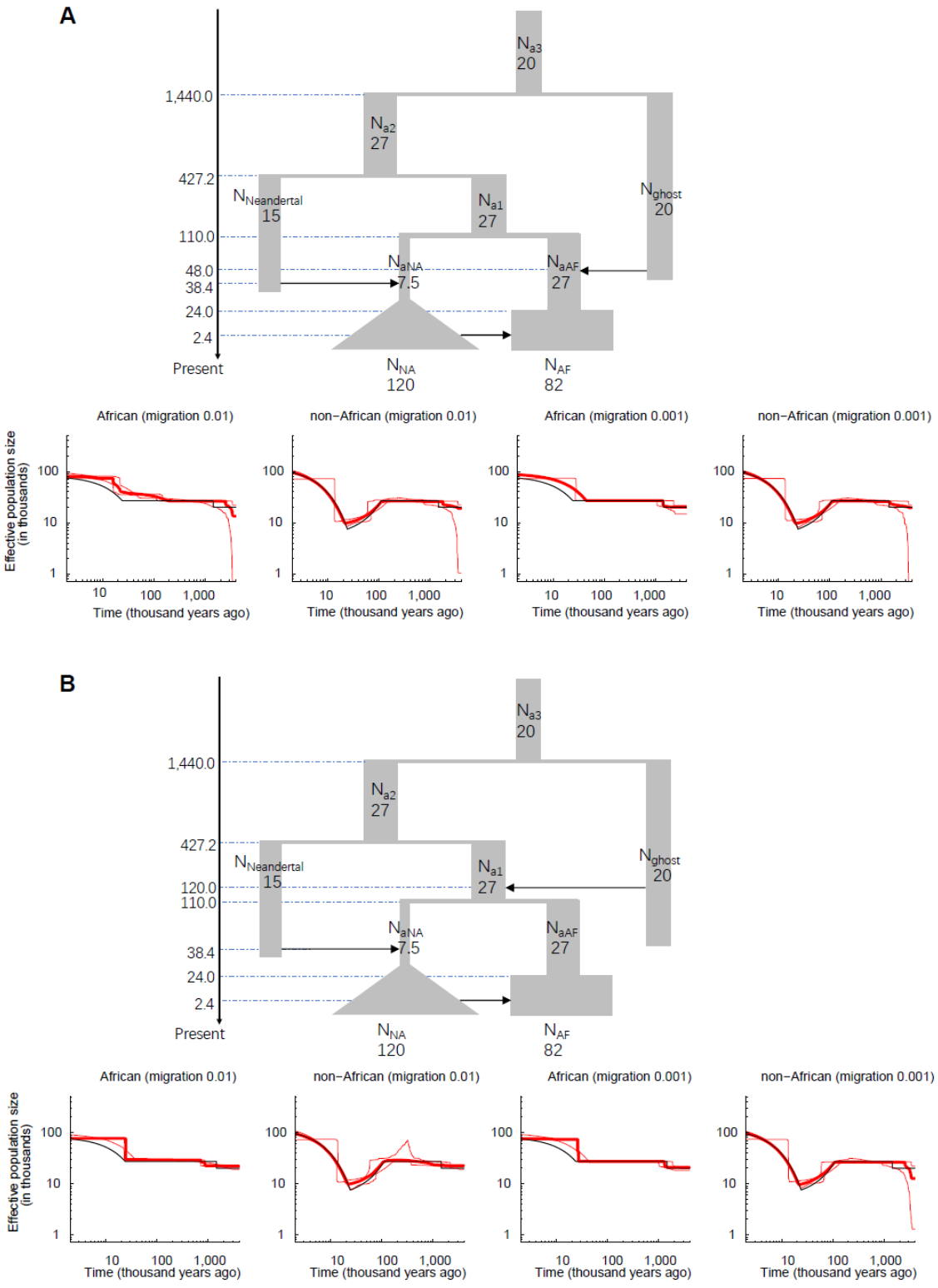

Fig. S21. Verification of inference accuracy with two archaic pulsed introgression models.
Values in the upper panel are those of time (unit: 1,000 years) and population sizes (unit: 1,000). The generation time is 24 years. NA: non-African; AF: African. The modelling was based on the following assumptions: (**A**) The African population received gene flow from the ghost

population 2,000 generations ago. The African population received $0.04N_{NA}$ 100 generations ago, and the non-African population received $0.02N_{Neanderthal}$ 1,600 generations ago. N_{NA} and $N_{Neanderthal}$ are effective population size of non-African and Neanderthal populations, respectively. (**B**) Both African and non-African populations received gene flow from a ghost population 5,000 generations ago. 200 simulated replicates were analyzed to obtain the confidence interval of estimated history. For each replicate, 800 Mb sequences were generated by simulating 8 fragments of 100 Mb each. The sample size is 188 for African population and 194 for non-African population. Black lines indicate the true models. Thick red lines indicate the medians of FitCoal estimated values; thin red lines denote 2.5 and 97.5 percentiles of the values.

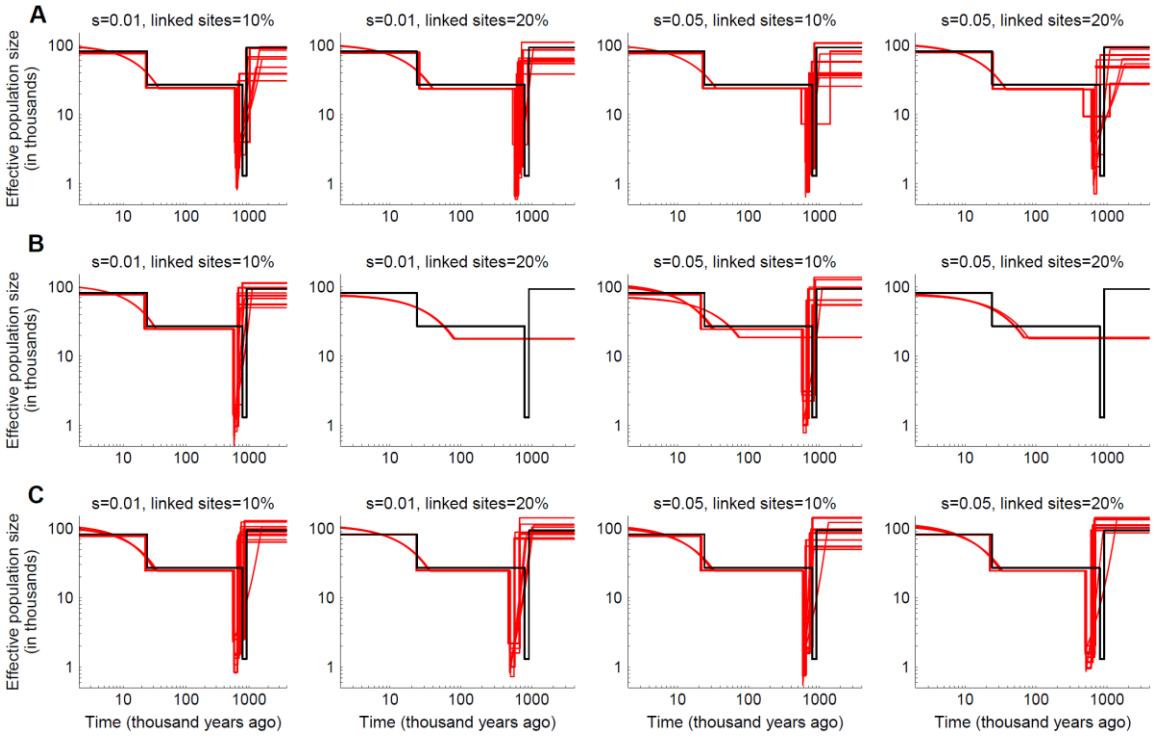

Fig. S22. Effects of positive selection on FitCoal analysis with a bottleneck model mimicking African human populations.

$n = 202$. Each scenario was examined with 10 replications. The true model was indicated by black line. Inferred population size histories were presented with red lines.

(**A**) Inferred population size histories using truncated SFSs. The last 21 SFS categories with high frequency mutations were excluded from the analysis.

(**B**) Inferred population size histories using full size (complete) SFSs.

(**C**) Inferred population size histories using full size (complete) SFSs with four time intervals.

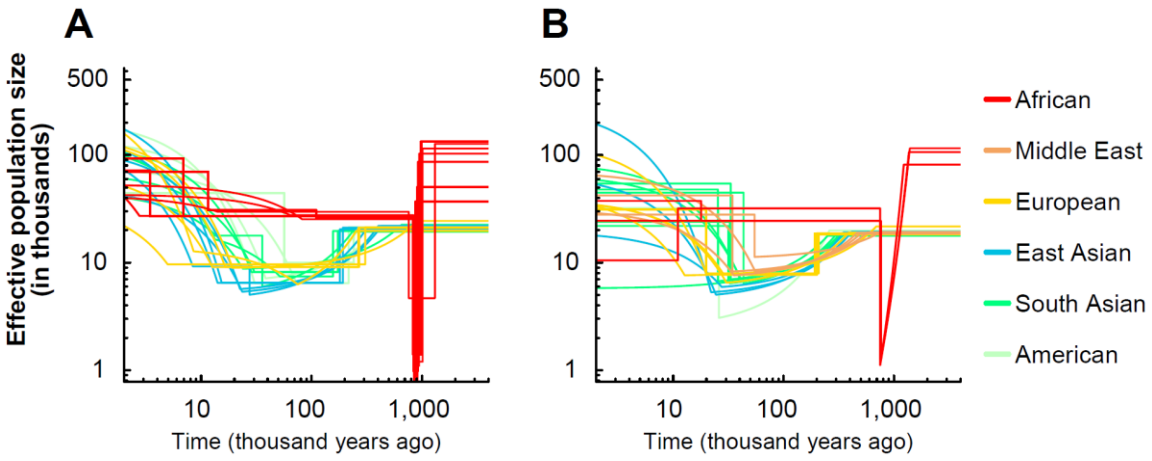

Fig. S23. FitCoal-inferred population size histories of human populations using remote non-coding regions at least 10kb away from coding regions.

(**A**) Inferred population size histories of 26 populations in 1000GP. (**B**) Inferred population size histories of 24 populations in the HGDP-CEPH panel. Various color lines indicate the following: red, African populations; yellow, European populations; brown, Middle East populations; blue, East Asian populations; green, Central or South Asian populations; and dark sea green, American populations.

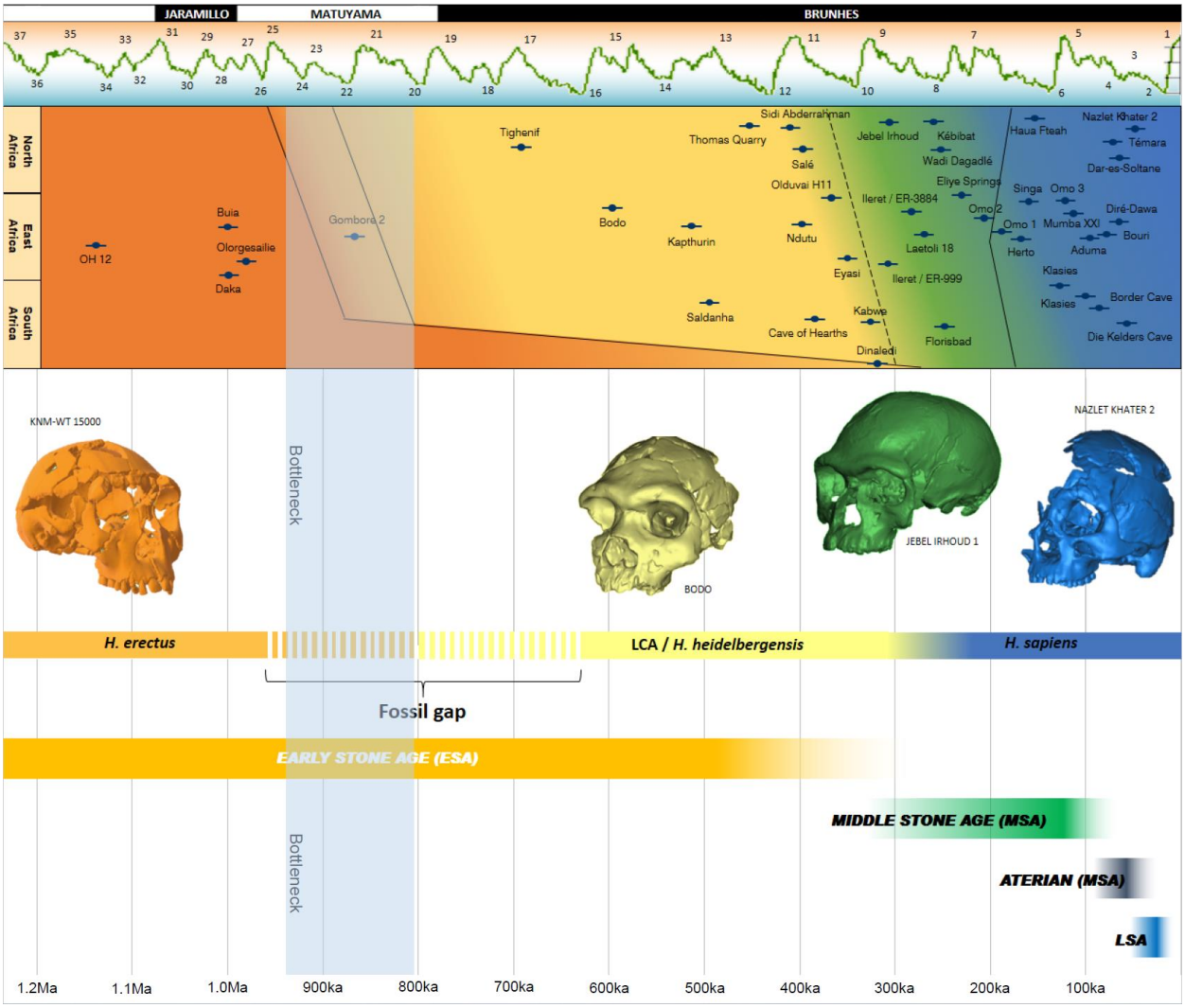

Fig. S24. Distribution of the hominin fossil record in Africa from late Early Pleistocene.
Sites in North, East, and South Africa with dated human fossil specimens are shown. Various colours indicate changes in morphology and lithic culture. Images of crania are purely indicative (the skull KNM-WT 15000 is about 1.6 Ma). Records of paleomagnetic dates, climatic changes (above), and major stages of the African Palaeolithic (below) are also shown. A gap with very few fossil samples is apparent between roughly 950 and 650 kyr BP. This period coincides with the time span of the severe bottleneck (930 – 813 kyr BP, highlighted in pale blue). Data were adopted and modified from a variety of previous studies (*91-95*) and images were surface scans of hominin casts produced by the Laboratory of Paleoanthropology and Bioarchaeology of Sapienza University in Rome.

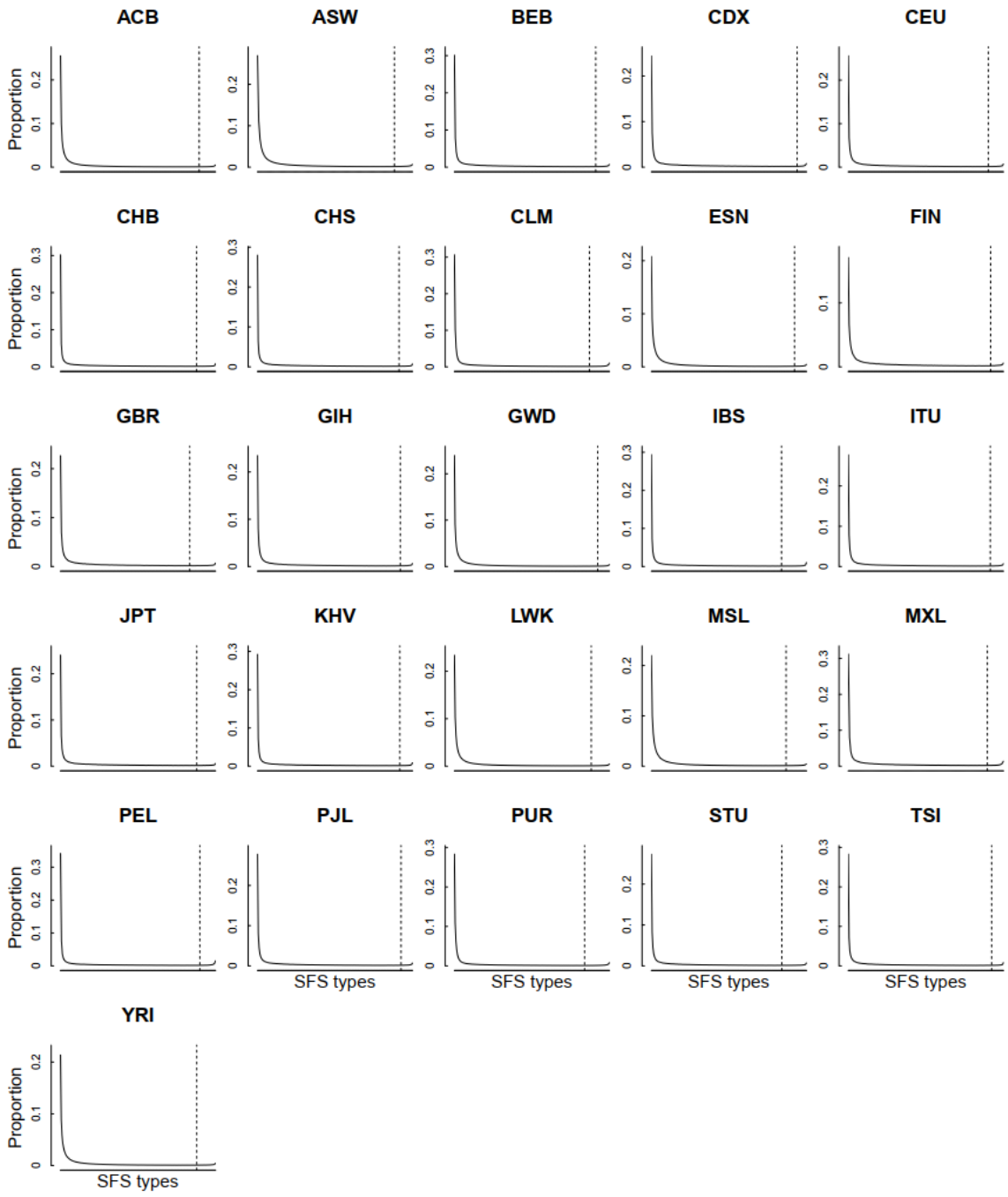

Fig. S25. Observed SFSs of populations in 1000GP.

Solid lines indicate observed SFSs. The *x*-axis represents SFS types (categories) with values ranging from 1 to $(n-1)$. The left side of the *x*-axis indicates rare mutations, and the right side indicates high frequency mutations. The y-axis indicates proportions of mutations. Dashed lines indicate the cut-off threshold for SFS truncation.

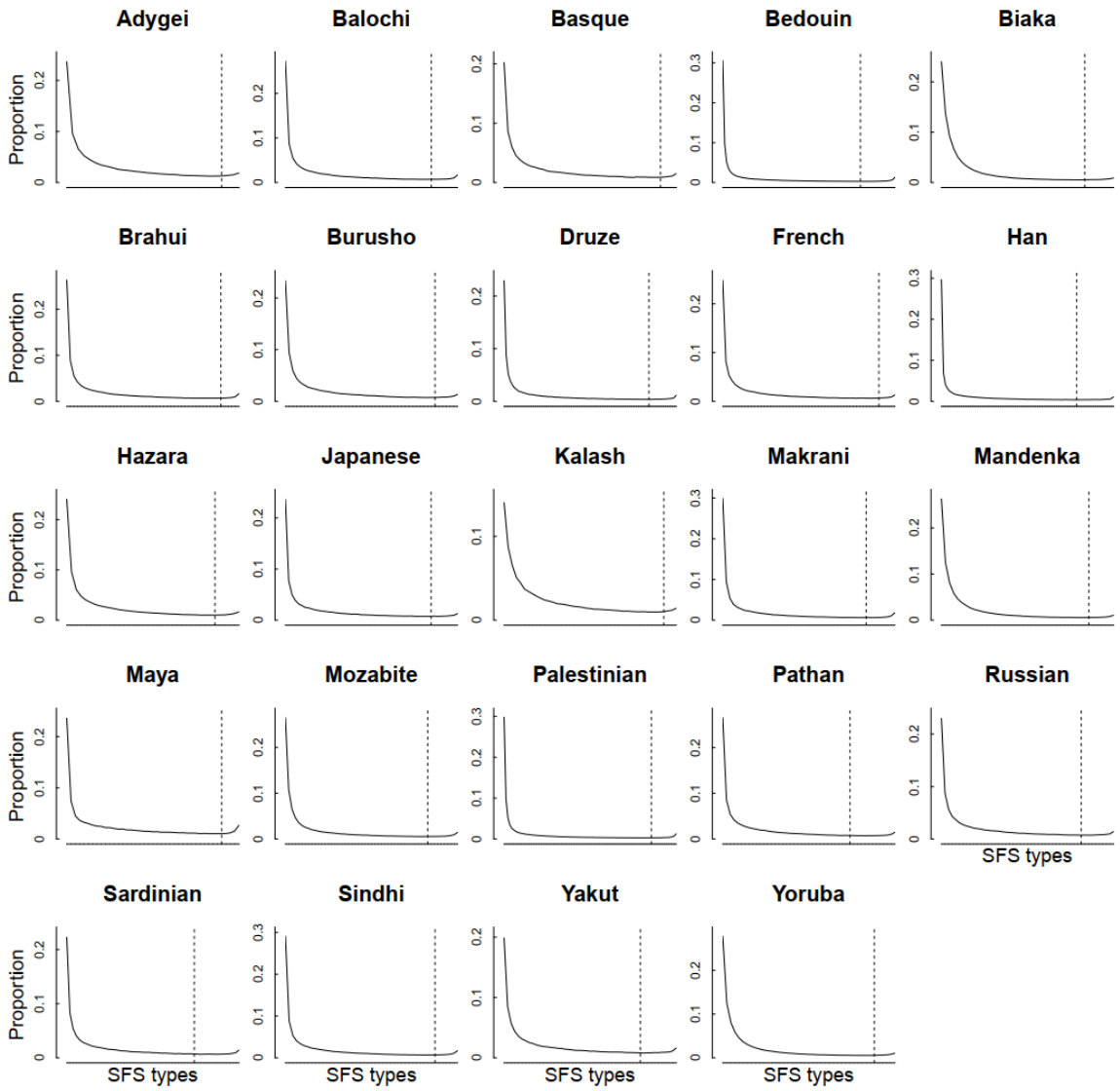

Fig. S26. Observed SFSs without missing data of populations in the HGDP-CEPH panel. Solid lines indicate observed SFSs. The *x*-axis represents SFS types (categories) with values ranging from 1 to $(n-1)$. The left side of the *x*-axis indicates rare mutations, and the right side indicates high frequency mutations. The y-axis indicates proportions of mutations. Dashed lines indicate the cut-off threshold for SFS truncation.

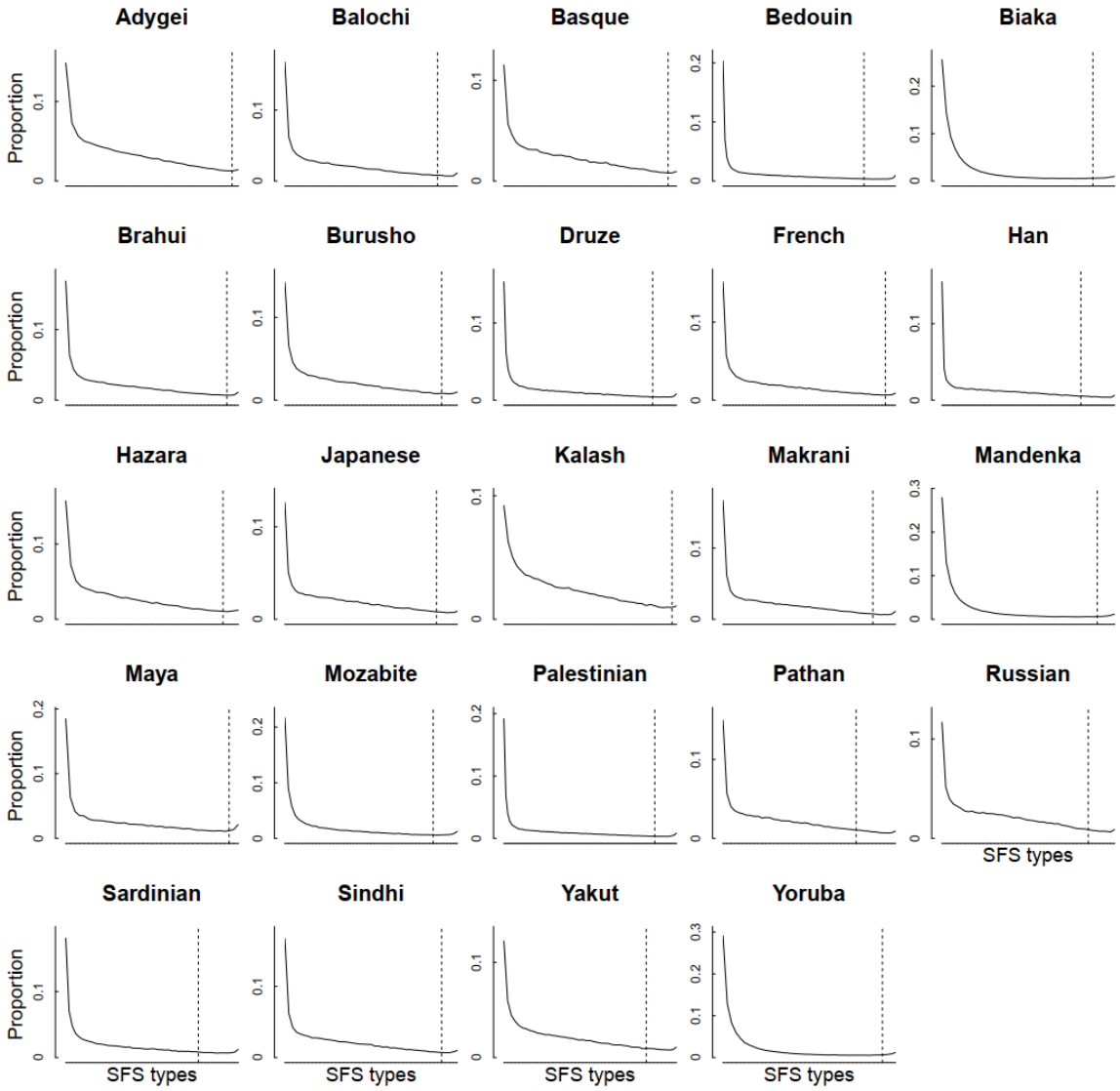

Fig. S27. Observed SFSs (with one individual missing) of populations in the HGDP-CEPH panel.

Solid lines indicate observed SFSs. The *x*-axis represents SFS types (categories) with values ranging from 1 to $(n-3)$. The left side of the *x*-axis indicates rare mutations, and the right side indicates high frequency mutations. The y-axis indicates proportions of mutations. Dashed lines indicate the cut-off threshold for SFS truncation.

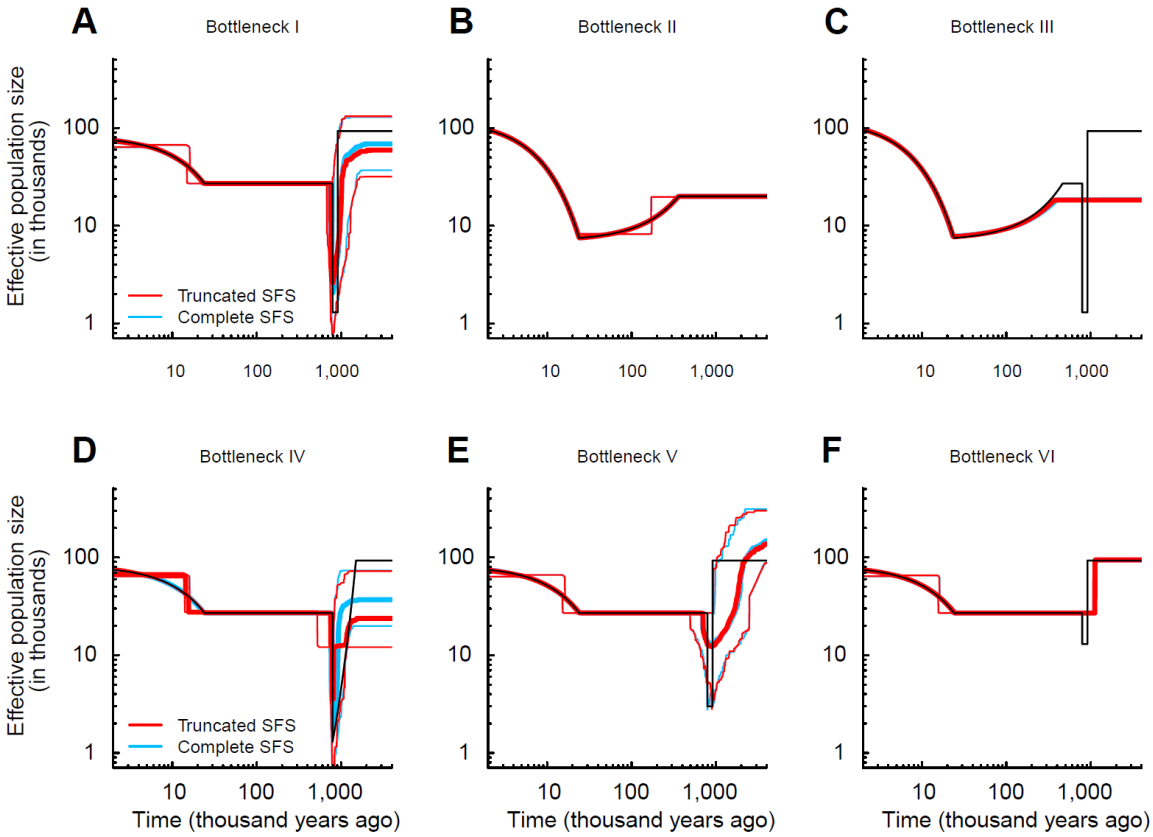

Fig. S28. FitCoal-inferred population size histories with six different models using complete and truncated SFSs.

Black lines indicate the true models as those presented in Fig. 4. Thick red lines indicate the medians, and thin red lines indicate 2.5 and 97.5 percentiles of FitCoal estimated values using truncated SFSs. Thick blue lines indicate the medians of FitCoal estimated values, and thin blue lines indicate 2.5 and 97.5 percentiles of the values using complete SFSs.

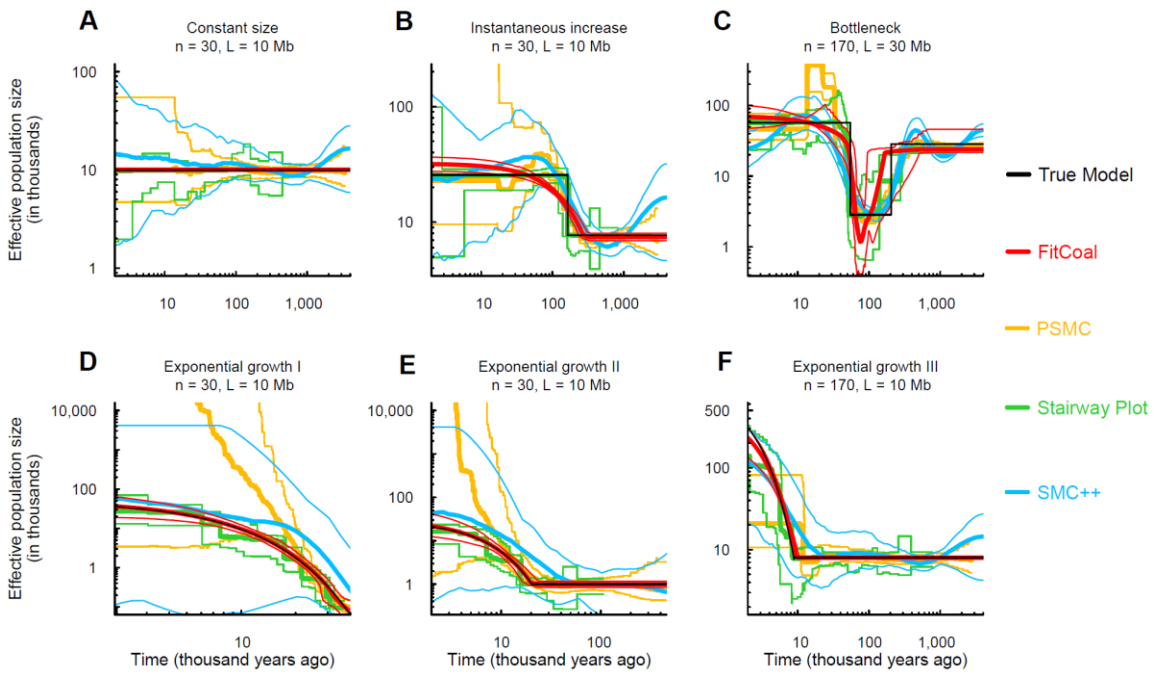

Fig. S29. Population size histories inferred by FitCoal (conditional on exponential changes), PSMC, Stairway Plot, and SMC++ using simulated samples.

(**A**) Constant size model. (**B**) Instantaneous increase model. (**C**) Bottleneck model. (**D**) Exponential growth I model. (**E**) Exponential growth II model. (**F**) Exponential growth III model. *L* is the length of simulated sequences, and *n* is the number of sequences. Black lines indicate the true models. Thick red lines are the medians of FitCoal estimated values. Yellow, green and blue lines indicate the population size histories inferred by PSMC, Stairway Plot, and SMC++, respectively. Other parameters are the same as those in Fig. 2.

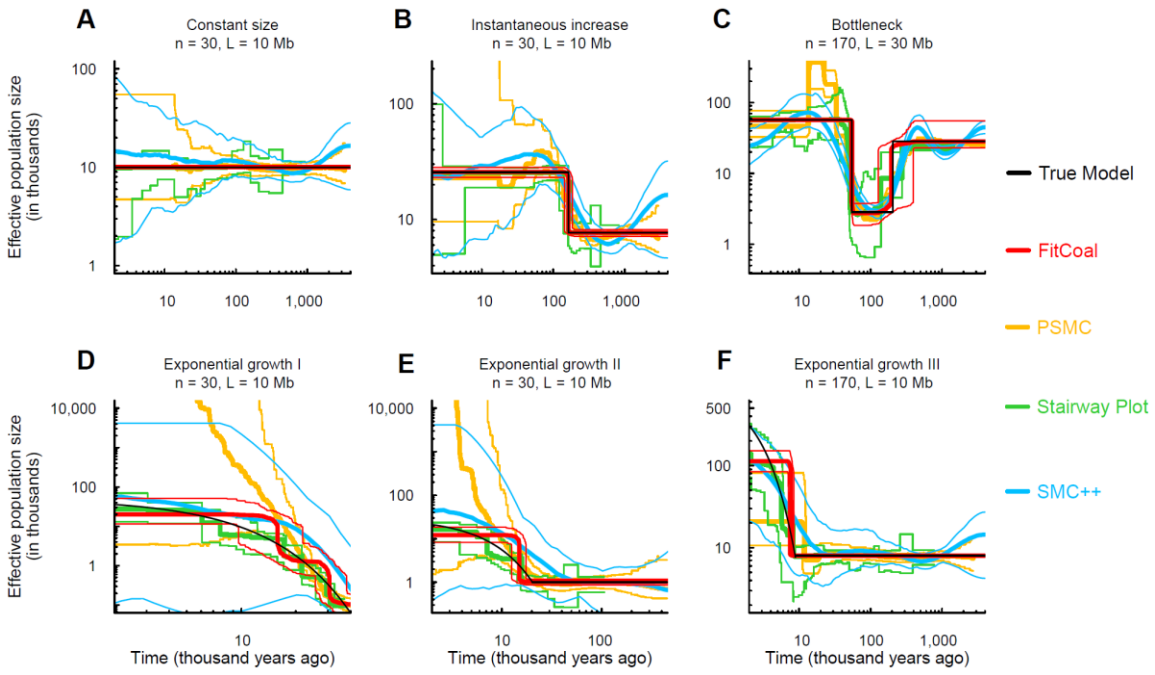

Fig. S30. Population size histories inferred by FitCoal (conditional on instantaneous changes), PSMC, Stairway Plot, and SMC++ using simulated samples.

(**A**) Constant size model. (**B**) Instantaneous increase model. (**C**) Bottleneck model. (**D**) Exponential growth I model. (**E**) Exponential growth II model. (**F**) Exponential growth III model. *L* is the length of simulated sequences, and *n* is the number of sequences. Black lines indicate the true models. Thick red lines are the medians of FitCoal estimated values. Yellow, green and blue lines indicate the population size histories inferred by PSMC, Stairway Plot, and SMC++, respectively. Other parameters are the same as those in Fig. 2.

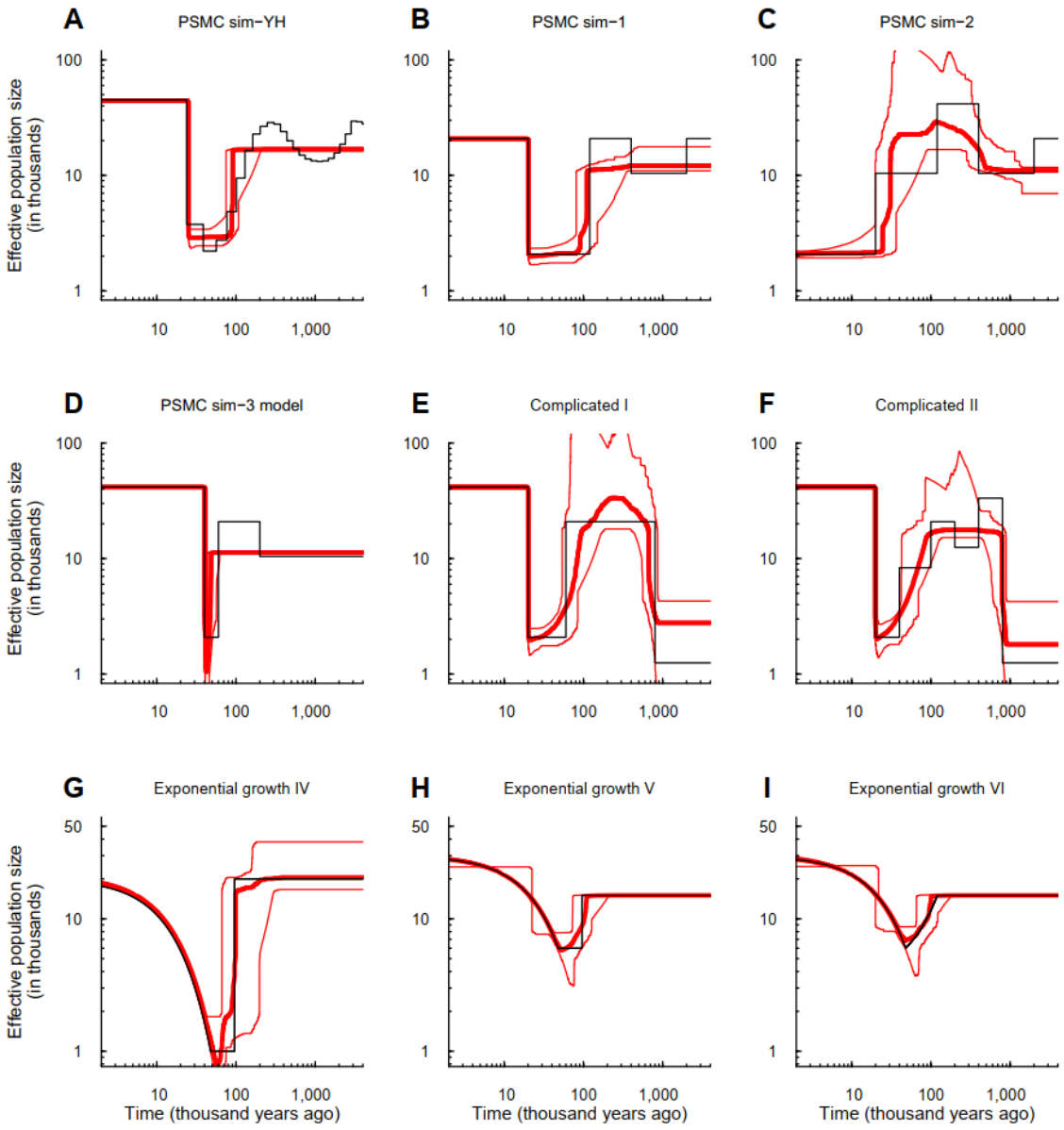

Fig. S31. Verification of FitCoal accuracy in simulations using complete SFSs under more complexed models.

(**A**) PSMC sim-YH model. (**B**) PSMC sim-1 model. (**C**) PSMC sim-2 model. (**D**) PSMC sim-3 model. (**E**) Complicated I model. (**F**) Complicated II model. (**G**) Exponential growth IV model. (**H**) Exponential growth V model. (**I**) Exponential growth VI model. Black lines indicate the true models. Thick red lines are the medians of FitCoal estimated values; thin red lines represent 2.5 and 97.5 percentiles of the values. The number of simulated sequences is 170, and the length of each simulated sequence is 100Mb. Complete SFSs were used in the analysis. Other parameters are the same as those in Fig. 2.

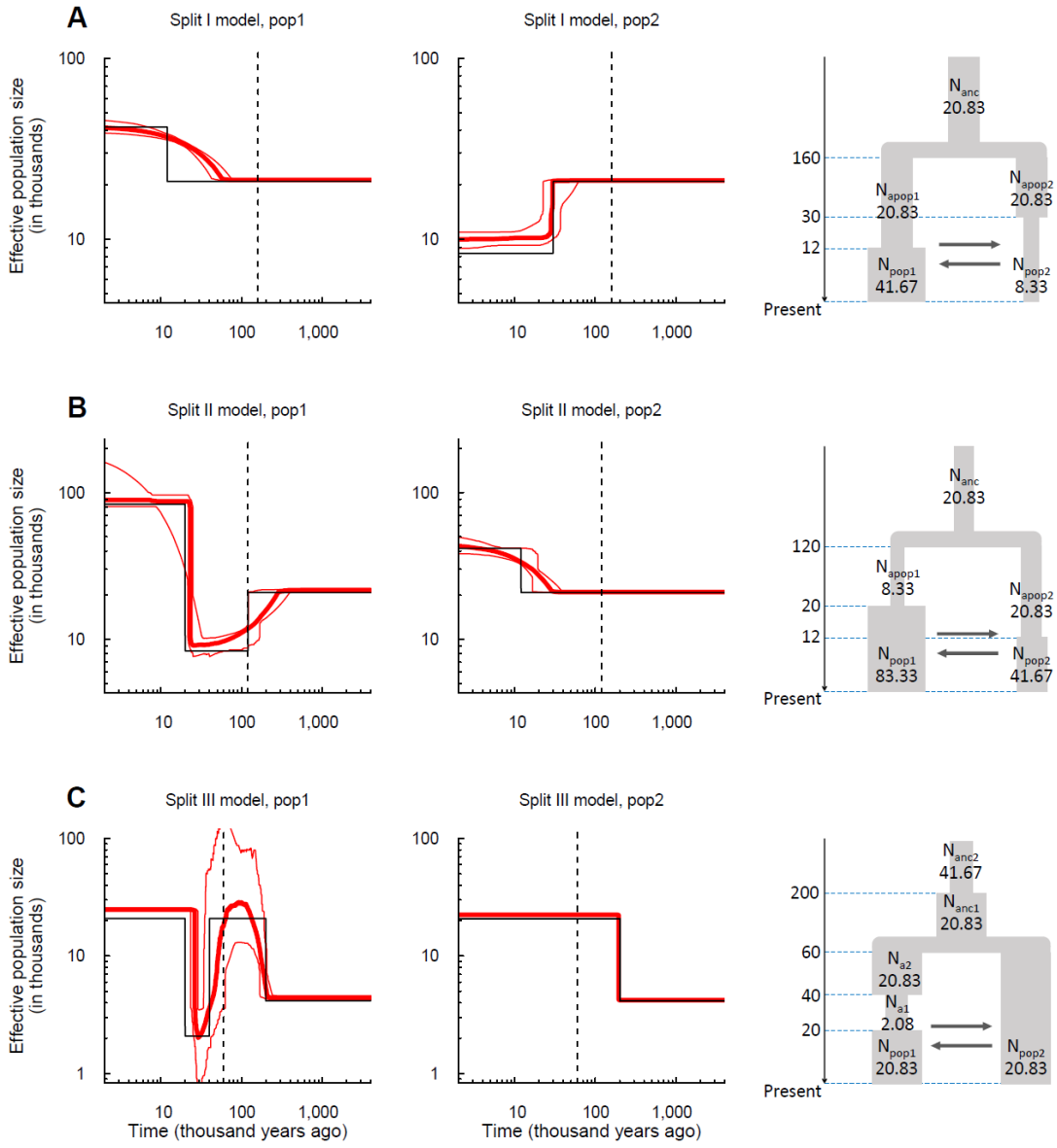

Fig. S32. Verification of FitCoal accuracy with three migration models.

Values in right panels are those of time (unit: 1,000 years) and population sizes (unit: 1,000). Solid black lines indicate the true models. Black dashed lines indicate the time of population split. Thick red lines are the medians of FitCoal estimated values; thin red lines are 2.5 and 97.5 percentiles of the values. The number of simulated sequences is 170, and the migration rate ($4Nm$) is 4. The length of simulated sequences each is 30Mb in models A and B, and 100Mb each in model C. Other parameters are the same as those in Fig. 2.

(**A**) Inferred demographic histories of two populations (pop1 and pop2) with Split I model. This model assumes that the two populations split at 160 kyr BP, that the first population had an instantaneous growth, and that the second one had a population size decline. Migration occurred between the two populations. (**B**) Inferred demographic histories of two populations (pop1 and pop2) with Split II model. (**C**) Inferred demographic histories of two populations (pop1 and pop2) with Split III model.

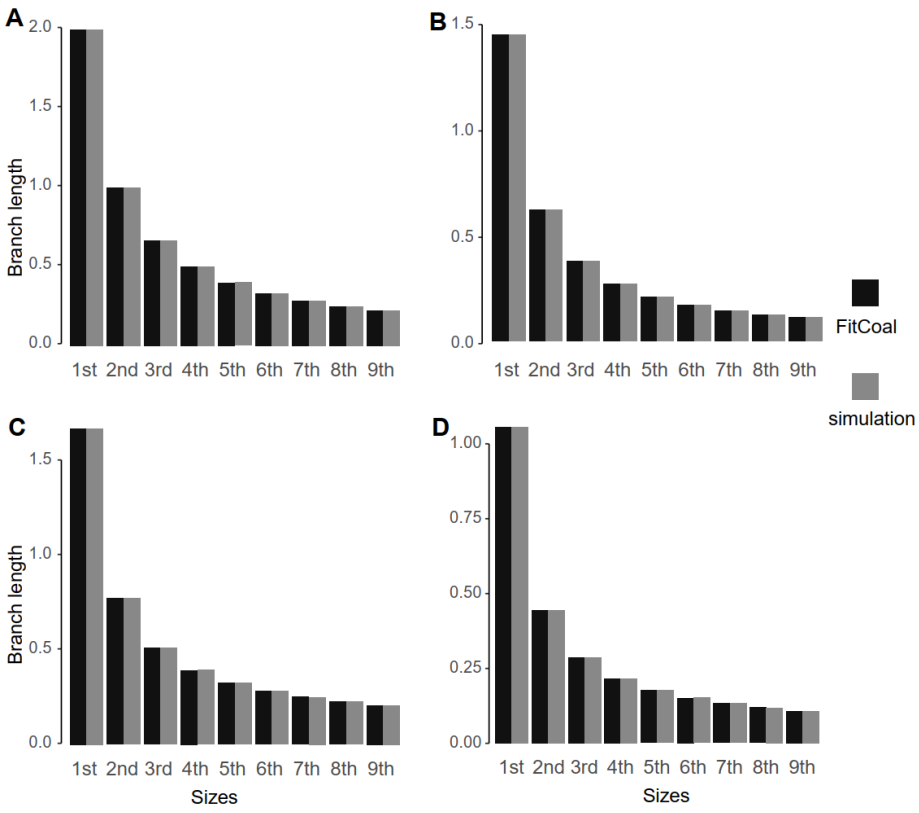

Fig. S33. Comparison of expected branch lengths of FitCoal and average branch lengths derived from coalescent simulations.

(**A**) Constant size model. (**B**) Exponential growth model. (**C**) Bottleneck model. (**D**) Complex model. $n = 10$. Average values of branch lengths were derived from 10^6 iterations in coalescent simulations.

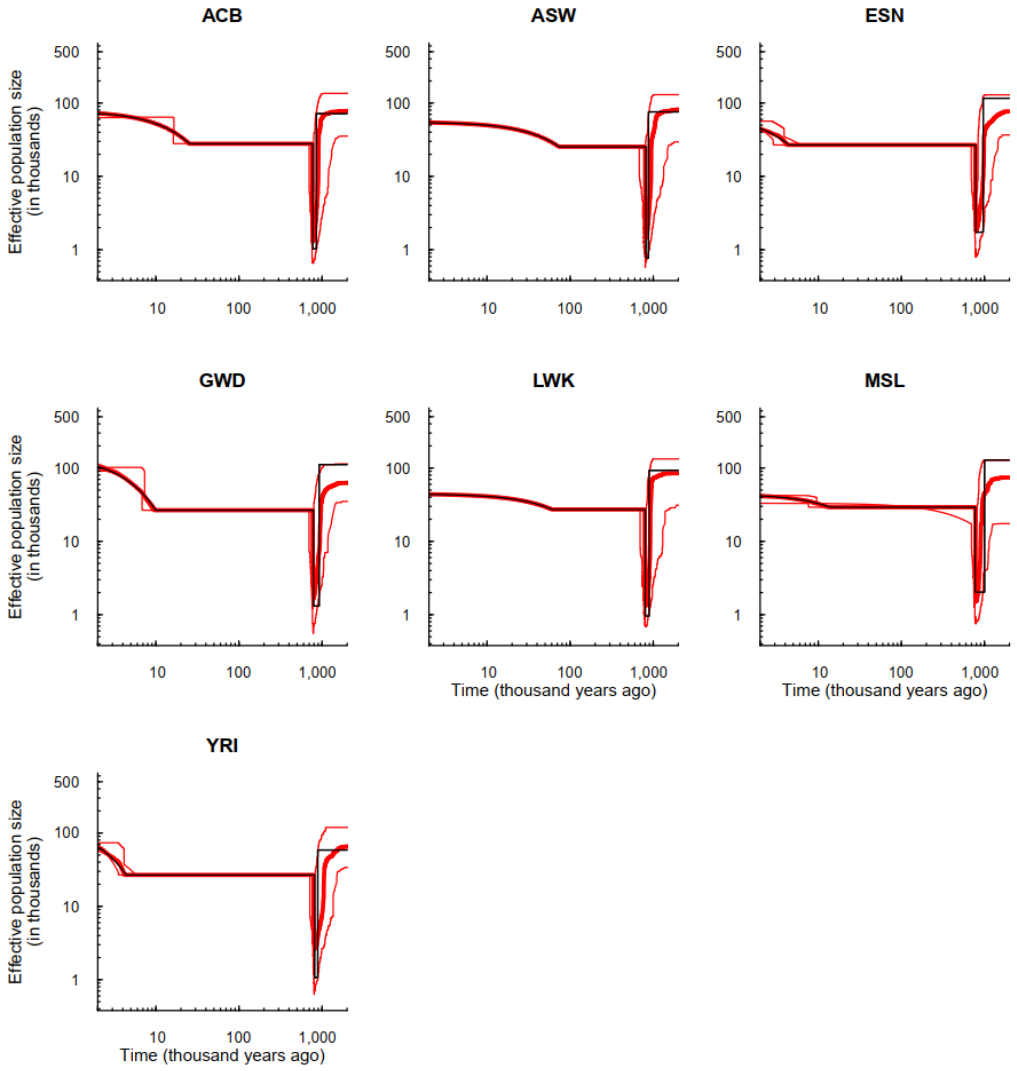

Fig. S34. 95% confidence intervals of African populations in 1000GP.

ACB: African Caribbeans in Barbados; ASW: Americans of African Ancestry in SW USA; ESN: Esan in Nigeria; GWD: Gambian in Western Divisions in the Gambia; LWK: Luhya in Webuye, Kenya; MSL: Mende in Sierra Leone; YRI: Yoruba in Ibadan, Nigeria.
For each population, simulations were conducted with proper sample size. Black lines indicate the true models (i.e., FitCoal-inferred population size histories shown in Fig. 3). Thick red lines indicate the medians of FitCoal estimated values; thin red lines are 2.5 and 97.5 percentiles of the values. Truncated SFSs were used.

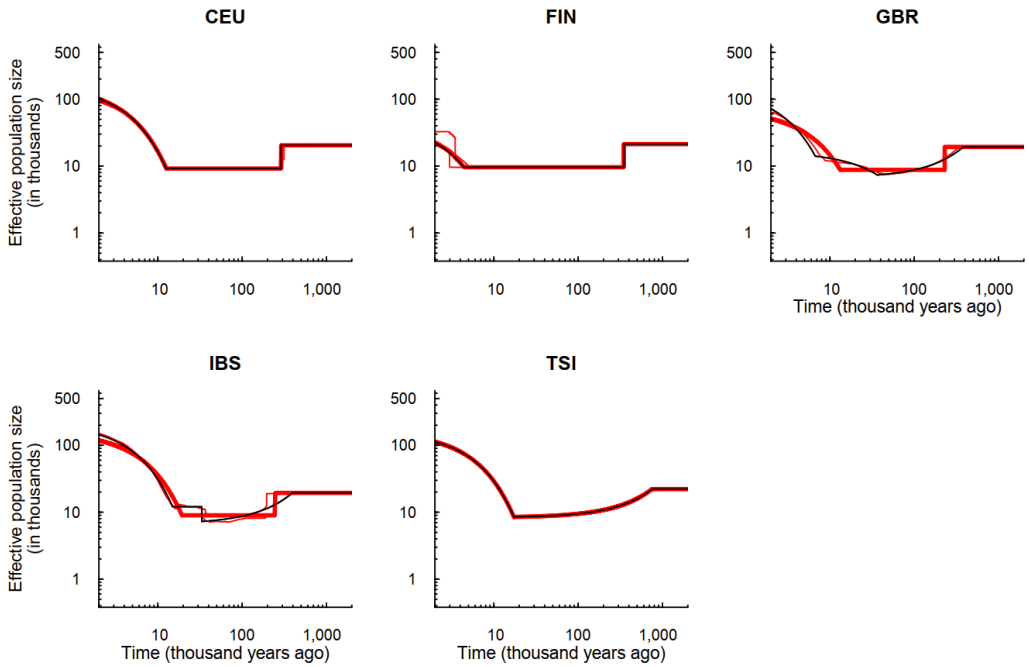

Fig. S35. 95% confidence intervals of European populations in 1000GP.

CEU: Utah Residents (CEPH) with Northern and Western European Ancestry; FIN: Finnish in Finland; GBR: British in England and Scotland; IBS: Iberian Population in Spain; TSI: Toscani in Italy.

For each population, simulations were conducted with proper sample size. Black lines indicate the true models (i.e., FitCoal-inferred population size histories shown in Fig. 3). Thick red lines indicate the medians of FitCoal estimated values; thin red lines are 2.5 and 97.5 percentiles of the values. Truncated SFSs were used.

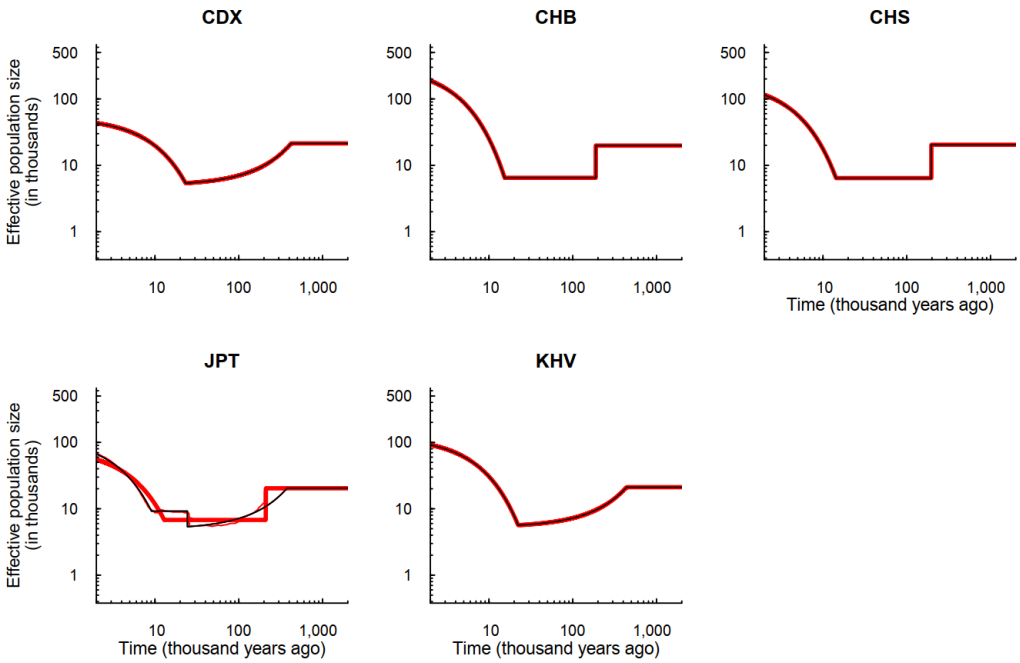

Fig. S36. 95% confidence intervals of East Asian populations in 1000GP.

CDX: Chinese Dai in Xishuangbanna, China; CHB: Han Chinese in Beijing, China; CHS: Southern Han Chinese; JPT: Japanese in Tokyo, Japan; KHV: Kinh in Ho Chi Minh City, Vietnam.

For each population, simulations were conducted with proper sample size. Black lines indicate the true models (i.e., FitCoal-inferred population size histories shown in Fig. 3). Thick red lines indicate the medians of FitCoal estimated values; thin red lines are 2.5 and 97.5 percentiles of the values. Truncated SFSs were used.

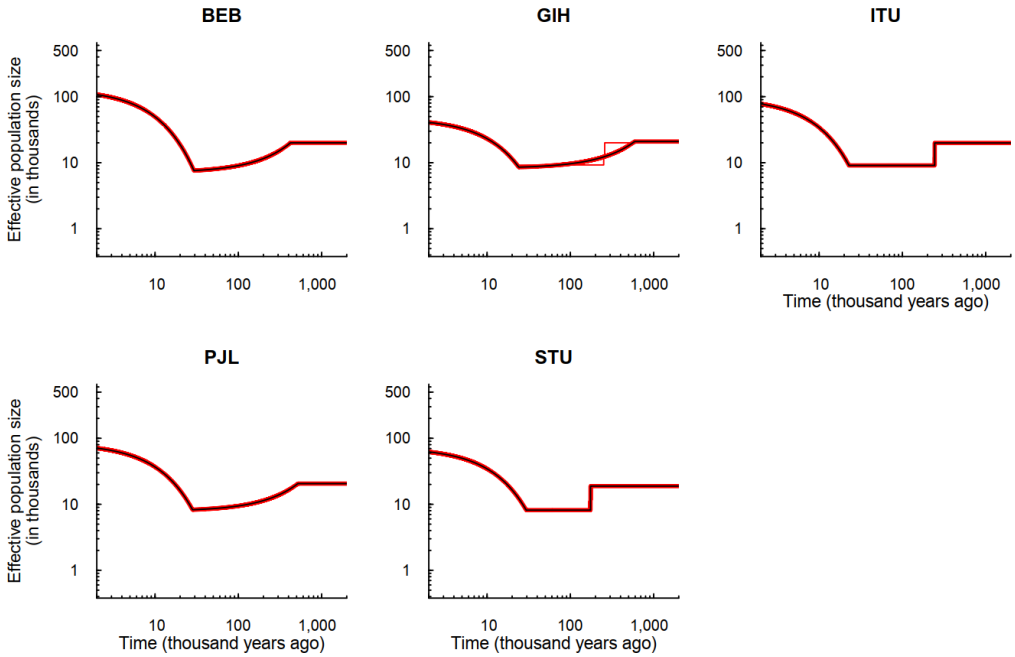

Fig. S37. 95% confidence intervals of South Asian populations in 1000GP.

BEB: Bengali in Bangladesh; GIH: Gujarati Indian from Houston, Texas; ITU: Indian Telugu from the UK; PJL: Punjabi from Lahore, Pakistan; STU: Sri Lankan Tamil from the UK. For each population, simulations were conducted with proper sample size. Black lines indicate the true models (i.e., FitCoal-inferred population size histories shown in Fig. 3). Thick red lines indicate the medians of FitCoal estimated values; thin red lines are 2.5 and 97.5 percentiles of the values. Truncated SFSs were used.

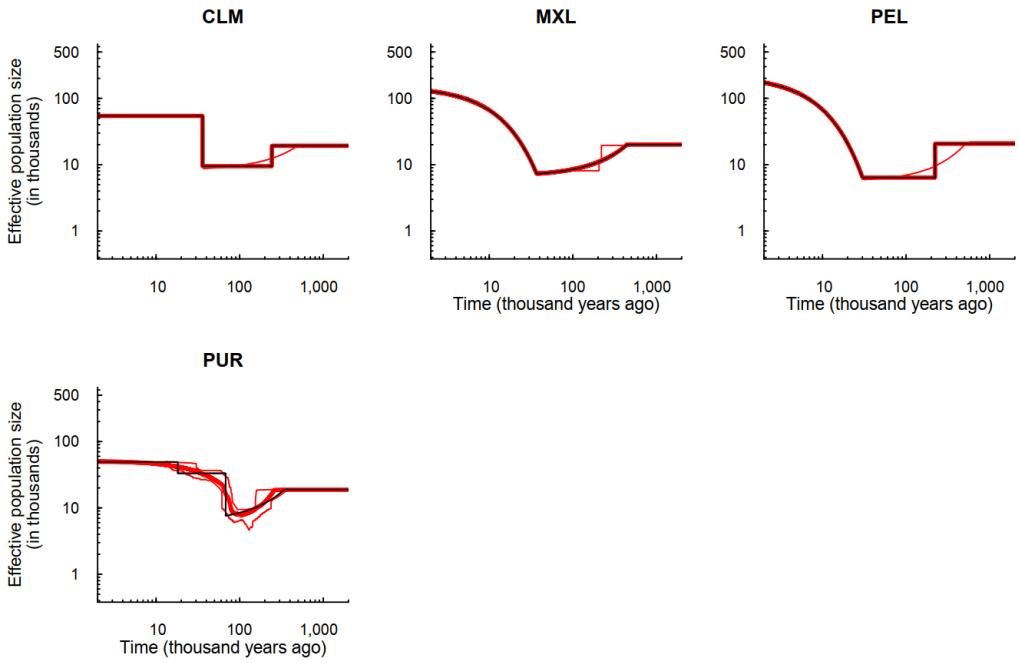

Fig. S38. 95% confidence intervals of American populations in 1000GP.

CLM: Colombians from Medellin, Colombia; MXL: Mexican Ancestry from Los Angeles USA; PEL: Peruvians from Lima, Peru; PUR: Puerto Ricans from Puerto Rico.

For each population, simulations were conducted with proper sample size. Black lines indicate the true models (i.e., FitCoal-inferred population size histories shown in Fig. 3). Thick red lines indicate the medians of FitCoal estimated values; thin red lines are 2.5 and 97.5 percentiles of the values. Truncated SFSs were used.

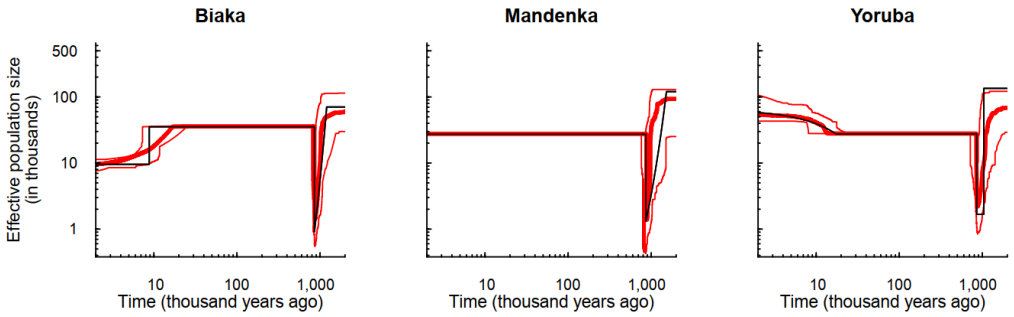

Fig. S39. 95% confidence intervals of African populations in the HGDP-CEPH panel.

For each population, simulations were conducted with proper sample size. Black lines indicate the true models (i.e., FitCoal-inferred population size histories shown in Fig. 3). Thick red lines indicate the medians of FitCoal estimated values; thin red lines are 2.5 and 97.5 percentiles of the values. Truncated SFSs were used.

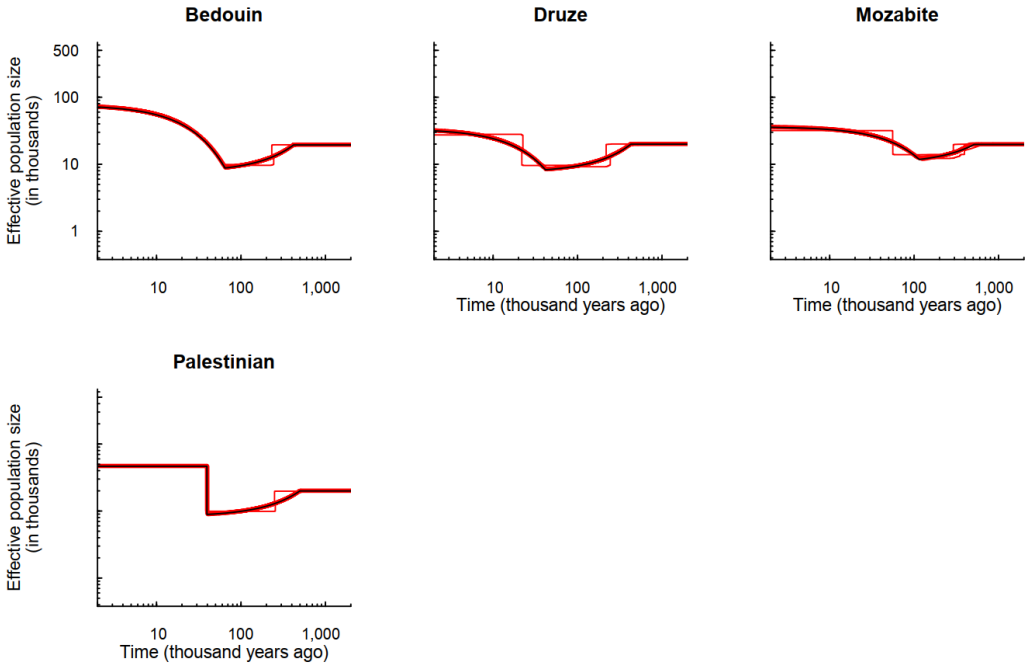

Fig. S40. 95% confidence intervals of Middle East populations in the HGDP-CEPH panel.
For each population, simulations were conducted with proper sample size. Black lines indicate the true models (i.e., FitCoal-inferred population size histories shown in Fig. 3). Thick red lines indicate the medians of FitCoal estimated values; thin red lines are 2.5 and 97.5 percentiles of the values. Truncated SFSs were used.

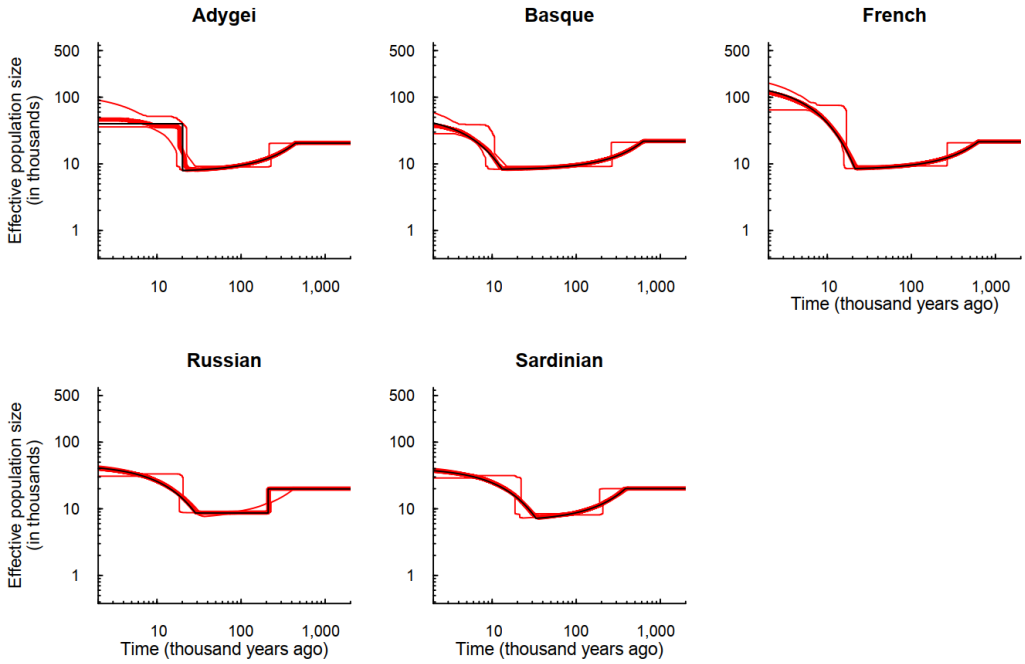

Fig. S41. 95% confidence intervals of European populations in the HGDP-CEPH panel.

For each population, simulations were conducted with proper sample size. Black lines indicate the true models (i.e., FitCoal-inferred population size histories shown in Fig. 3). Thick red lines indicate the medians of FitCoal estimated values; thin red lines are 2.5 and 97.5 percentiles of the values. Truncated SFSs were used.

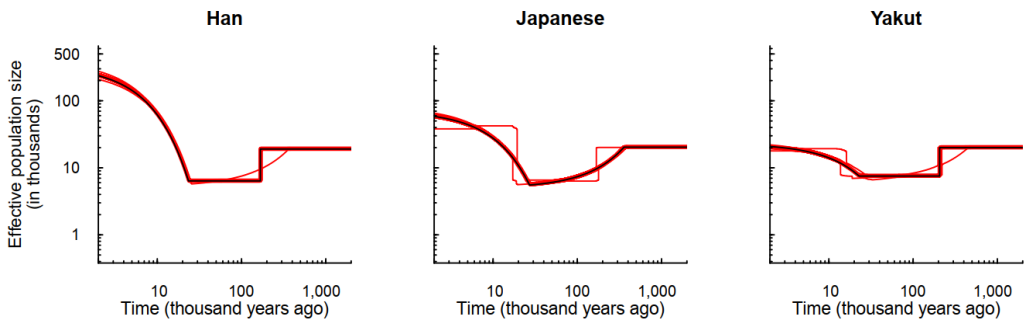

Fig. S42. 95% confidence intervals of East Asian populations in the HGDP-CEPH panel.

For each population, simulations were conducted with proper sample size. Black lines indicate the true models (i.e., FitCoal-inferred population size histories shown in Fig. 3). Thick red lines indicate the medians of FitCoal estimated values; thin red lines are 2.5 and 97.5 percentiles of the values. Truncated SFSs were used.

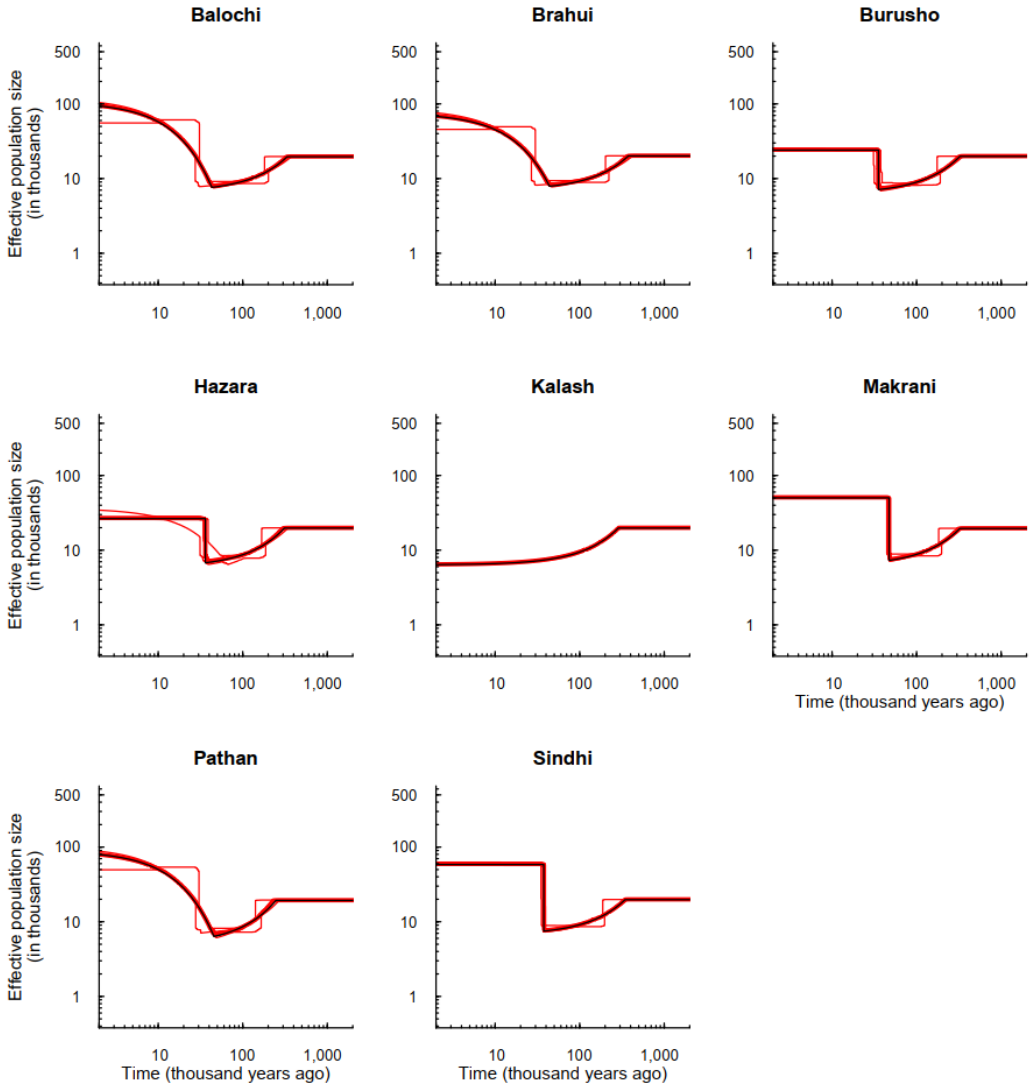

Fig. S43. 95% confidence intervals of Central & South Asian populations in the HGDP-CEPH panel.

For each population, simulations were conducted with proper sample size. Black lines indicate the true models (i.e., FitCoal-inferred population size histories shown in Fig. 3). Thick red lines indicate the medians of FitCoal estimated values; thin red lines are 2.5 and 97.5 percentiles of the values. Truncated SFSs were used.

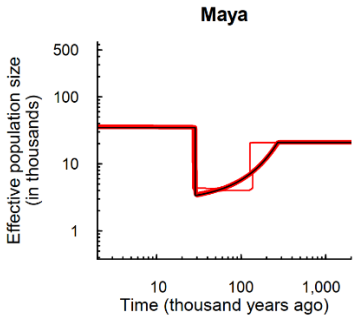

Fig. S44. 95% confidence intervals of American population in the HGDP-CEPH panel.

For the population, simulations were conducted with proper sample size. Black lines indicate the true models (i.e., FitCoal-inferred population size histories shown in Fig. 3). Thick red lines indicate the medians of FitCoal estimated values; thin red lines are 2.5 and 97.5 percentiles of the values. Truncated SFSs were used.

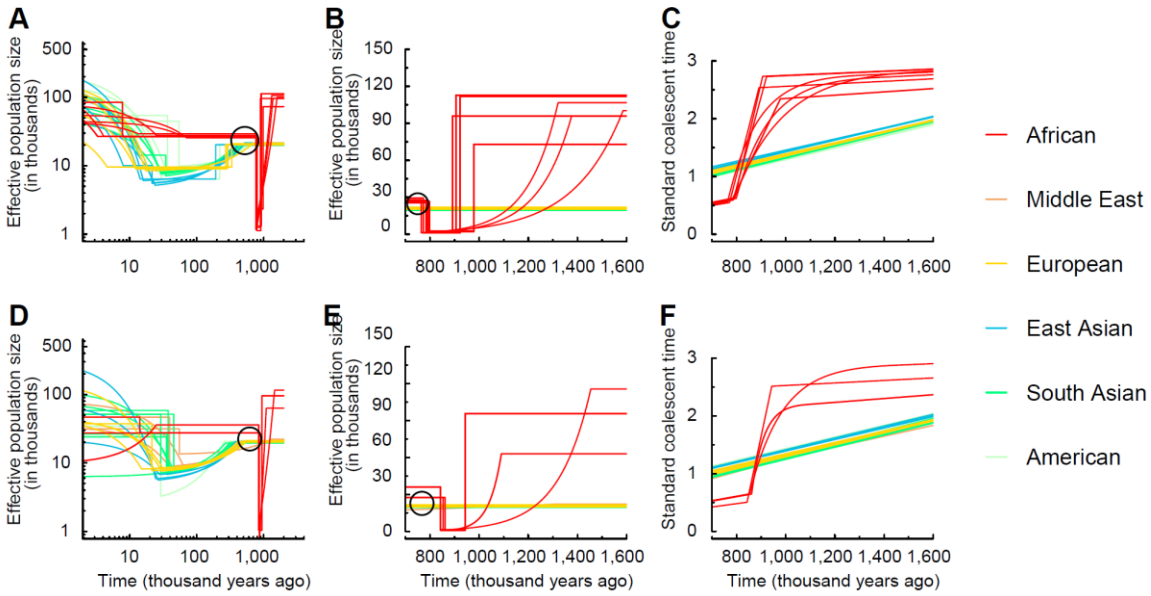

Fig. S45. FitCoal-inferred demographic histories of populations in 1000GP and HGDP-CEPH panels using the same proportion of SFS truncation.

(**A**) FitCoal-inferred demographic histories of 26 populations in 1000GP. (**B**) Linear-scaled histories of populations in 1000GP during the severe bottleneck. (**C**) Calendar time *vs* standard coalescent time of the estimated histories of populations in 1000GP. (**D**) FitCoal-inferred demographic histories of 24 populations in the HGDP-CEPH panel. (**E**) Linear-scaled histories of populations in the HGDP-CEPH panel during the severe bottleneck. (**F**) Calendar time *vs* standard coalescent time of the estimated histories of populations in the HGDP-CEPH panel. Various colored lines represent different populations as follows: red, African populations; yellow, European populations; brown, Middle East populations; blue, East Asian populations; green, Central or South Asian populations; dark sea green, American populations. Black circles show size difference between African agriculturalist populations and non-African populations. 10% SFS types of populations in 1000GP and 15% SFS types of HGDP-CEPH populations were discarded. A mutation rate of 1.2×10^{-8} per base per generation and a generation time of 24 years were assumed.

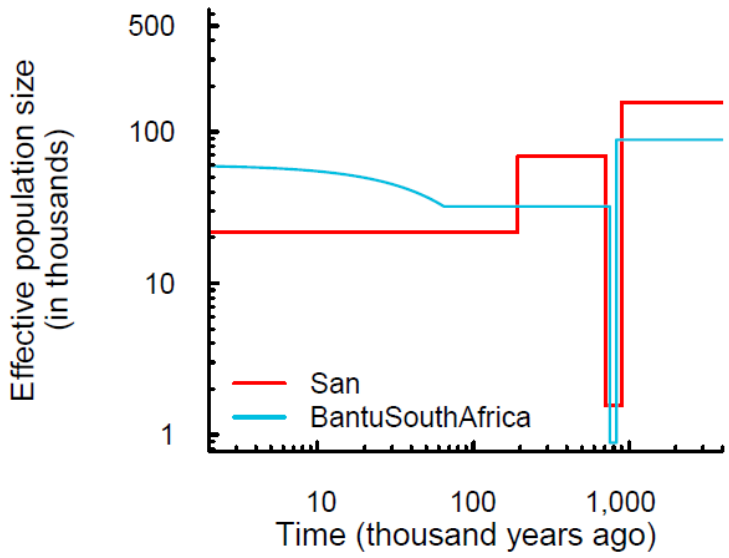

Fig. S46. FitCoal-inferred population size histories of two South African populations in the HGDP-CEPH panel.

The number of sampled individuals was 6 for San and 8 for BantuSouthAfrica populations.

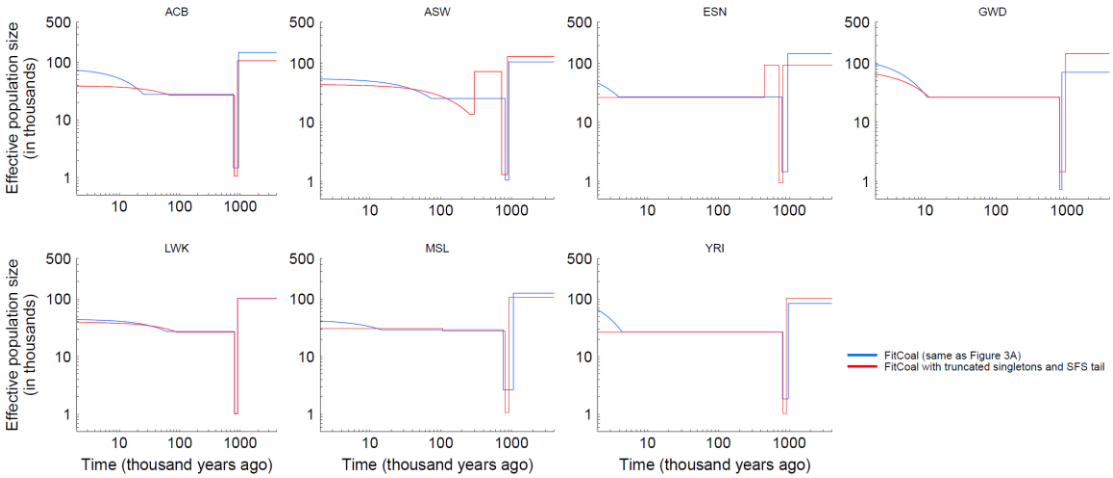

Fig. S47. FitCoal-inferred population size histories of seven African populations in 1000GP with singletons and high frequency mutations excluded.

Blue lines: FitCoal re-estimated population size histories using the same parameters as those used in Fig. 3A; Red lines: FitCoal-inferred population size histories with singletons and high frequency mutations excluded from the analysis. The cut-off thresholds for SFS truncation are shown in table S17.

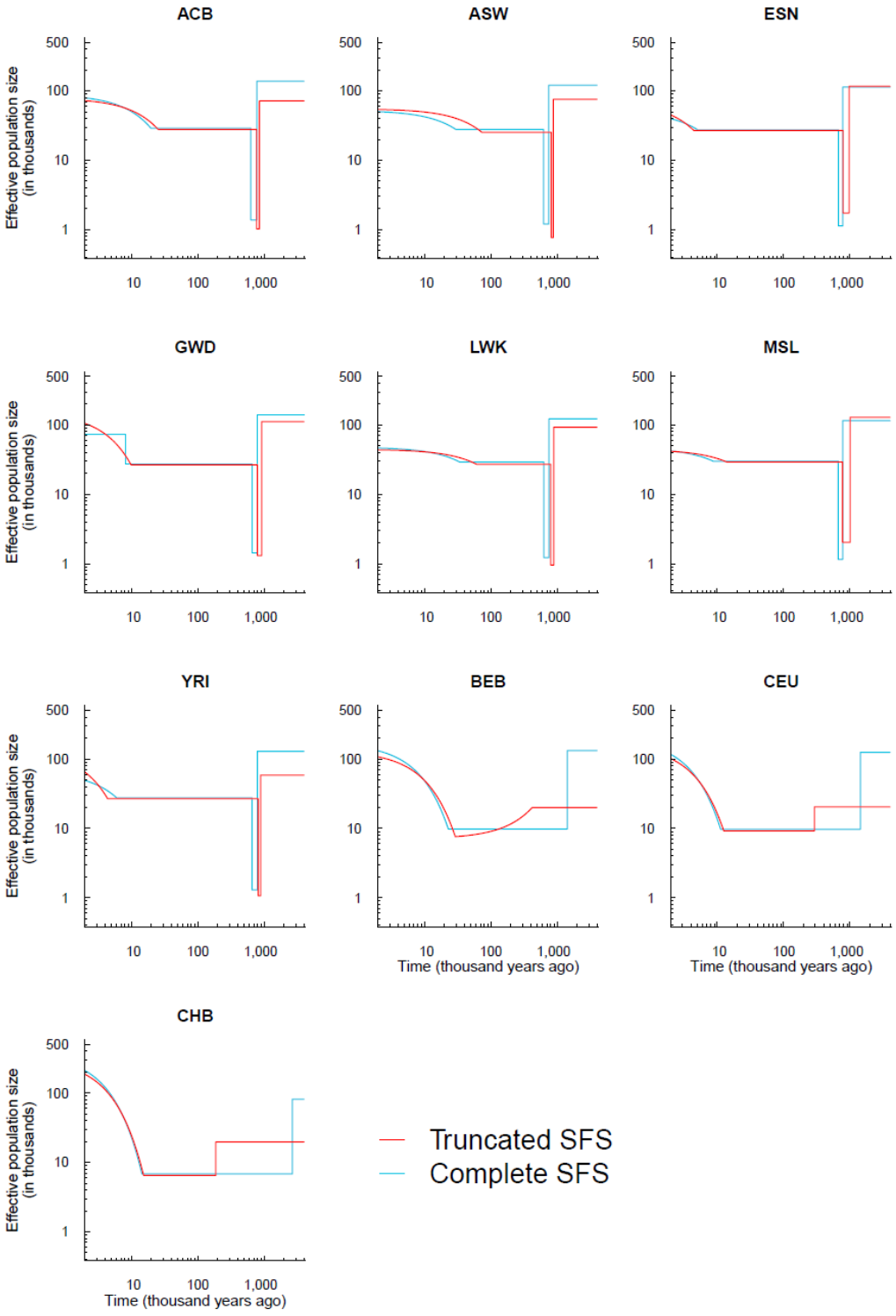

Fig. S48. FitCoal-inferred population size histories using complete and truncated SFSs of populations in 1000GP.

ACB: African Caribbeans in Barbados; ASW: Americans of African Ancestry in SW USA; ESN: Esan in Nigeria; GWD: Gambian in Western Divisions in the Gambia; LWK: Luhya in Webuye,

Kenya; MSL: Mende in Sierra Leone; YRI: Yoruba in Ibadan, Nigeria; BEB: Bengali in Bangladesh; CEU: Utah Residents (CEPH) with Northern and Western European Ancestry; CHB: Han Chinese in Beijing, China. Red lines indicate the inferred population size histories using truncated SFSs (Fig. 3A and fig. S6). Blue lines indicate those estimated using complete SFSs. The analyses were conducted with the same number of inference time intervals.

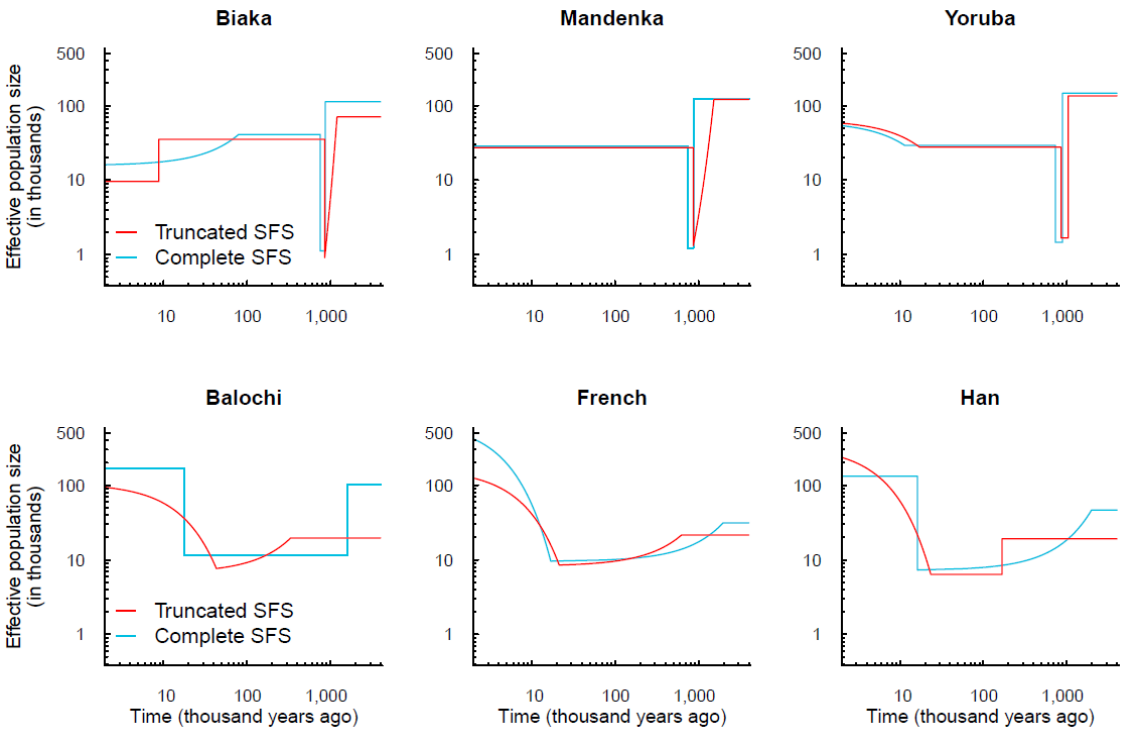

Fig. S49. FitCoal-inferred population size histories using complete and truncated SFSs of populations in the HGDP-CEPH panel.

Red lines indicate the inferred population size histories using truncated SFSs (Fig. 3A and fig. S6). Blue lines indicate those estimated using complete SFSs. The analyses were conducted with the same number of inference time intervals.

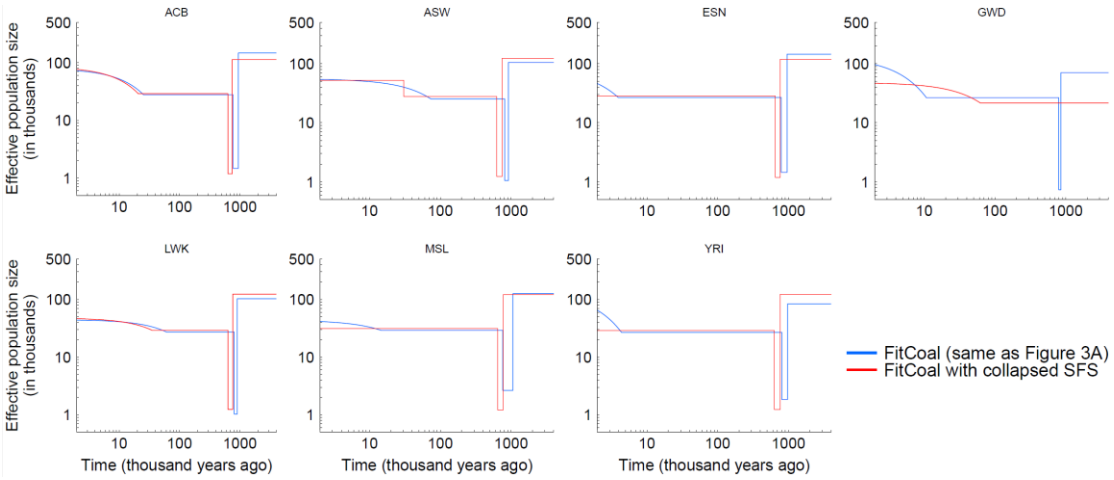

Fig. S50. FitCoal-inferred demographic histories of seven African populations in 1000GP with high frequency mutations combined (collapsed) into one category.

Blue lines: FitCoal re-estimated population size histories using the same parameters as those used in Fig. 3A; Red lines: FitCoal-inferred population size histories using collapsed SFS. The cut-off thresholds for SFS collapse are shown in table S17.

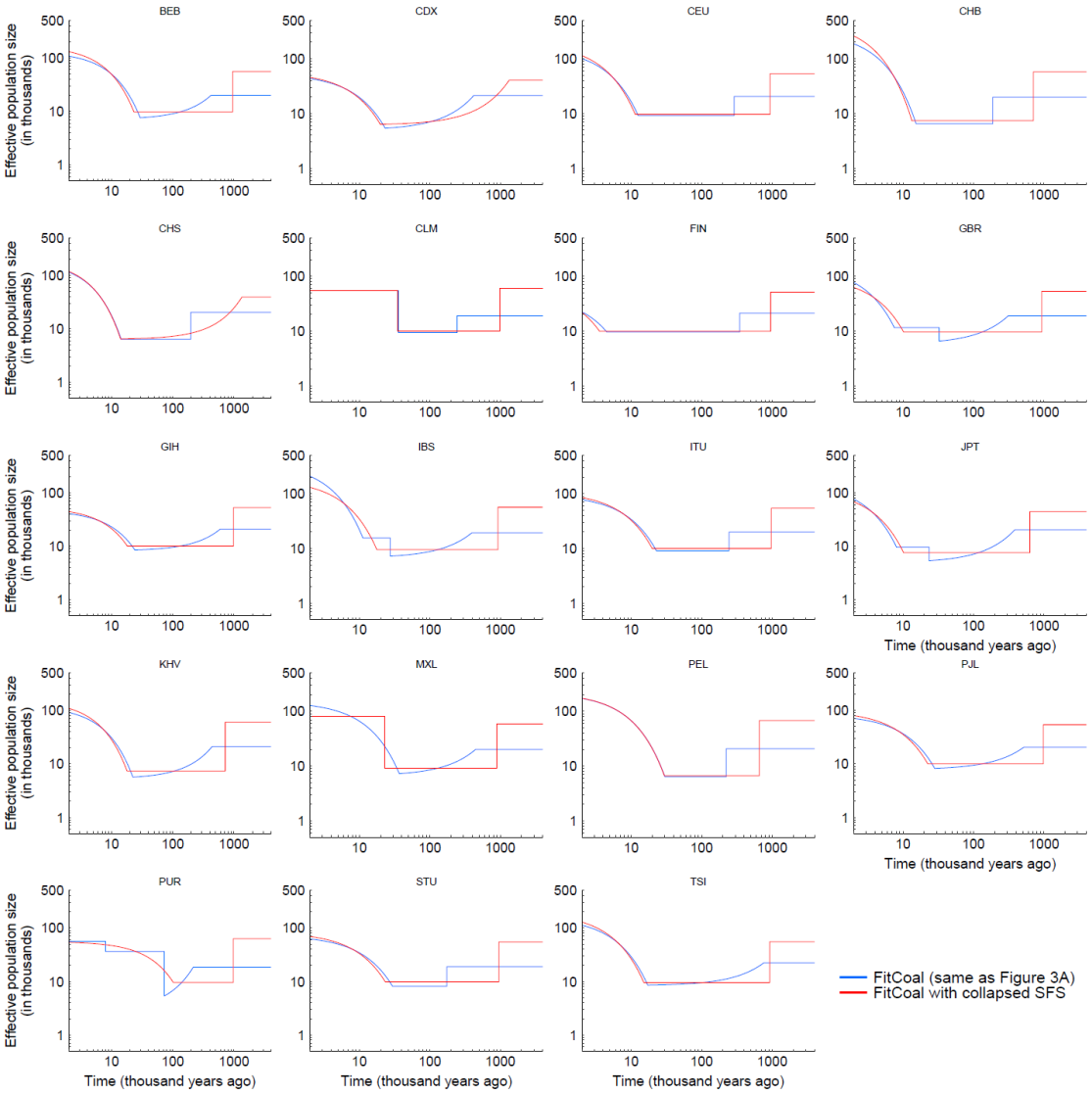

Fig. S51. FitCoal-inferred demographic histories of 19 non-African populations in 1000GP with high frequency mutations combined (collapsed) into one category.

Blue lines: FitCoal re-estimated population size histories using the same parameters as those used in Fig. 3A; Red lines: FitCoal-inferred population size histories using collapsed SFS. The cut-off thresholds for SFS collapse are shown in table S17.

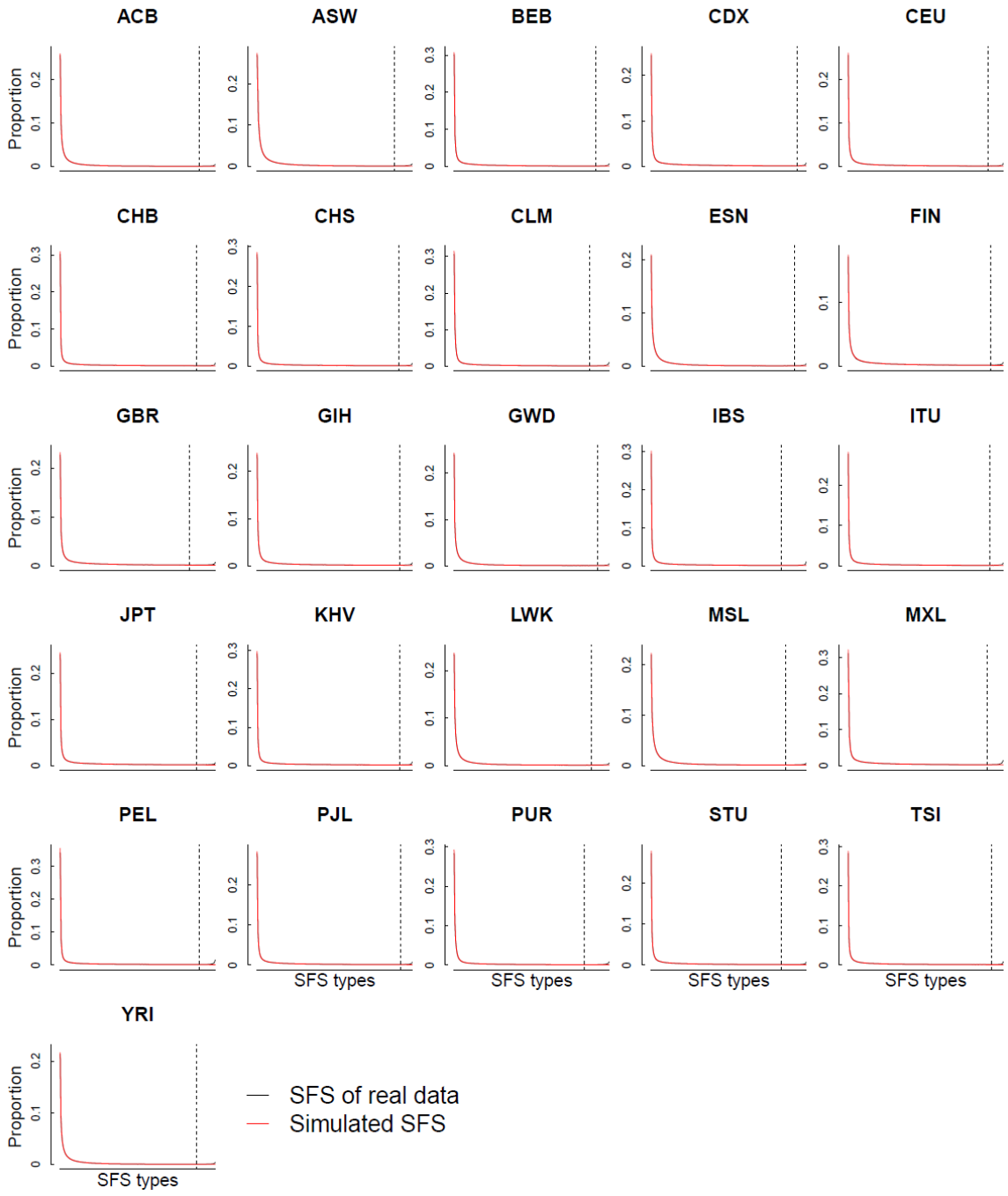

Fig. S52. Observed and simulated SFSs of populations in 1000GP.

Black solid lines indicate observed SFSs. The *x*-axis represents SFS types (categories) with values ranging from 1 to (*n*-1). The y-axis indicates proportions of mutations. Red solid lines indicate the means of SFSs of the 200 data sets simulated for each population. Dashed black lines indicate the cut-off thresholds for SFS truncation.

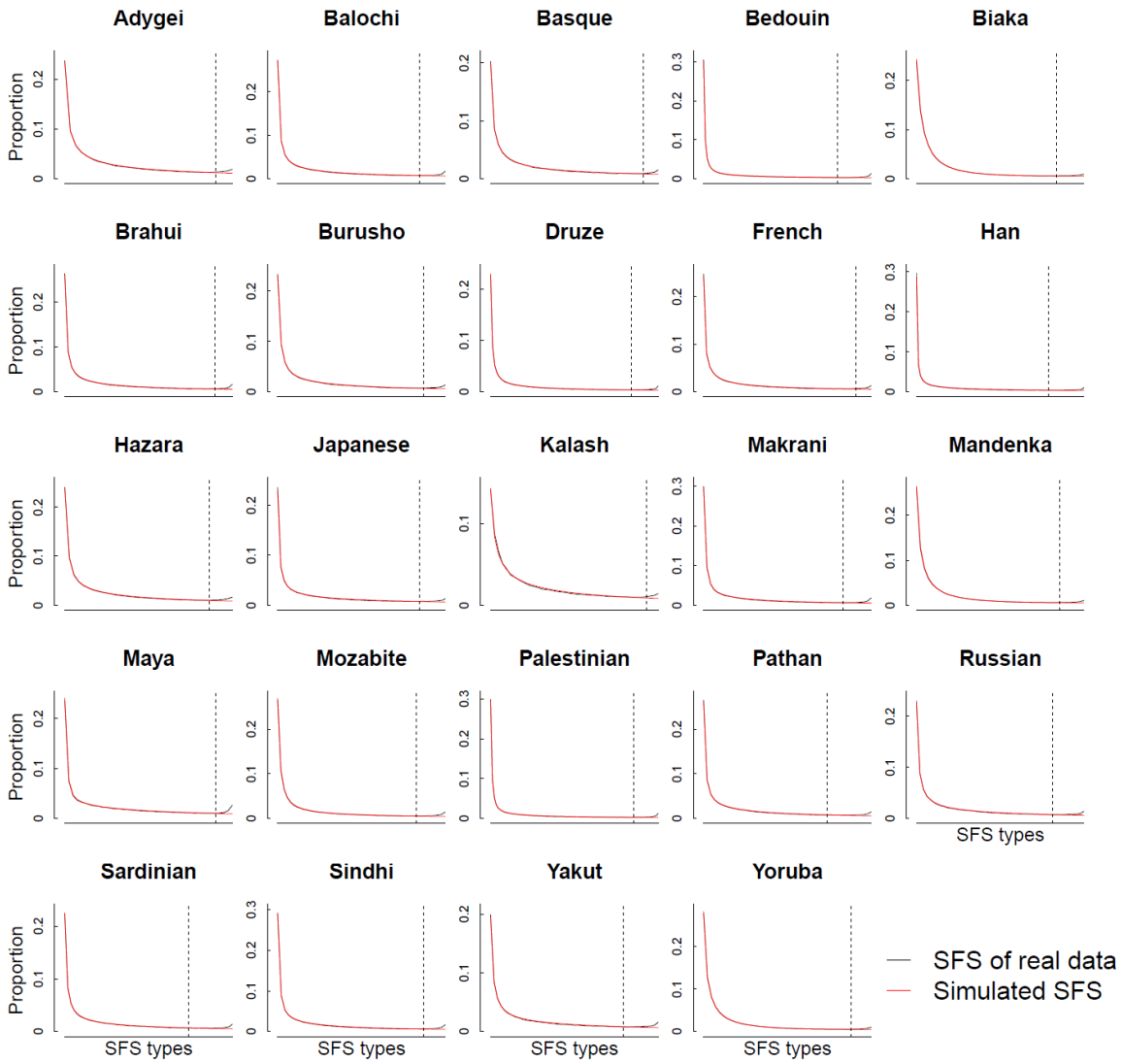

Fig. S53. Observed SFS without missing data and simulated SFS of populations in the HGDP-CEPH panel.

Black solid lines indicate observed SFSs. The *x*-axis represents SFS types (categories) with values ranging from 1 to (*n*-1). The y-axis indicates proportions of mutations. Red solid lines indicate the means of SFSs of the 200 data sets simulated for each population. Dashed black lines indicate the cut-off thresholds for SFS truncation.

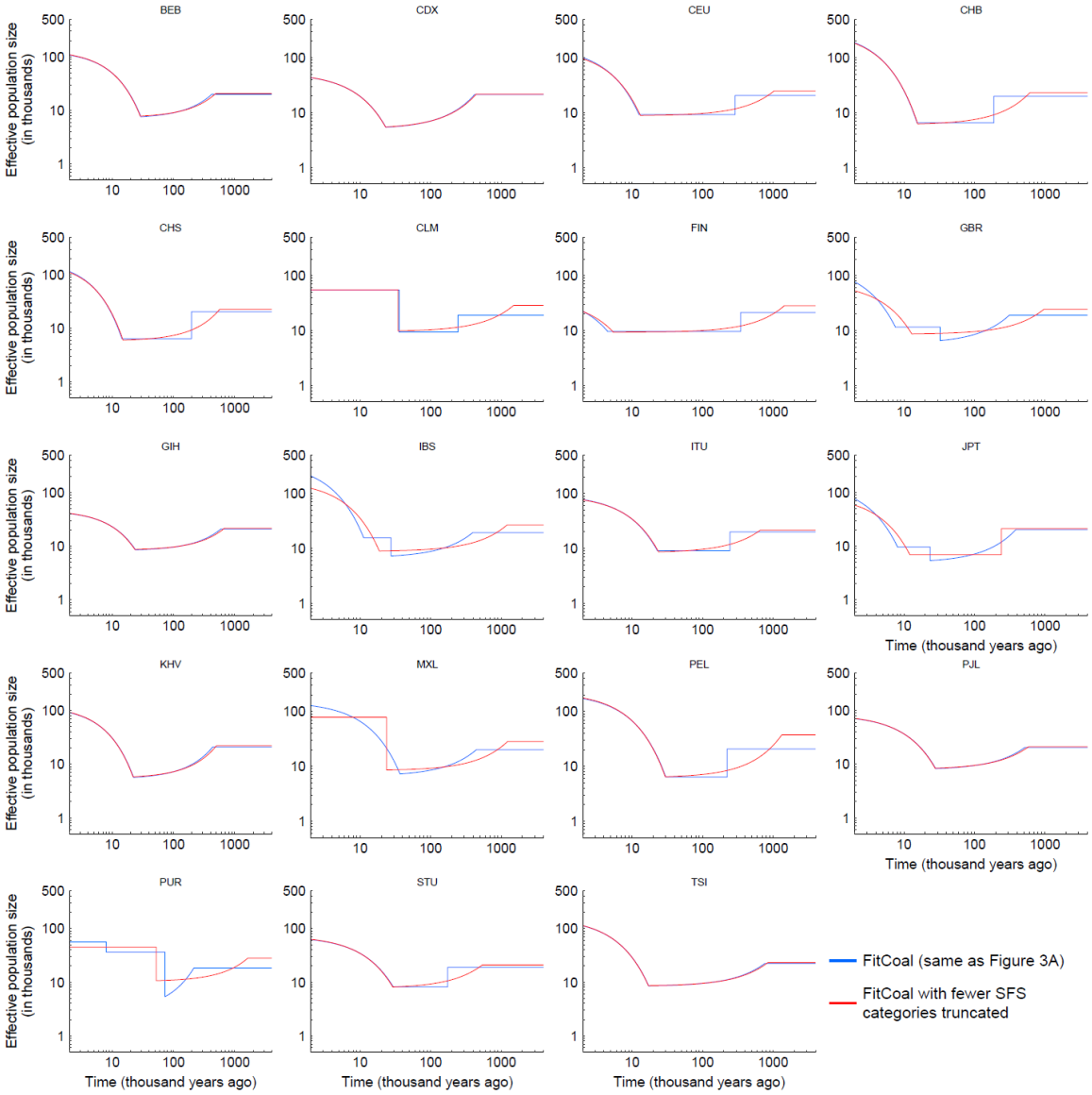

Fig. S54. FitCoal-inferred demographic histories of 19 non-African populations in 1000GP with 3.22% SNPs excluded for analysis.

Blue lines: FitCoal re-estimated population size histories using the same parameters as those used in Fig. 3A; Red lines: FitCoal-inferred population size histories with fewer SFS categories truncated. The proportion of SNPs excluded from the analysis is the same as that for African populations in 1000GP.

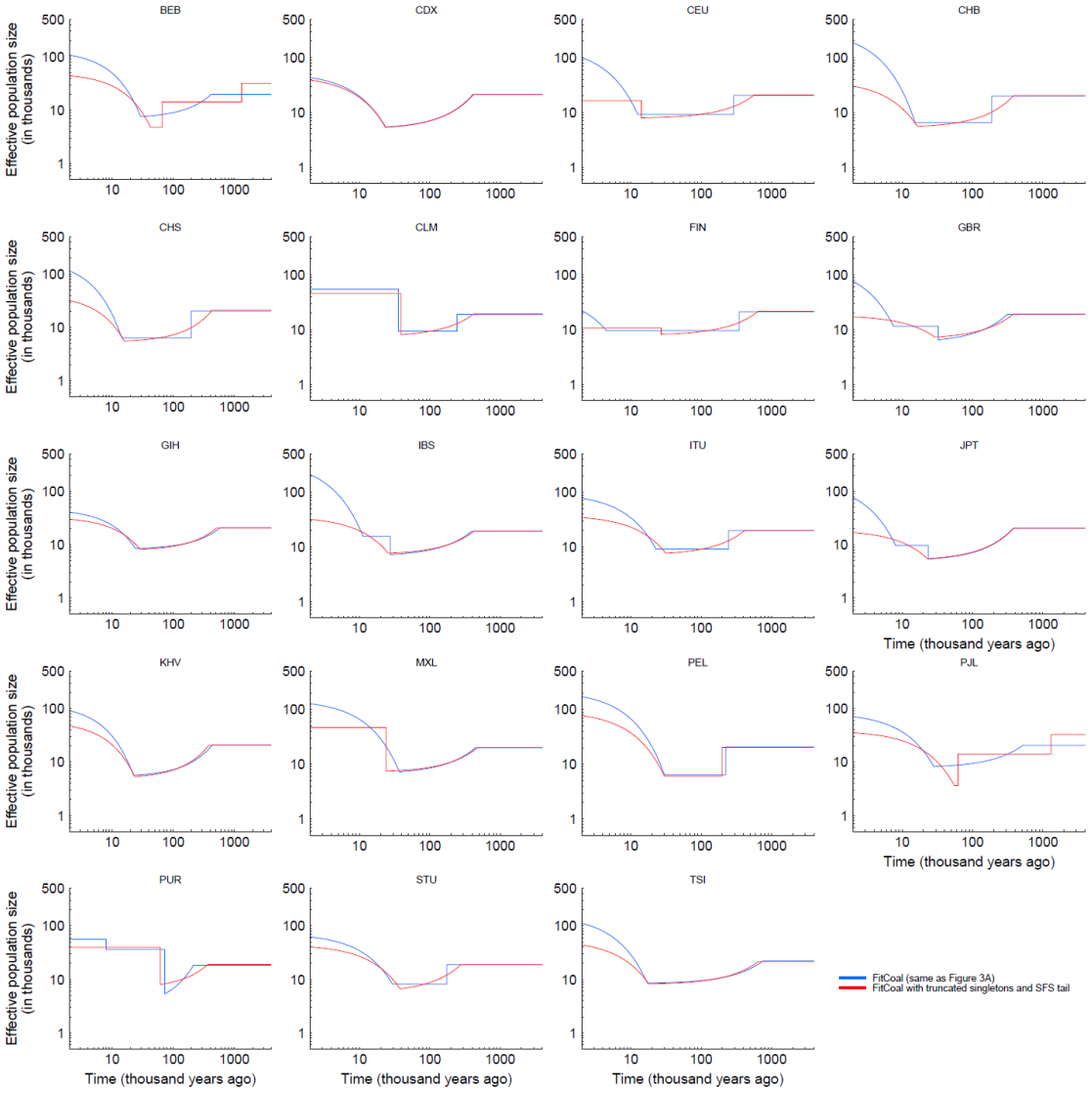

Fig. S55. FitCoal-inferred demographic histories of 19 non-African populations in 1000GP with singletons and high frequency mutations excluded (truncated).

Blue lines: FitCoal re-estimated population size histories using the same parameters as those used in Fig. 3A; Red lines: FitCoal-inferred population size histories with singletons and high frequency mutations excluded from the analysis. The cut-off thresholds for SFS truncation are shown in table S17.

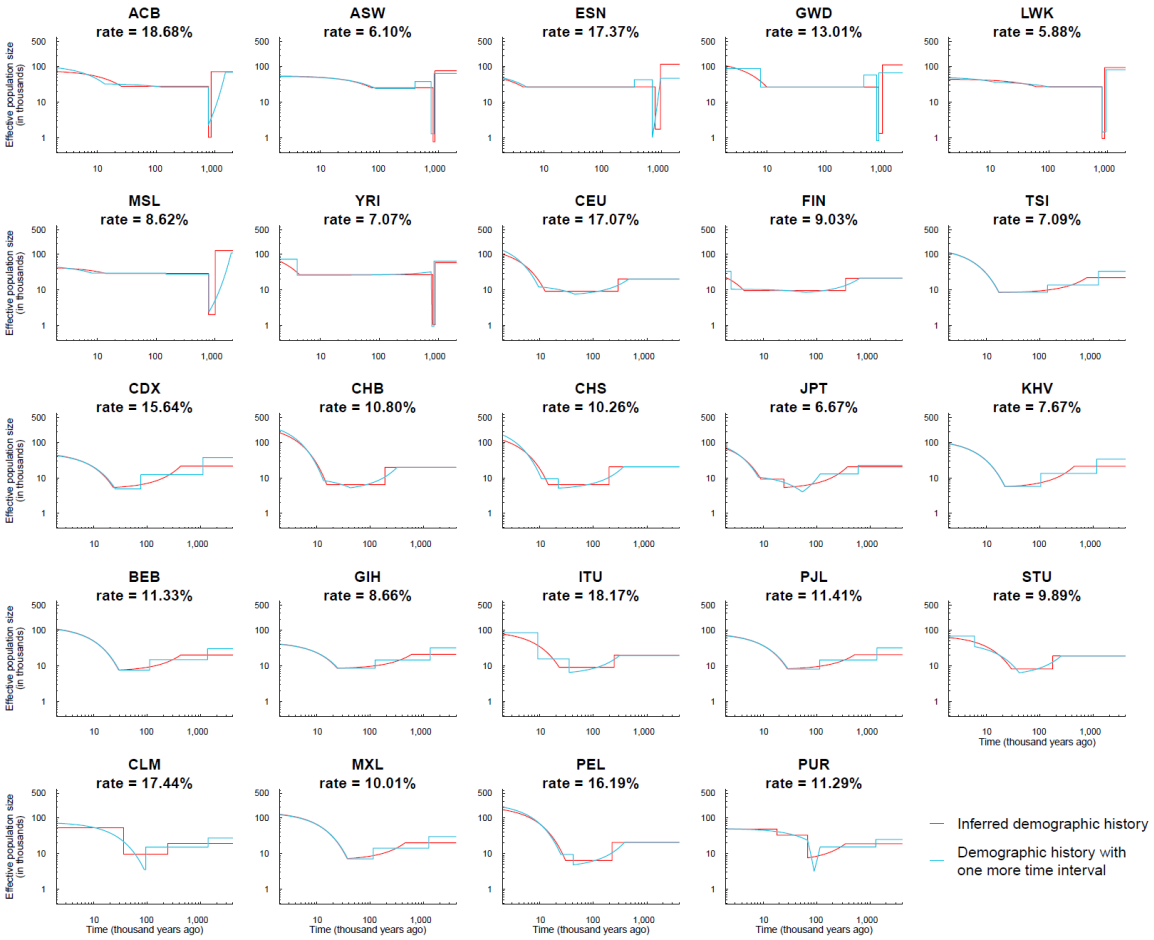

Fig. S56. FitCoal-inferred population size histories with different numbers of time intervals of populations in 1000GP.

Red lines indicate FitCoal-inferred population size histories, and blue lines indicate FitCoal population size histories inferred with one additional time interval. The log-likelihood promotion rates of different populations vary as indicated (from 5.88 to 18.68%).

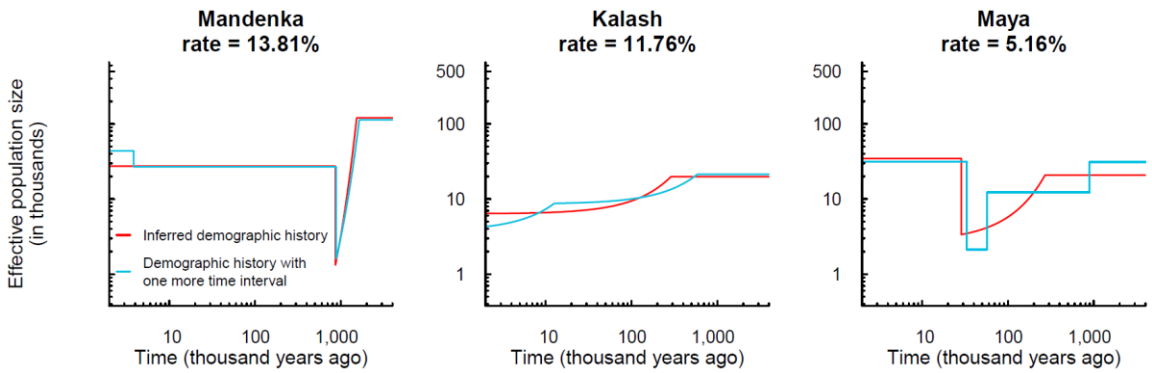

Fig. S57. FitCoal-inferred population size histories with different numbers of time intervals of American populations in the HGDP-CEPH panel.

Red lines indicate FitCoal-inferred population size histories, and blue lines indicate FitCoal population size histories inferred with one additional time interval. The log-likelihood promotion rates vary (5.16, 11.76, and 13.81%) for different populations.

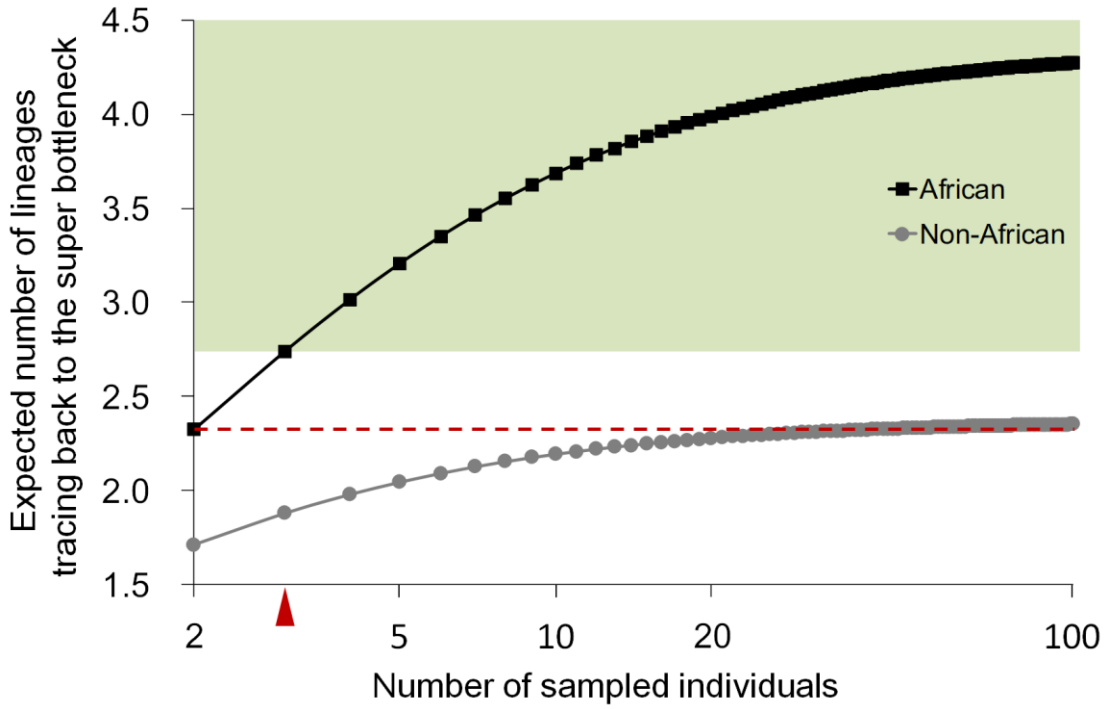

Fig. S58. Theoretical minimum number of sampled African individuals to detect the ancient severe bottleneck.

The black curve denotes the expected number of African lineages tracing back to the severe bottleneck ($t = 0.5$), where t is the standard coalescent time. The gray curve shows the expected number of non-African lineages tracing back to the severe bottleneck ($t = 1.0$). The number of lineages remained is larger in African samples than in non-African ones because non-African populations went through the out-of-Africa dispersal. The green shadow marks the sampling range in which the ancient severe bottleneck can be detected. The red triangle indicates the theoretical minimum number of sampled individuals for detection of the ancient severe bottleneck by FitCoal.

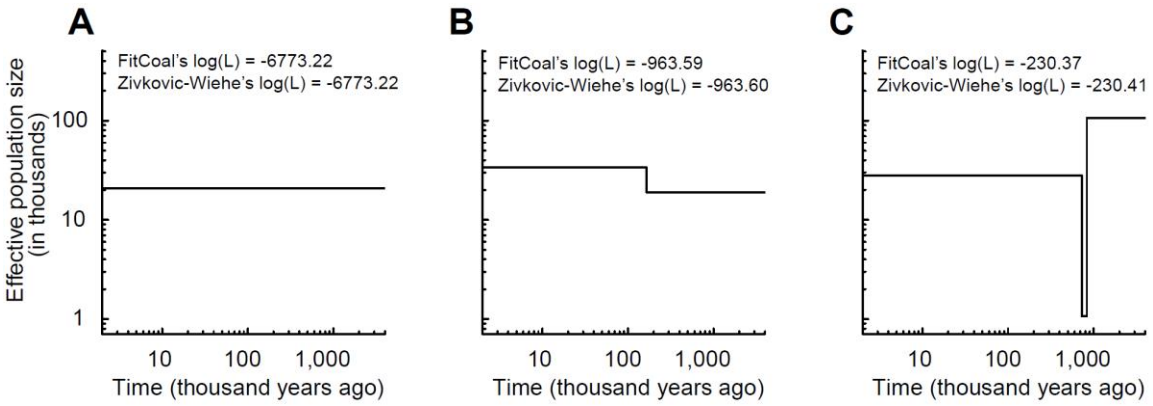

Fig. S59. Likelihood of the ancient severe bottleneck calculated by Živković-Wiehe's method.

Population size histories were inferred by FitCoal with the fixed number of inference time intervals. An YRI subsample with three individuals was used. The data has been deposited at Mendeley (https://doi.org/10.17632/xmf5r8nzrn.3), and the chosen data index was seven (Fig. S12). The full SFS was used for analyses because excessive high frequency mutations were not found. The value of log(L) is shown for each population size history inferred.
(**A**) Population size history inferred with one time interval. (**B**) Population size history inferred with two time intervals. (**C**) The ancient severe bottleneck inferred with three time intervals.

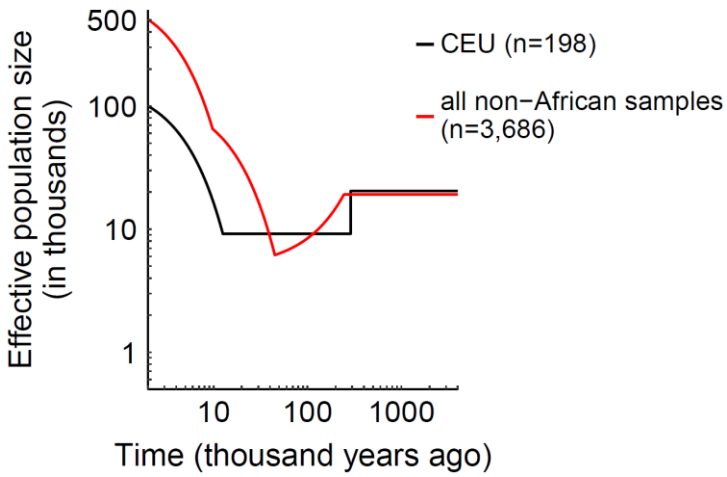

Fig. S60. FitCoal-inferred demographic history of combined non-African population.

Table S1. Proportion of the most recent population changes inferred from six models.

Model	Proportion
Constant size	100%
Instantaneous increase	85.5%
Bottleneck	100%
Exponential growth I	41.5%
Exponential growth II	61%
Exponential growth III	67%

Table S2. Resources table.

Resource	Source	Web link to download
Deposited data		
1000 Genomes project, phase 3	1000 GP	http://ftp.1000genomes.ebi.ac.uk/vol1/ftp/release/20130502/
Human Genome Diversity Project – Centre d'Etude du Polymorphisme Humain (HGDP-CEPH) panel	HGDP-CEPH	ftp://ngs.sanger.ac.uk/production/hgdp
Observed SFSs and raw data for figures	This study	https://doi.org/10.17632/xmf5r8nzrn.3
Software		
FitCoal	This study	https://doi.org/10.5281/zenodo.7857456 http://www.sinh.ac.cn/evolgen/ and http://www.egps-software.net/

Table S3. Parameters of the ancient severe bottleneck in African populations in 1000GP.

Population (Num. of ind.)	Ancestral *Ne*	Start time of the bottleneck		*Ne* during the bottleneck	End time of the bottleneck		*Ne* immediately after the bottleneck
		Time[a]	Change type[b]		Time[a]	Change type[b]	
ACB (96)	71,705	854,288	I	1,021	772,422	I	27,802
ASW (61)	75,746	877,763	I	767	815,473	I	25,302
ESN (99)	116,216	966,439	I	1,735	785,741	I	26,785
GWD (113)	111,486	922,296	I	1,311	790,048	I	26,546
LWK (99)	92,952	891,086	I	954	802,498	I	27,142
MSL (85)	128,666	1,002,553	I	2,031	773,633	I	29,183
YRI (108)	58,563	887,367	I	1,066	812,636	I	26,796
Average	93,619	914,542		1,269	793,207		27,079

Note: [a]Time is in years BP.
[b]I represents instantaneous change. *Ne*: effective population size.

Table S4. Parameters of the ancient severe bottleneck in African populations in the HGDP-CEPH panel.

Population (Num. of ind.)	Ancestral *Ne*	Start time of the bottleneck		*Ne* during the bottleneck	End time of the bottleneck		*Ne* immediately after the bottleneck
		Time[a]	Change type[b]		Time[a]	Change type[b]	
Biaka (22) [c]	70,583	1,202,743	E	908	855,778	I	35,329
Mandenka (22)	120,452	1,526,972	E	1,319	864,078	I	27,306
Yoruba (22)	134,958	1,041,950	I	1,670	856,750	I	27,569
Average	108,664	1,257,222		1,299	858,869		27,438 [d]

Note: [a]Time is in years BP.
[b]I represents instantaneous change, and E represents exponential change.
[c]The Biaka, an African hunter-gatherer population, had a large population size of 35,329 after the severe bottleneck was relieved, suggesting a deep divergence between this and other agriculturalist populations (*68-70*).
[d]The average size of the two African agriculturalist populations (Mandenka and Yoruba).

Table S5. Parameters of out-of-Africa dispersal in non-African populations in 1000GP.

Region	Population (Num. of ind.)	Ancestral *Ne*	Start time of out-of-Africa dispersal		*Ne* during the bottleneck
			Time[a]	Change type[b]	
EUR	CEU (99)	20,414	290,251	I	9,168
	GBR (91)	19,334	383,068	E	7,343
	FIN (99)	21,278	348,509	I	9,612
	IBS (107)	19,393	391,678	E	7,270
	TSI (107)	22,215	756,179	E	8,505
EAS	CDX (93)	21,362	421,701	I	5,374
	CHB (103)	19,887	188,134	E	6,484
	CHS (105)	20,406	196,219	I	6,414
	JPT (104)	20,417	377,347	E	5,363
	KHV (99)	21,123	439,168	E	5,657
SAS	BEB (86)	19,998	422,436	E	7,584
	GIH (103)	20,941	591,769	E	8,554
	ITU (102)	19,912	244,308	I	9,091
	PJL (96)	20,556	518,059	E	8,257
	STU (102)	18,848	174,620	I	8,157
AMR	CLM (94)	19,252	242,526	I	9,482
	MXL (64)	20,063	444,463	E	7,266
	PEL (85)	20,666	222,966	I	6,384
	PUR (104)	18,917	344,023	E	7,606
Average		20,262	368,285	-	-

Note: [a]Time in years.
[b]I represents instantaneous change, and E represents exponential change. *Ne*: effective population size.

Table S6. Parameters of out-of-Africa dispersal in non-African populations in the HGDP-CEPH panel.

Region	Population (Num. of ind.)	Ancestral *Ne*	Start time of out-of-Africa dispersal		*Ne* during the bottleneck
			Time[a]	Change type[b]	
Middle East	Bedouin (46)	19,410	420,348	E	8,793
	Druze (42)	19,930	428,504	E	8,275
	Mozabite (27)	19,932	497,224	E	8,904
	Palestinian (46)	19,733	513,178	E	11,795
European	Adygei (16)	20,467	443,402	E	7,934
	Basque (23)	21,848	627,518	E	8,315
	French (28)	21,469	623,958	E	8,496
	Russian (25)	19,836	209,860	I	8,647
	Sardinian (28)	20,065	385,155	E	7,183
East Asian	Han (43)	19,055	167,289	I	6,365
	Japanese (27)	20,303	357,997	E	5,532
	Yakut (25)	20,012	206,684	I	7,526
Central & South Asian	Balochi (24)	19,618	334,493	E	7,635
	Brahui (25)	20,095	375,825	E	7,897
	Burusho (24)	19,846	325,186	E	7,127
	Hazara (19)	19,765	310,990	E	6,780
	Kalash (22)	19,766	286,505	E	6,346
	Makrani (25)	19,497	324,241	E	7,297
	Pathan (24)	19,283	245,899	E	6,364
	Sindhi (24)	19,758	344,223	E	7,493
American	Maya (21)	20,847	270,478	E	3,365
Average		20,025	366,617	-	-

Note: [a]Time in years.
[b]I represents instantaneous change, and E represents exponential change. *Ne*: effective population size.

Table S7. Ancient severe bottleneck parameters of Bottleneck I model with long, simulated DNA fragments.

Parameter	Value	Median of estimated values	Lower bound of 95% CI	Upper bound of 95% CI
Start time of the bottleneck	912,000	1,028,512	810,039	1,916,513
End time of the bottleneck	792,000	760,318	677,525	792,662
Population size before the bottleneck	93,000	59,347	31,808	130,198
Population size during the bottleneck	1,300	2,173	549	6,267
Population size after the bottleneck	27,000	26,904	27,077	27,261

Note: 200 replications were simulated. For each replication, 800 Mb of data were generated by simulations using eight DNA fragments of 100 Mb each.

Table S8. Ancient severe bottleneck parameters of Bottleneck I model with short, simulated DNA fragments (fig. S9A).

Parameter	Value	Median of estimated values	Lower bound of 95% CI	Upper bound of 95% CI
Start time of the bottleneck	912,000	978,024	790,776	1,890,528
End time of the bottleneck	792,000	764,376	685,656	794,784
Population size before the bottleneck	93,000	62,224	32,334	130,445
Population size during the bottleneck	1,300	1,907	546	5,838
Population size after the bottleneck	27,000	27,069	26,936	27,230

Note: 200 replications were simulated. For each replication, 800 Mb of data were generated by simulations using 80,000 DNA fragments of 10 kb each.

Table S9. Verification of the ancient severe bottleneck using the parameters from the HGDP-CEPH panel (fig. S10A).

Parameter	Value	Median of estimated values	Lower bound of 95% CI	Upper bound of 95% CI
Start time of the bottleneck	984,000	1,072,368	894,648	1,899,288
End time of the bottleneck	864,000	854,256	774,360	873,672
Population size before the bottleneck	110,000	72,408	31,934	140,463
Population size during the bottleneck	1,300	1,677	638	5,536
Population size after the bottleneck	28,000	27,965	27,817	28,203

Note: 200 replications were simulated. For each replication, 800 Mb of data were generated by simulations using 80,000 DNA fragments of 10 kb each.

Table S10. Parameters of the ancient severe bottleneck in 19 non-African populations in 1000GP.

Population	maxLogL1	maxLogL2	Ancestral *Ne*	Start time of the bottleneck (in years BP)	*Ne* during the bottleneck	End time of the bottleneck (in years BP)
BEB	-2,427.69	-2,263.67	90,343	860,271	917	783,636
CDX	-2,526.27	-2,338.19	136,728	811,705	1,509	653,241
CEU	-2,600.35	-2,500.18	79,237	778,766	793	714,537
CHB	-2,038.48	-1,973.84	101,941	811,997	1,586	662,973
CHS	-2,687.83	-2,496.00	64,221	646,386	1,049	570,307
CLM	-1,931.68	-1,834.08	94,133	877,926	1,206	770,672
FIN	-2,473.67	-2,399.66	168,470	1,132,501	3,359	718,299
GBR	-1,611.94	-1,545.07	118,384	930,569	1,552	777,483
GIH	-2,768.80	-2,650.20	133,030	982,416	1,645	815,018
IBS	-1,757.40	-1,720.66	77,247	947,910	985	873,960
ITU	-3037.74	-2,789.85	87,413	772,696	1,167	670,668
JPT	-1,940.53	-1,908.79	138,119	963,480	1,506	806,733
KHV	-2,534.19	-2,464.42	129,833	926,471	1,660	758,835
MXL	-1,315.49	-1,250.08	84,044	933,773	1,240	835,087
PEL	-1,655.60	-1,654.89	87,845	1,388,867	2,359	1,202,850
PJL	-2,952.41	-2,762.79	110,248	911,288	1,437	776,633
PUR	-1,790.24	-1,495.38	82,153	813,624	858	744,856
STU	-1,951.48	-1,917.00	91,376	1,003,759	1,566	869,631
TSI	-2,957.45	-2,911.04	89,664	1,002,058	1,142	914,520
Average			103,391	920,867	1,450	785,260

Note: maxLogL1 is the maximum log(likelihood) value obtained from FitCoal. maxLogL2 is the maximum log(likelihood) value obtained from R-extended FitCoal, which was used to detect the severe bottleneck in non-African populations. The average log-likelihood promotion rate is 5.17%.

Table S11. Computing time (in hours) for YRI population in 1000GP and Yoruba population in the HGDP-CEPH panel using FitCoal, PSMC, SMC++, Stairway Plot, and Relate.

Population (num. of indv.)	FitCoal[a] (in hours)	PSMC[b] (in hours)	SMC++ (in hours)	Stairway Plot (in hours)	Relate (in hours)
YRI (108)	13.13	305.19	48.78	37.65	36.55
Yoruba (22)	9.37	51.36	2.33	2.67	5.37

Note: [a]The optimization was repeated 200 times for each estimation.
[b]The time required to infer 108 and 22 population size histories because PSMC is based on individual genome sequences.

Table S12. Computing time (in seconds) to analyze one simulated data in fig. 4 using FitCoal, PSMC, SMC++, Stairway Plot, and Relate.

Model (num. of indv.)	FitCoal [a] (in seconds)	PSMC [b] (in seconds)	SMC++ (in seconds)	Stairway Plot (in seconds)	Relate (in seconds)
Bottleneck I (94)	1,953	5,198	268,569	51,188	85,000
Bottleneck II (97)	651	2,367	185,582	55,132	65,051
Bottleneck III (97)	668	2,366	194,629	57,356	53,893
Bottleneck IV (94)	1,438	2,396	297,223	44,975	79,111
Bottleneck V (94)	2,756	2,327	199,033	44,956	119,859
Bottleneck VI (94)	709	2,392	210,394	48,001	181,136

Note: [a]The optimization was repeated 10 times for each estimation.
[b]The time required to infer multiple population size histories because PSMC is based on individual genome sequences.

Table S13. Comparison of accuracy between FitCoal and Ž-W's method.

Constant size model		
size	Ž-W's method	FitCoal
1	1.9999999999	2.0000000000
2	0.9999999999	1.0000000000
3	0.6666666666	0.6666666666
4	0.4999999999	0.5000000000
5	0.3999999999	0.4000000000
6	0.3333333333	0.3333333333
7	0.2857142857	0.2857142857
8	0.2499999999	0.2500000000
9	0.2222222222	0.2222222222
Instantaneous growth model		
size	Ž-W's method	FitCoal
1	1.7547171613	1.7547229380
2	0.7797340922	0.7797375358
3	0.4686921135	0.4686939043
4	0.3218480766	0.3218487511
5	0.2394397929	0.2394397658
6	0.1883537444	0.1883533260
7	0.1545070379	0.1545064537
8	0.1309436073	0.1309430117
9	0.1138668845	0.1138663751
Bottleneck model		
size	Ž-W's method	FitCoal
1	1.6737287481	1.6737374623
2	0.7744529188	0.7744538197
3	0.5109730563	0.5109715354
4	0.3927621211	0.3927603900
5	0.3264269184	0.3264256821
6	0.2832102142	0.2832095492
7	0.2519772704	0.2519770488
8	0.2277455013	0.2277455704
9	0.2080244642	0.2080247051

Table S14. Comparison of theoretical and FitCoal calculated branch lengths with the constant size model.

$n = 5$		
Type	Theoretical length	FitCoal length
1	2.000000000000	2.000000000000
2	1.000000000000	1.000000000000
3	0.666666666667	0.666666666667
4	0.500000000000	0.500000000000
$n = 1{,}000$		
Type	Theoretical length	FitCoal length
1	2.000000000000	2.000000000000
100	0.020000000000	0.020000000000
200	0.010000000000	0.010000000000
300	0.006666666667	0.006666666667
400	0.005000000000	0.005000000000
500	0.004000000000	0.004000000000
600	0.003333333333	0.003333333333
700	0.002857142857	0.002857142857
800	0.002500000000	0.002500000000
900	0.002222222222	0.002222222222
999	0.002002002002	0.002002002002

Table S15. Comparison between the two methods that calculate expected branch length ($\boldsymbol{BL_i(N(\cdot))}$) for each SFS component.

	Živković and Wiehe (2008) (*17*)	FitCoal (this study)
Theory	Joint probability density function of coalescent times	FitCoal
Limits on sample size	$n \leq 50$	Small to very large sample sizes.
Coalescent model	Kingman's coalescent	Based on Kingman's coalescent. Can be extended to other coalescent models, such as the exact coalescent (*96*).
Accelerated calculation	N/A	Yes
Software	Mathematica code	https://www.sinh.ac.cn/evolgen/
Supported demographic models	Multiple instantaneous/exponential changes in population size	Multiple instantaneous/exponential changes in population size

Table S16. Effect of different thresholds of log-likelihood promotion rate on FitCoal analysis.

Model	30%			20%			10%		
	Underfitting	Correct	Overfitting	Underfitting	Correct	Overfitting	Underfitting	Correct	Overfitting
Constant size	…	100%	0	…	100%	0	…	93%	2%
Instantaneous increase	0	100%	0	0	100%	0	0	99.5%	0.5%
PSMC “standard”	0	100%	0	0	100%	0	0	100%	0
Exponential growth II	0	100%	0	0	100%	0	0	99.5%	0.5%
Exponential growth III	0	100%	0	0	100%	0	0	100%	0
PSMC sim-YH	0	100%	0	0	100%	0	0	99.5%	0.5%
PSMC sim-1	0	100%	0	0	100%	0	0	100%	0
PSMC sim-2	20%	80%	0	0	100%	0	0	100%	0
PSMC sim-3	0	100%	0	0	100%	0	0	98%	2%
Complicated I	0	100%	0	0	100%	0	0	100%	0
Complicated II	0	100%	0	0	100%	0	0	100%	0
Exponential growth IV	0	100%	0	0	100%	0	0	100%	0
Exponential growth V	0	100%	0	0	100%	0	0	100%	0
Exponential growth VI	0	100%	0	0	100%	0	0	100%	0
Split I pop 1	0	100%	0	0	100%	0	0	99.5%	0.5%
Split I pop 2	0	100%	0	0	100%	0	0	99.5%	0.5%
Split II pop 1	0	100%	0	0	100%	0	0	100%	0
Split II pop 2	0	100%	0	0	100%	0	0	100%	0
Split III pop 1	0	100%	0	0	100%	0	0	100%	0
Split III pop 2	0	100%	0	0	100%	0	0	100%	0

Table S17. Sample size and truncated SFS of populations in 1000GP.

Population	Sample size (number of genomes)	SFS types discarded (start – end)[a]	Proportion of truncated SFS types (%)	Proportion of truncated SNPs (%)
African populations				
ACB	192	171 – 191	10.99	3.17
ASW	122	107 – 121	12.40	3.66
ESN	198	182 – 197	8.12	2.67
GWD	226	208 – 225	8.00	2.59
LWK	198	174 – 197	12.18	3.39
MSL	170	147 – 169	13.61	3.63
YRI	216	189 – 215	12.56	3.50
(Average)			11.12	3.23
Non-African populations				
BEB	172	156 – 171	9.36	4.00
CDX	186	174 – 185	6.49	3.56
CEU	198	178 – 197	10.15	4.39
CHB	206	180 – 205	12.68	5.34
CHS	210	191 – 209	9.09	4.17
CLM	188	163 – 187	13.37	5.49
FIN	198	181 – 197	8.63	4.19
GBR	182	151 – 181	17.13	6.60
GIH	206	189 – 205	8.29	3.75
IBS	214	179 – 213	16.43	6.29
ITU	204	186 – 203	8.87	3.88
JPT	208	182 – 207	12.56	5.26
KHV	198	181 – 197	8.63	4.21
MXL	128	114 – 127	11.02	5.49
PEL	170	152 – 169	10.65	6.21
PJL	192	177 – 191	7.85	3.54
PUR	208	174 – 207	16.43	5.77
STU	204	171 – 203	16.26	5.79
TSI	214	197 – 213	7.98	3.78
(Average)			11.15	4.83

Note: [a]Both values are inclusive.

Table S18. Proportion of SNPs without or with missing data of populations in the HGDP-CEPH panel.

Population	No missing data (%)	Missing samples ≤ 2 chromosomes (%)
Adygei	92.58	98.80
Balochi	91.01	98.37
Basque	92.66	98.83
Bedouin	87.00	97.30
Biaka	93.25	98.03
Brahui	90.76	98.37
Burusho	91.30	98.55
Druze	89.60	97.86
French	88.78	98.14
Han	84.54	97.14
Hazara	92.53	98.76
Japanese	87.45	97.96
Kalash	90.57	98.48
Makrani	91.10	98.29
Mandenka	91.93	98.13
Maya	94.98	99.13
Mozabite	93.21	98.58
Palestinian	87.22	97.32
Pathan	91.74	98.60
Russian	92.68	98.68
Sardinian	93.04	98.81
Sindhi	90.73	98.43
Yakut	86.66	97.80
Yoruba	92.78	98.02

Table S19. Sample size and truncated SFS of populations in the HGDP-CEPH panel.

Population	Sample size (number of genomes)	SFS types discarded (start – end)[a]	Proportion of truncated SFS types (%)	Proportion of truncated SNPs (%)
		African populations		
Biaka	44	36 – 43	18.60	4.93
Mandenka	44	37 – 43	16.28	4.75
Yoruba	44	38 – 43	13.95	4.14
(Average)			16.28	4.61
		Non-African populations		
Adygei	32	28 – 31	12.90	5.65
Balochi	48	40 – 47	17.02	7.22
Basque	46	41 – 45	11.11	6.18
Bedouin	92	73 – 91	20.88	9.52
Brahui	50	44 – 49	12.24	5.21
Burusho	48	41 – 47	14.89	6.57
Druze	84	70 – 83	16.87	8.24
French	56	50 – 56	10.91	5.59
Han	86	67 – 85	22.35	8.72
Hazara	38	32 – 37	16.22	6.72
Japanese	54	45 – 53	16.98	6.95
Kalash	44	40 – 43	9.30	5.22
Makrani	50	41 – 49	18.37	7.24
Maya	42	37 – 41	12.20	7.20
Mozabite	54	44 – 53	18.87	7.43
Palestinian	92	78 – 91	15.38	8.53
Pathan	48	35 – 49	27.66	10.12
Russian	50	40 – 49	20.41	8.06
Sardinian	56	51 – 55	27.27	11.65
Sindhi	48	41 – 47	14.89	6.35
Yakut	50	39 – 49	22.45	10.02
(Average)			17.10	7.54

Note: [a]Both values are inclusive.

Table S20. Comparison of accuracy between FitCoal and coalescent simulations.

Constant size model		
Type	Simulation method	FitCoal
1	1.999529551	2.000000000
2	0.999720720	1.000000000
3	0.667102715	0.666666667
4	0.500240165	0.500000000
5	0.400967708	0.400000000
6	0.333256388	0.333333333
7	0.285465389	0.285714286
8	0.249471384	0.250000000
9	0.222272679	0.222222222
Exponential growth model		
Type	Simulation method	FitCoal
1	1.441789518	1.441673129
2	0.616556332	0.616508244
3	0.376438453	0.376742859
4	0.269168704	0.268510338
5	0.207984340	0.208373096
6	0.170848693	0.170519652
7	0.144555420	0.144603091
8	0.125837330	0.125751908
9	0.111364011	0.111402445
Bottleneck model		
Type	Simulation method	FitCoal
1	1.673321651	1.673741394
2	0.775051787	0.774457584
3	0.510960086	0.510974557
4	0.394262151	0.392762519
5	0.325116671	0.326426966
6	0.284039310	0.283210115
7	0.251717509	0.251977042
8	0.228240338	0.227745129
9	0.207539986	0.208023953
Complex model		
Type	Simulation method	FitCoal
1	1.055607245	1.055592252
2	0.444340081	0.444812747
3	0.285522751	0.285501081
4	0.215995323	0.215622470
5	0.176447487	0.176540331
6	0.151750997	0.151231289
7	0.133173783	0.133109779
8	0.118845125	0.119172375
9	0.107810932	0.107898957

Table S21. Likelihood promotion rate of inferred demographic histories of populations in 1000GP with different numbers of time intervals.

Region	Population	Rate (%) for various inference time intervals			
		2	3	4	5
AFR	ACB	1384.26	350.31	60.09	18.68
	ASW	3538.08	130.56	93.48	6.10
	ESN	714.05	35.23	126.18	17.37
	GWD	590.15	302.50	112.43	13.01
	LWK	2925.80	91.55	70.91	5.88
	MSL	2935.78	43.91	60.37	8.62
	YRI	861.84	166.36	69.09	7.07
EUR	CEU	135.51	2471.16	17.07	…
	FIN	341.55	541.28	9.03	…
	GBR	65.68	2900.65	22.20	2.50
	IBS	384.43	2289.75	25.85	4.34
	TSI	236.98	2286.49	7.09	…
EAS	CDX	49.99	4430.87	15.64	…
	CHB	175.03	5343.87	10.80	…
	CHS	111.49	4384.47	10.26	…
	JPT	56.37	4100.17	24.05	6.76
	KHV	153.13	4242.29	7.67	…
SAS	BEB	319.95	2491.42	11.33	…
	GIH	101.31	1982.75	8.66	…
	ITU	261.16	1836.98	18.17	…
	PJL	254.33	1884.50	11.41	…
	STU	284.42	2590.84	9.89	…
AMR	CLM	834.67	1867.06	17.44	…
	MXL	347.01	4258.47	10.01	…
	PEL	359.65	5549.64	16.19	…
	PUR	1335.08	967.44	22.39	11.29

Table S22. Likelihood promotion rate of inferred demographic histories of populations in the HGDP-CEPH panel with different numbers of time intervals.

Region	Population	Rate (%) for various inference time intervals			
		2	3	4	5
AFR	Biaka	387.67	931.28	58.4	0.42
	Mandenka	2350.47	31.56	13.81	…
	Yoruba	3157.91	24.28	67.73	0.35
ME	Bedouin	282.02	87.97	1.89	…
	Druze	33.15	218.35	1.68	…
	Mozabite	275.41	130.64	2.99	…
	Palestinian	195.99	102.86	1.2	…
EUR	Adygei	179.37	98.23	0.37	…
	Basque	336.87	42.2	0.78	…
	French	48.25	201.88	0.58	…
	Russian	75.68	97.53	0.27	…
	Sardinian	105.69	649.27	1.04	…
EAS	Han	59.53	201.39	0.95	…
	Japanese	86.6	154.89	0.41	…
	Yakut	287.46	43.19	0.23	…
CSA	Balochi	40.25	244.48	0.78	…
	Brahui	27.24	276.49	0.6	…
	Burusho	75.72	115.73	0.21	…
	Hazara	95.97	159.24	1.05	…
	Kalash	1465.6	11.76	…	…
	Makrani	106.68	112.25	0.35	…
	Pathan	28.68	218.83	0.31	…
	Sindhi	69.31	170.14	0.29	…
AMR	Maya	136.19	1813.04	5.16	…

Table S23. Probabilities of each coalescent state (the number of ancestral lineages remained) at time t.

Standard coalescent time	*n*	Number of ancestral lineages remained							
		1	2	3	4	5	6	7	else
0.6	30	1.92%	17.22%	38.16%	30.57%	10.39%	1.62%	0.12%	<0.01%
0.6	40	1.64%	15.62%	36.9%	31.85%	11.78%	2.03%	0.17%	0.01%
0.6	50	1.49%	14.67%	36.06%	32.55%	12.68%	2.32%	0.21%	0.01%
0.6	180	1.11%	12.05%	33.27%	34.28%	15.53%	3.37%	0.37%	0.02%
0.6	200	1.09%	11.96%	33.15%	34.34%	15.65%	3.42%	0.38%	0.02%
0.6	220	1.08%	11.88%	33.05%	34.38%	15.74%	3.46%	0.38%	0.02%
0.8	30	7.32%	36.36%	40.14%	14.22%	1.86%	0.1%	<0.01%	<0.01%
0.8	40	6.73%	34.93%	40.68%	15.36%	2.17%	0.12%	<0.01%	<0.01%
0.8	50	6.38%	34.05%	40.96%	16.08%	2.38%	0.14%	<0.01%	<0.01%
0.8	180	5.44%	31.41%	41.56%	18.27%	3.09%	0.22%	0.01%	<0.01%
0.8	200	5.4%	31.31%	41.58%	18.36%	3.12%	0.22%	0.01%	<0.01%
0.8	220	5.37%	31.22%	41.59%	18.43%	3.15%	0.22%	0.01%	<0.01%
1.0	30	15.99%	48.88%	29.75%	5.09%	0.28%	0.01%	<0.01%	<0.01%
1.0	40	15.18%	48.17%	30.73%	5.58%	0.33%	0.01%	<0.01%	<0.01%
1.0	50	14.7%	47.72%	31.32%	5.89%	0.36%	0.01%	<0.01%	<0.01%
1.0	180	13.35%	46.29%	33%	6.88%	0.48%	0.01%	<0.01%	<0.01%
1.0	200	13.29%	46.23%	33.06%	6.92%	0.48%	0.01%	<0.01%	<0.01%
1.0	220	13.25%	46.18%	33.12%	6.95%	0.49%	0.01%	<0.01%	<0.01%
1.2	30	26.31%	53.05%	18.95%	1.65%	0.04%	<0.01%	<0.01%	<0.01%
1.2	40	25.42%	52.97%	19.75%	1.82%	0.05%	<0.01%	<0.01%	<0.01%
1.2	50	24.89%	52.89%	20.23%	1.93%	0.05%	<0.01%	<0.01%	<0.01%
1.2	180	23.37%	52.6%	21.69%	2.27%	0.07%	<0.01%	<0.01%	<0.01%
1.2	200	23.31%	52.59%	21.74%	2.29%	0.07%	<0.01%	<0.01%	<0.01%
1.2	220	23.26%	52.58%	21.79%	2.3%	0.07%	<0.01%	<0.01%	<0.01%

Note: The shadowed area shows the probability for the number of ancestral lineages remained is ≤ 3 in more than 90% cases when the standard coalescent time is $t \geq 1.0$.